UILU-ENG-72-2001

CIVIL ENGINEERING STUDIES
STRUCTURAL RESEARCH SERIES NO. 375
Illinois Cooperative Highway Research Program
Series No. 126

FIELD INVESTIGATION OF A PRESTRESSED CONCRETE HIGHWAY BRIDGE LOCATED IN DOUGLAS COUNTY, ILLINOIS

By
D. M. HOUDESHELL
T. C. ANDERSON
W. L. GAMBLE

Issued as a Documentation Report on
The Field Investigation of Prestressed
Reinforced Concrete Highway Bridges
Project IHR-93
Illinois Cooperative Highway Research Program
Phase I

Conducted by

THE STRUCTURAL RESEARCH LABORATORY
DEPARTMENT OF CIVIL ENGINEERING
ENGINEERING EXPERIMENT STATION
UNIVERSITY OF ILLINOIS

in cooperation with

THE STATE OF ILLINOIS
DIVISION OF HIGHWAYS

and

THE U.S. DEPARTMENT OF TRANSPORTATION
FEDERAL HIGHWAY ADMINISTRATION

UNIVERSITY OF ILLINOIS
URBANA, ILLINOIS

FEBRUARY 1972

UILU-ENG-72-2001

FIELD INVESTIGATION OF A PRESTRESSED CONCRETE HIGHWAY BRIDGE LOCATED IN DOUGLAS COUNTY, ILLINOIS

by

D. M. Houdeshell
T. C. Anderson
W. L. Gamble

Issued as a Documentation Report on
The Field Investigation of Prestressed
Reinforced Concrete Highway Bridges
Project IHR-93
Illinois Cooperative Highway Research Program
Phase I

Conducted by

THE STRUCTURAL RESEARCH LABORATORY
DEPARTMENT OF CIVIL ENGINEERING
ENGINEERING EXPERIMENT STATION
UNIVERSITY OF ILLINOIS

in cooperation with

THE STATE OF ILLINOIS
DIVISION OF HIGHWAYS

and

THE U. S. DEPARTMENT OF TRANSPORTATION
FEDERAL HIGHWAY ADMINISTRATION

UNIVERSITY OF ILLINOIS
URBANA, ILLINOIS
FEBRUARY 1972

ABSTRACT

Houdeshell, D. M., T. C. Anderson, and W. L. Gamble, "Field Investigation of a Prestressed Concrete Highway Bridge Located in Douglas County, Illinois," Civil Engineering Studies, Structural Research Series No. 375, Department of Civil Engineering, University of Illinois, Urbana, February 1972.

Key Words: Prestressed, concrete, bridges, structures, creep, shrinkage, strain, camber, construction, research, reinforcement

Camber, strain, creep, and shrinkage measurements were made over a period of two years on a three-span prestressed concrete highway bridge and concrete specimens. The precast I-section girders 72 ft. 9 in. long were made continuous for live-load forces by reinforcement cast in the deck. The construction of the bridge is described, as is the instrumentation used.

Although the most important changes in camber of the beams occurred within the first 200 days after release of prestress, measurable movements were still occurring after more than two years. The strain measurements exhibited annual cyclical expansions and contractions, probably due to changes in average relative humidity at different times of the year. Measurable shortening of the bottom fiber of the girders occurred for more than two years after release of the prestressing force, but was obscured by the large cyclical variations.

The major portion of the loss of prestress occurred during the first few weeks after release, but the losses continued at a slow rate throughout the test period.

The creep and shrinkage measurements show that the shrinkage in the field was much less than in the laboratory, but that the creep values were comparable in the two environments. Further work is required to define the magnitude of creep of concrete subjected to variable environmental conditions, as most accepted present concepts are not adequate.

TABLE OF CONTENTS

TABLE OF CONTENTS (Con't.)

1. INTRODUCTION

1.1 Introductory Remarks

The introduction of prestressed concrete as a construction material in the past two decades prompted many laboratory investigations into the strength and behavior, in both short and long term tests, of prestressed members and structures. However, there have been relatively few long-term investigations under field conditions where the varying environment is a factor affecting behavior.

The Department of Civil Engineering and the Engineering Experiment Station of the University of Illinois in cooperation with the Illinois Division of Highways and the Federal Highway Administration undertook, in 1965, a field study of the long-term behavior of prestressed concrete bridges in order to produce some relevant information.

This report describes the results of measurements made on the second bridge studied in the project. The initial measurements were made at the time the girders were manufactured in December, 1968, and the results of the measurements for the first two years of the life of the bridge are presented in this report.

The work reported herein covers parts of Phase 1 (b), (c), (d), and (e), Field Instrumentation, Field Measurements, and Data Evaluation, of the project's work schedule.

1.2 Object and Scope

This report describes the investigation into the long-term behavior of a three-span prestressed reinforced concrete highway bridge. Each span consists of six I-section precast girders, and the structure was made continuous for live loads by means of non-prestressed reinforcement in the composite deck.

The results of strand-force, concrete strain, and girder deflection measurements are given for two girders in the structure. The strain and deflection measurement records extend for two years at the time of preparation of this report.

Anchorage zone cracking was observed in the girders, and these cracks are described.

The strain and deflection measurements are discussed and compared with theoretical values. The implications of the measurements, in terms of loss of prestress, flexural cracking, and changes in camber with time, are discussed.

The test structure is described in Chapter 2, as are the methods of construction and the properties of the materials used in the structure. The instrumentation used in the test structure is described in Chapter 3, as are the various test specimens used to determine the long-term behavior of the concrete used in the girders and deck. The results of the measurements made on the bridge are presented in Chapter 4, and the results of shrinkage and creep measurements on concrete specimens are presented in Chapter 5. The test results are discussed in Chapter 6, and Chapter 7 is a summary.

1.3 Acknowledgments

This study was carried out as a part of the research under the Illinois Cooperative Highway Research Program, Project IHR-93, "Field Investigation of Prestressed Reinforced Concrete Highway Bridges." The work on the project was conducted by the Department of Civil Engineering, University of Illinois, in cooperation with Division of Highways, State of Illinois, and the U. S. Department of Transportation, Federal Highway Administration. At the University, the work covered by this report was carried out under the general administrative supervision of D. C. Drucker, Dean of the College of Engineering,

Ross J. Martin, Director of the Engineering Experiment Station, N. M. Newmark, Head of the Department of Civil Engineering, and Ellis Danner, Director of the Illinois Cooperative Highway Research Program and Professor of Highway Engineering.

At the Division of Highways of the State of Illinois, the work was under the administrative direction of Richard H. Golterman, Chief Highway Engineer, R. D. Brown, Jr., Deputy Chief Highway Engineer, and J. E. Burke, Engineer of Research and Development.

The program of investigation has been guided by a Project Advisory Committee consisting of the following members:

Representing the Illinois Division of Highways:

J. E. Burke, Engineer of Research and Development

F. K. Jacobsen, Engineer of Bridge Research

C. E. Thunman, Jr., Engineer of Bridge and Traffic Structures, Bureau of Design.

Representing the Federal Highway Administration:

Robert J. Deatrick, Assistant Bridge Engineer

Edward L. Tyk, Assistant Bridge Engineer

Representing the University of Illinois:

Narbey Khachaturian, Professor of Civil Engineering

C. P. Siess, Professor of Civil Engineering

Acknowledgment is due to Mr. R. C. Mulvey and Mr. R. Bradford, Illinois Division of Highways, who contributed materially to the guidance and progress of the program.

Thanks are also due to Mr. Jacob Whitlock and Mr. Eugene L. Peck of Midwest Prestressed Concrete Co., Springfield and Rochelle, Illinois, and to Mr. Charles Reinhardt of Howell Asphalt Co., Mattoon, Illinois, for aid

and cooperation during the construction phases of the contract. The bridge contract was held by a joint-venture group consisting of Howell Asphalt Co., A. J. Walker Construction Co., and Huckaba and Sons Construction Co., all of Mattoon, Illinois.

Construction inspection and supervision was provided by Homer L. Chastain and Associates, Decatur, Illinois, under a contract with the Illinois Division of Highways. Mr. F. C. Skinner and Mr. John Perry provided immediate supervision.

This investigation is directed by Dr. M. A. Sozen, Professor of Civil Engineering, as Project Supervisor. Immediate supervision of the investigation is provided by Dr. W. L. Gamble, Associate Professor of Civil Engineering, as Project Investigator.

The following Research Assistants in Civil Engineering have participated in the design and installation of the instrumentation, and the collection and analysis of the data: T. C. Anderson, V. C. Corsetti, D. M. Houdeshell, V. Mossiossian, S. Sithichaikasem, and J. B. Wojakowski.

This report has been prepared in cooperation with the U. S. Department of Transportation, Federal Highway Administration.

The opinions, findings, and conclusions expressed in this publication are those of the authors and not necessarily those of the State of Illinois, Division of Highways, or of the Department of Transportation.

2. DESCRIPTION OF TEST STRUCTURE

2.1 Description of Test Structure

The test structure is a three-span bridge carrying Interstate Route 57 over Hayes Branch and is shown in Fig. 2.1. The test structure carries the south-bound lanes of the highway. The north-bound lanes are carried on an identical parallel structure, with the roadways on 88 ft centers. Each span contains six precast I-section girders, and the bridge was made continuous for live loads by means of the reinforcement in the composite deck. The design live load was HS-20.

The test structure is located in Douglas County, Illinois, one-half mile east of the town of Tuscola. The bridge was constructed as a part of Section 21-28(VB & B) Project I-IG-57-5(68)212, HPR-PR-1(3).

The plan of the bridge is shown in Fig. 2.2. The bridge is skewed 30^{o}, left-hand side advanced. It is on a vertical curve sloping upward from north to south with elevation difference of 3.5 ft between the bridge ends. All girders were 72 ft 9 in. long and 48 in. deep. Cast-in-place diaphragms were placed as shown in the figure. The diaphragms were connected to the girders by means of threaded rods screwed into inserts cast into the girders.

The elevation of a typical girder is shown in Fig. 2.3 and an elevation of the structure is shown in Fig. 2.4. Locations of the 7/16-in. diam pre-stressing strands are shown in Fig. 2.3. The girder cross-section showing the strand spacing is shown in Fig. 2.5. There were no end-blocks.

Non-prestressed longitudinal reinforcement and stirrups were spaced in the beams as shown in the above referenced figures.

A cross-section of the bridge is shown in Fig. 2.6. The girders were spaced at 7 ft 2 1/2 in. centers, and the deck was 7 in. thick. A small fillet was provided at the girder-deck interface to facilitate corrections

for camber of the girders when setting the deck forms. The form of this fillet is shown in Fig. 2.8. The deck was reinforced continuously both top and bottom and in both directions. The reinforcement in the areas near the piers is shown in Fig. 2.6, and that near mid-span in Fig. 2.7.

Three different types of bearing devices were used in the structure. At the north pier, all beams were supported on rubber-impregnated fabric bearing pads which were 6 in. by 18 in. by 1/2 in. thick. The pads were centered 6 in. from the beam ends. In addition, dowel bars extended from the pier into the transverse diaphragm over the pier. The bridge consequently was not free to move relative to the north pier.

At the south pier, the girders were supported on elastomeric bearing pads. The pads were 9 in. by 18 in. by 2 7/8 in. thick, were made of Grade 70 (Shore A Durometer) neoprene, and contained 5 bonded metallic shims. The pads were centered 7 in. from the ends of the beams.

At the abutments, metal bearing devices were used to accommodate the longitudinal motions and the rotations. The sliding elements were self-lubricating bronze plates set between two steel plates. Rocker plates machined to a 24 in. radius were attached to the girders, and bear on flat steel plates. The bearings were centered 8 in. from the ends of the girders.

The two piers were solid reinforced concrete, 2 ft 6 in. thick with a 3 ft 6 in. thick cap, and were supported on spread footings bearing on hard, gray, clay loam till. The abutments were also reinforced concrete and were supported on 36 ft concrete bearing piles driven into hard, brown, sandy, clay loam till.

The girders of the test bridge were manufactured during December, 1968, and January, 1969. The south pier was cast in November, 1968, and the north pier and abutments were cast in the spring of 1969. The girders were placed on the piers during May and June of 1969. The central portion of the deck

and diaphragms was cast on 5 August 1969, and the structure was finished the same month.

Wooden scaffolding was hung below the bridge to allow access to the gage lines on the two test beams as shown in Figs. 2.9 and 2.10. A metal ladder attached to the south bridge pier supplied access to the scaffolding from below the bridge.

The roadway over the bridge was opened to traffic on 22 December 1970, and the last complete set of strain readings reported herein were taken on 20 February 1971, 782 days after release of the prestressing force on the test girders.

2.2 Construction of Bridge

2.2.1 Manufacturing of Girders

The girders were manufactured in the Rochelle, Illinois, plant of Midwest Prestressed Concrete Co. All girders were cast in steel forms on a single 200-ft long prestressing bed. The prestressing bed, one of 11 in the plant, was set up to make two girders during one cycle. The bed was inside a building which was heated only by steam used in curing concrete.

The times at which various operations were started and completed are listed in Table 2.1, for a 71-hour period from 27 December to 30 December 1968. The times indicated apply to the construction of two girders, designated BX-3 and BX-4, in which instrumentation was installed as described in Chapter 3. The starting point for the cycle is taken as the time when the prestressing bed was empty and the holddowns were set.

Starting with a clean, empty, prestressing bed with the side forms removed, the hardware for holding strands down at the drape points and up at a point between the two beams was installed, as were the end bulkheads for the beam

forms. The 38 strands were strung through the end anchorages, bulkheads, lower loops of non-prestressed reinforcement, and holddowns. The bottom straight strands were placed first and the draped top strands later.

Tensioning of the 7/16 in. diam strands started immediately after the last strand was in place. A hydraulic ram and a pressure gage which previously had been calibrated against a load cell by Illinois Division of Highways personnel were used to control the pretensioning force.

The remaining non-prestressed reinforcement had been tack welded into cages, and the cages were placed on the bed and worked into the proper positions after all strands had been stressed. The side forms were then placed.

The first concrete was placed soon after the forms were finished. The concrete was placed in the form in three lifts. The first lift approximately filled the lower flange of the beam, the second filled most of the web, and the third finished the beam. All lifts of concrete were compacted with internal electrical vibrators. A great deal of vibration was used, as the concrete was quite stiff.

The concrete was placed in about two hours, and the beams had been struck off and finished with a wooden float within an additional 20 minutes. The top of the beam was covered with burlap. Steam curing was started about two hours later with steam lines under the prestressing bed. The side forms were removed from the beam 15 hours after the last of the concrete was placed, and the beam was covered with rubberized canvas.

The prestressing force was released about 60 hours after the beams had been cast. The strands were flame cut, starting with the draped strands. After the draped strands were cut, the holddowns were released and the straight strands cut. The sequence was to cut 2 or 3 strands at one end of the bed, move to the space between the two beams and cut 2 or 3 strands, cut a few

strands at the second end, and then move back toward the starting point. The strands were heated over several inches to relax the stress in the wires before the oxygen was turned on in the torch to finish burning the strands.

The beams were then moved from the stressing bed to a storage area inside the plant. One day later they were moved to an outdoor storage area, where they remained until being shipped to the bridge site. The girders were shipped to the construction site during May and June of 1969.

The locations of the girders at various times during construction of the bridge are listed in Table 2.2. The girders were placed on temporary supports, and the locations of these supports when the beams were in their various locations are shown in Fig. 2.12.

2.2.2 Construction of Deck

Construction was stopped for the winter of 1968-1969 after the south pier had been cast. Construction of the deck and diaphragm forms started in July, 1969. The formwork was entirely supported from the girders, except that the bottoms of the diaphragms over the interior supports were supported from the piers.

The forms were made of wood. Most of the material was either nominal 2 by 6 in. stock or 3/4 in. plywood. The forms were supported from the girders by means of steel rods which screwed into steel brackets placed across the tops of the girders. A view of the formwork for a diaphragm over an interior pier is shown in Fig. 2.11. The diaphragm reinforcement and part of the deck reinforcement is in place.

It was discovered that the south pier was constructed about three in. too short. In order to provide the correct deck profile, the fillets, as

shown in Fig. 2.8, were up to 3 1/8 in. high over this pier instead of being less than one in. as is the normal case.

The deck and diaphragm reinforcement were placed. The reinforcement was assembled by tying with 16 gage soft iron wire, and was supported on bar chairs.

The deck concrete was cast on 5 August 1969, a clear, bright, and calm day. The concrete was delivered to the job site in mixer trucks, and concreting started at the south end of the structure. Concrete at the ends was dumped directly from the truck into the forms, but most of the concrete was placed with a crane and bucket. The casting operation took about eight hours, and included the following steps:

1. Place concrete from truck or bucket.
2. Vibrate with internal vibrators.
3. Screed with a screed having two separate screeds two ft apart, sprinkling water on the concrete between the screeds by hand using a large paint brush.
4. Float surface with long-handled float moved transversely across deck.
5. Straight-edge surface with six-ft long straight-edge moved transversely across deck.
6. Refloat surface, with frequent sprinkling of water on deck. This was done two to three hours after placement of concrete.
7. Hand-float problem areas.
8. Broom surface to get rough textured surface.

It appeared that the upper layer of concrete in the deck was often badly overworked by the time the finishing operation was complete.

The deck was covered with burlap and plastic sheeting and kept wet for at least a week following casting of the concrete.

The forms for the longitudinal construction joints in the deck were coated with retarder before the central portion of the deck was cast. The joints were cleaned with water sprays and sand-blasting before the edge strips were cast in order to obtain a well bonded joint. The edge sections of the deck were cast within a week after the central strip, and the curb sections were cast after another week.

2.3 Materials Used in Bridge

2.3.1 Concrete

The concrete used in the girders had a specified cylinder strength of f'_c = 5,000 psi at 28 days, and a required minimum strength of 4,000 psi at the time of the release of the pretensioning force.

The mix used in the girders was made with 7.5 sacks of Type III cement per cubic yard. The proportions were 1:1.36:2.78, cement:sand:gravel, by weight. The coarse aggregate was crushed limestone with a 1 in. maximum particle size. Darex air entraining agent was added at the rate of 2 oz. per sack of cement. The ratio of added water to cement was 0.35, but this was not representative of the mix since the aggregates were used wet. The actual water cement ratio is not known, but probably was between 0.4 and 0.5. The concrete was mixed in a horizontal pan mixer of 1 cu yd capacity.

The air content of the concrete placed in the beams varied from 4.6 to 6.2 per cent, and the specifications called for 4 to 7 per cent. The measured slump varied from 2 to 3 in., with the average about 2 1/2 in.

The concrete had an average value of f'_c = 4,940 psi at 60 hours after casting, and this was used to control the release of the pretensioning.

The compressive strengths and initial values of Young's Modulus at various ages of test cylinders stored in the field with the bridge girders and in the University of Illinois Structural Research Laboratory are listed in Table 2.3. A representative stress-strain curve is shown in Fig. 2.13a.

A temperature study was made on two cylinders made from the beam concrete to determine the coefficient of thermal expansion. The results are graphed in Fig. 2.14, and show $\alpha = 4.9 \times 10^{-6}$/°F for concrete one month old.

The deck concrete was specified as Class X, and under the specifications in effect at the time, the compressive strength was to be a minimum of $f'_c = 3{,}500$ psi and the modulus of rupture at least $f_r = 650$ psi, both at 14 days. The compressive strengths and initial values of Young's Modulus at various ages are shown in Table 2.4 for concrete specimens stored at the bridge site and in the laboratory. The air content, by volume, was to be in the range of 4 to 7 per cent.

The concrete mix used contained 6 sacks of Type I cement per cubic yard, and the mix proportions were 1:2.08:3.43, cement:sand:gravel, by weight. The ratio of added water to cement was 0.37, but wet aggregates were used. The coarse aggregate was crushed limestone, and the maximum size was between 1 and 1.5 in. Darex air entraining agent was used, but the rate was not recorded. Daratard retarding admixture was used at the rate of 9 oz. per sack of cement. The concrete was mixed in truck-mounted transit mixers.

Air content and slump tests were made by inspection personnel at the site. The air content as recorded in official test data ranged from 4.1 to 6.5 per cent, and averaged 5.2 for 30 tests. Project personnel were informed, during casting of the deck specimens, that the specimens were from a batch with an air content of 1.9 per cent. Three cylinders of hardened concrete were later cut and polished for an air content determination, follow-

ing ASTM C-457, 67-T, Modified Point-Count Method. The air contents found were 4.1, 2.5, and 2.9 percent, for an average of 3.2 percent. The slump ranged from 3 in. to 4 in. A representative stress-strain curve is shown in Fig. 2.13b.

Samples of the concrete used in both the girders and deck were taken and specimens for strength, shrinkage, and creep tests were made. These specimens and the results of the creep and shrinkage measurements are discussed later in this report.

2.3.2 Reinforcement

The prestressed reinforcement was 7/16 in. diam, 7-wire strand meeting the requirements of ASTM A-416. The specified minimum ultimate stress is 248 ksi, and the minimum elongation is 3.5 per cent in a 24 in. gage length.

The strands used in the beams came from two separate rolls which had significantly different properties. One roll was used for the nineteen strands on the west half of the beams, and the other roll was used for the nineteen strands on the east half of the beams. The west roll was old and had a thin coating of rust. The east roll was newer and still had a shiny blue surface. Two samples from each roll were tested.

The west roll had an average failure stress of 298 ksi with an elongation in a 12 inch gage length of 17 per cent across the fractured section. The average Young's Modulus was $E = 28{,}700$ ksi, and yield stress at 0.1 per cent offset was $\sigma_y = 258$ ksi.

The east roll had an average failure stress of 269 ksi, an average Young's Modulus of $E = 27{,}600$ ksi, and an offset yield stress of $\sigma_y = 236$ ksi. The elongation at failure was not determined precisely because of the locations of the fractures, but was in excess of 3.7 percent.

The Young's Modulus used in analyzing the beams is the average value of all four tests, $E = 28{,}200$ ksi. A typical stress-strain curve is shown in Fig. 2.15.

Special precautions as described in Ref. 1* were taken during testing of the strands to insure that failures did not occur within the grips.

The non-prestressed reinforcement was specified as ASTM A-15, intermediate grade, reinforcing bars (equivalent current specification: ASTM A-615, Grade 40). It was discovered during the placing of the deck reinforcement that much of the steel was marked as Grade 60 instead of the specified Grade 40. A count was made of the bars on the bridge site, and it was found that all of the #4, #7, and #8 bars, and about half of the #5 bars were Grade 60. Only the #6 bars were all Grade 40. All of the girder reinforcement was marked as Grade 40.

Two samples of each size of bar used in the deck and girders were tested. All reinforcement exceeded the required yield stress of 40 ksi. The average yield and ultimate stresses for each size bar are listed in Table 2.5, as are the values of ultimate elongation. Typical stress-strain curves are shown in Fig. 2.16.

*References, which are also listed as numbers enclosed in parentheses, are listed in Chapter 8 of this report.

3. INSTRUMENTATION AND CONTROL SPECIMENS

3.1 Introduction

The instrumentation used in determining the strand forces, deflections, strain distributions, temperatures, and cracking are described in this chapter. The locations of the various devices are described, and essential details given. In addition, the specimens providing auxiliary information on the strength, creep, and shrinkage properties of the concrete are described.

Many of the details of the instrumentation are described in Ref 2.

3.2 Strand Force Measurements

Forces were measured in 12 of the 38 strands at the anchorage end of the prestressing bed during the prestressing operation and at intervals until the strands were released. The locations of the 12 strands are shown in Fig. 3.1. The force in a draped strand was also measured at the jacking end of the prestressing bed.

The force measurements were made with aluminum sleeve dynamometers which were instrumented with bonded wire electrical resistance strain gages, with the four gages on each sleeve arranged as a four-arm bridge. The sleeves were of 6061-T6 aluminum, 1-3/8 in. OD, 5/8 in. ID, and 6 in. long. The sensitivity of the dynamometers was about 48 lb per dial division deviation on a portable strain indicator.

Forces were measured in each strand just after it was tensioned and immediately after all 38 strands had been tensioned. The readings were repeated when the steam curing cycle was started and just before and after release of the prestressing strands.

3.3 Strain Measuring Instrumentation for Girders

3.3.1 Electrical Strain Gages

Six Carlson Elastic Wire Strain Meters were installed in the forms for each beam before the concrete was cast, and were located as shown in Figs. 3.2 and 3.3. Six additional gages were installed in the deck above the girders, and their locations are shown in the same figures.

The lead wires for the gages embedded in the girder were brought out through the top surfaces of the beams near the gage locations. The lead wires were full length so no field splicing would be necessary, and were left coiled on top of the beams until the deck formwork had been completed. The lead wires were then strung along the top of the girders to a point near mid-span of the south end-span of the bridge. The wires were led to holes drilled in the formwork above an instrumentation platform on the back-slope below the end-span. A 2 1/2 in. pipe elbow and a short nipple were inserted into each hole, the wires were led through the pipes, and the pipes were stuffed full of rags to seal against concrete.

The Carlson Strain Meters, as described in Refs 2 and 3 are unbonded wire resistance gages. Each gage contains two arms of a Wheatstone bridge circuit, and the remaining arms are in a portable measuring set.

There were some difficulties with the particular version of the gages used, as discussed in Ref 1, and the strain readings obtained were apparently substantially higher than the true strains.

3.3.2 Mechanical Strain Gage

One hundred fourteen mechanical strain gage lines were installed in each test beam before the prestressing force was released. A 10 in. gage length Whittemore gage was used to make the readings. It is a direct reading

mechanical gage with no multiplication of movement. It is equipped with spherical tips (diam 0.089 in.) which fit into conical holes drilled into gage points rigidly attached to the beams.

The locations and designations of the strain gage lines at mid-span and the quarter points are shown in Fig. 3.4. Locations and designations of the strain gage lines near the ends of the beams are shown in Fig. 3.5. Identical patterns were used on both sides of the beams with the designations changed to indicate east or west.

Several steps were involved in the installation of gage points in the hardened concrete. The sequence was as follows for each gage point:

1. A 1/4 in. diameter by 3/4 in. deep hole was drilled with an electric hammer-drill.
2. The hole was cleaned by blowing out with a tire pump.
3. The hole was partially filled with an epoxy which has a setting time of about 20 minutes at room temperature.
4. A 1/4 in. diameter by 1/2 in. long stainless steel hex-head cap screw was inserted into the epoxy filled hole, and the epoxy was allowed to set.
5. The head of the cap screw was lightly marked with a punch specially made to mark the desired 10 in. gage length.
6. A conical hole was drilled through the mark with a #1 center drill in a high speed electric drill, using cutting oil as a lubricant.
7. The cuttings and cutting oil were cleaned away from the bolt head using a pressure can of television-tuner cleaner equipped with a flexible plastic tube nozzle to direct the spray into the drilled hole.

A cross-section of the completed gage point is shown in Fig. 3.6. The conical hole had a 60 degree included angle and a 1/8 in. maximum diameter. The heads of the cap screws protruded by their thickness from the surface of the concrete, but this was not a problem and no serious difficulties with physical damage to the gage points have been experienced to date. The stainless steel bolts have been quite successful and there have been no corrosion difficulties after more than four years of field exposure on a similar test structure at Jefferson County (1).

The epoxy used was "Concresive" No. 1201, manufactured by the Adhesive Engineering Company. This material is no longer available, and will probably be replaced with "Aerobond" No. 2209, which has similar properties and is made by the same company.

All strain gage lines were read immediately before the prestressing strands were cut and again immediately afterward. The readings have been repeated at appropriate intervals since that time.

Temperature compensation has been provided by the use of a steel standard bar with the mechanical strain gage. The relatively heavy steel bar, 2 in. square, has been used so that it would respond to temperature changes relatively slowly and in addition would be so stiff that perfectly uniform bearing conditions would not have to be provided under the bar before repeatable readings could be obtained.

A thermometer inserted longitudinally in the center of the standard bar was used to determine the time when the bar reached ambient temperature. The readings were also used as an aid in interpreting the result of the strain readings.

It must be recognized that completely adequate temperature compensation is probably not possible in the case of a structure where some parts are in

shade and others in direct sun. The technique that was adopted as standard was to place the standard bar on the concrete structure, but always in the shade, and allow it to come to temperature equilibrium before taking strain readings. An additional problem is that the coefficients of expansion of the concrete and the steel standard bar are not quite the same, and the difference may become significant if a 50° F or greater temperature range occurs.

Temperature equilibrium occurs within a structure only occasionally, and the most likely time for the structure to be a uniform temperature throughout is just before dawn, or under heavy overcast conditions which have prevailed for several hours.

3.4 Deflection Measurements

Deflections were measured, by means of a precise surveyor's level and level rod, for the two beams designated BX-3 and BX-4 in Fig. 2.2. In each beam, deflection plates were cast into both the top and bottom surfaces of the beam near each end and at mid-span as shown in Fig. 3.7. The plates were set away from the ends of the beams in order to clear the faces of the piers when readings were taken from below the bridge. Elevation readings were made at each of three points on one surface of a beam, and the camber computed as the difference between the mid-span elevation and the average of the two readings at the ends of the girder, with a correction made for the initial irregularities in the surface profile. This eliminated the necessity of providing bench marks.

The deflection plates used were 1 by 1 by 1/4 in. stainless steel plates welded to a 2 in. length of #4 reinforcing bar. Plates were inserted into the top surface of the beam after the concrete finishers had completed striking off the concrete. Plates were also inserted into the deck concrete after

it had set by drilling holes into the deck with a masonry bit, chiseling a flat, depressed area for each plate, and grouting the plates into final position with the quick-hardening epoxy compound.

Level readings were taken on the upper surface of the girders immediately before and after release of the prestressing force and at appropriate time intervals later. After the girders were erected on the piers, readings were taken from below the bridge during the period when the deck was being cast and cured.

Readings from that time until the bridge was opened to traffic were taken from the bridge roadway surface. After the highway was opened to traffic, the readings again had to be taken from below.

A Wild N-3 precise level and a specially prepared level rod, as described in Ref 2, were used to make the readings. The minimum reading with this instrument is 0.0005 ft, with readings repeatable to 0.001 ft.

3.5 Temperature and Humidity Measurements

Temperatures were measured at two points near mid-span in each beam and in the deck above mid-span of each beam. Copper-constantan thermocouples encased in copper tubing were used, and were located as shown in Fig. 3.7.

The initially installed thermocouple wires extended only to the top surface of the girders, and additional lengths of copper and constantan wire were spliced on after the deck forms were in place. The wires were led through 1/4 in. ID plastic tubing along the top surface of the beams and then down through the deck form to the area under the south-end span where the concrete specimens were stored.

The thermocouples were used in order to obtain information about the differences between the temperature of the structure and that of the

surrounding air, and to check the temperature readings that were obtained from the Carlson Strain Meters.

A temperature-relative humidity recorder was used to obtain a record of weather conditions. The recorder was placed between the test girders during part of the time they were in the storage yard and then under the end-span of the test structure. Nearly continuous recordings were obtained for about 18 months. A typical recorder chart is reproduced in Fig. 3.8.

3.6 Cracking Observation

The end zones of the girders were examined for cracking immediately after release of the prestressing, two weeks later, and again five months later. Hand magnifying lenses were used to aid in tracing the ends of the cracks, and the widths of selected cracks were measured by the use of an optical comparator which had a reticle with various width lines ruled on it.

Cracks were noted in all four end zones at the junction of the lower flange with the web, and about 6 in. up on the web. A few very fine cracks were observed further up on some of the ends. Cracks did not seem to be time dependent.

3.7 Concrete Test Specimens

Concrete test specimens were made of concrete used in the girders and from concrete used in the deck. These samples were used for strength and Young's Modulus determinations, for shrinkage measurements, and for creep tests.

About sixty 6 by 12 in. cylinders were made of beam concrete, with the concrete being taken from buckets which were being used in BX-4. The cylinders were cast in disposable sheet-metal molds. In addition, six 2 ft long sections of girder were cast and used as shrinkage specimens. They were cast on the

same prestressing bed with the test girders at the beginning of the casting period. The short beam specimens all contain 38 prestressing strands. To prevent bonding of the strands in the shrinkage beams, the strands in four of the beams were covered by rubber hoses, and the strands in the remaining two beams were coated with Rugasol Retarder. The retarder was used on the strands in specimens F1 and L1.

Thirty-three cylinders of girder concrete were tested in compression at the various intervals shown in Table 2.3. The remaining cylinders were used as shrinkage or creep specimens, with half stored with the bridge girders and half in the laboratory.

In each cylinder in which strains were to be measured, three 10 in. gage lines were established for the Whittemore gage, with the lines spaced around the cylinders at 120 degree intervals. The six gage points in each cylinder were installed in anchors cast into the cylinders. The anchors consisted of 1 in. lengths of #4 reinforcing bar which had been drilled and tapped for the 1/4 in. cap screws. The anchors were attached to the disposable sheet metal cylinder molds by drilling holes in the molds and attaching the anchor to the inside of the mold by a cap screw through the hole. The cap screws were removed after the concrete set, the molds removed, and the stainless steel cap screws inserted and drilled with the center-drill. The cap screws were locked into the anchors by an application of a stud-locking solution to the threads. Ten cylinders were instrumented for shrinkage measurements and twelve for creep tests, half for the field and half for the laboratory storage conditions.

The creep specimens were loaded to a unit stress of 1,000 psi, and the load was maintained by means of a heavy coil spring. Each creep rack held three cylinders, and was arranged as shown in Fig. 3.9. The load was applied

by means of a 30-ton hydraulic jack, and then was held by tightening the nuts just above the plate over the spring by 1/4 turn from fingertight. The load was readjusted at every reading interval.

Two creep racks were loaded about 2 days after the beams were cast, and two were loaded at the time the deck was cast, approximately 220 days after casting of the girders.

The six 2 ft long beam sections were instrumented with strain gage lines, as shown in Fig. 3.10, for the 10 inch gage length Whittemore gage.

Approximately fifty 6 by 12 in. cylinders of deck concrete were made. In addition, six concrete prisms, each 7 by 14 by 28 in., were cast for use as shrinkage specimens. All deck specimens were cast from a single load of ready-mix concrete which was used near the middle of the center span of the bridge.

The 16 cylinders used for strain measurements (ten for shrinkage and six for creep measurements) were prepared for gage points in the same manner as that used on beam specimens. It was discovered immediately after stripping the forms that the concrete had settled from beneath many of the gage points, allowing them to move by as much as 0.003 in. A new set of shrinkage and creep specimens were therefore prepared with other cylinders of the same batch using the method of drilling and fixing bolts with epoxy.

Even though this problem did not appear in the beam concrete specimens, their gage points were then locked in place with epoxy as a preventive measure.

The prismatic shrinkage specimens of deck concrete were cast in wooden forms, and strain-gage lines were installed as shown in Fig. 3.11, after the concrete had hardened. The strain gage points were installed by drilling 1/4 in. holes with a masonry bit and then grouting 1/4 in. stainless steel

cap-screws into the holes with the quick-setting epoxy. After the epoxy had hardened, the tapered holes were drilled in the heads of the cap-screws.

Cylinders of deck concrete were tested at the intervals indicated in Table 2.4. Shrinkage measurements were made on five cylinders stored at the bridge site and five stored in the laboratory. Two creep racks were loaded 28 days after the deck was cast, with a set of specimens stored under each storage condition. Half of the prismatic specimens were left at the bridge site and half were taken to the laboratory.

4. RESULTS OF OBSERVATION ON BRIDGE STRUCTURE

4.1 General Remarks

The results of the first two years of observations on the bridge structure are presented in this chapter and will be discussed in Chapter 6. The measured deflections are presented in Sec. 4.2, and the measured strains are presented in Sec. 4.3 along with a discussion about the probable correctness of some of the observations. The strand force measurements, both as measured directly while beams BX-3 and BX-4 were being fabricated and as changes derived from the strain measurements, are presented in Sec. 4.4.

The observed end zone cracks are described in Sec. 4.5.

4.2 Measured Camber

The measured camber-time curves for the two beams, BX-3 and BX-4, are shown in Fig. 4.1.

Both curves show an initial camber of nearly one in. which occurred when the prestressing strands were cut. This initial camber was then followed by a rapid growth of camber with time. After about a month, the camber in the beams changed at a much slower rate than previously.

The girders were moved from inside to outside the prestressing plant at the age of three days. The approximate dates of movements are indicated in Table 2.2. With each move, the positions of the wooden blocks supporting the beams were changed, and the various positions are shown schematically in Fig. 2.12. The two girders were moved to the bridge site from the plant when they were about 155 days old. The combination of the transportation and the changes in span length resulted in some increase in camber when readings were taken after the move.

The camber remained approximately constant from the time the girders were placed on the piers until the deck construction was started. The weight of the formwork and deck reinforcement caused a deflection of 0.08 in., and the casting of the concrete deck caused an additional deflection of 0.40 in. in both beams, for a total deflection of 0.48 in. from the weight of the deck. There have been only small variations in the camber since the deck was cast.

4.3 Measured Strains in Concrete

4.3.1 Mid-Span Strains

The longitudinal strains measured at mid-span in BX-3 and BX-4 are plotted versus time in Figs. 4.2 and 4.3 respectively. The strain near the top of the girders, near the bottom, and at the centroid of the section, as determined with the Whittemore gage, are shown.

The girders were stored inside the plant for only three days after casting after which they were moved to outdoor storage where the temperature was initially about 0° F. The low temperatures quickly froze the free water in the girders, and continued low temperatures kept it frozen for several weeks. Because of this, the compressive strains increased at a slower rate than in previous tests (1).

The strain readings were corrected for temperature variations, and the temperature-induced movements are not included in the reported strains.

In general, all of the strains increased until the time the deck was cast at 218 days. Cold winter weather caused decrease in strains after 290 days until a minimum was reached at 411 days. A complete yearly cycle of increase and then decrease in strains is clearly shown between 411 and 782 days. The strain changes at the three levels in the girders have been nearly

equal, indicating that the girders are changing length, but that there are no appreciable changes in curvature. Similar strain changes occur at the quarter points as shown in Figs. 4.11 and 4.12.

All three strain-time traces for each beam show decreases in compressive strain during the winter months. These reversals are due to increased average relative humidity during the winter, and it was found that the same reversals also occurred in both the creep and shrinkage specimens stored in the field, as will be discussed in Chapter 5.

The mid-span strain distributions over the depth of the girders are plotted in Figs. 4.4 and 4.5 for a few selected time intervals. The strain distributions are approximately linear. Since the sections are at mid-span of long girders, this must support the general consistency of the strain readings rather than being viewed as a confirmation of the linear strain distribution.

The inclination of the strain distribution from the vertical axis is the curvature, and it can be seen that although the distributions indicate continued increases in strain, the changes in curvature have been small when compared with the curvature occurring within the first two weeks of the life of the girder.

The longitudinal strains were also measured by means of Carlson meters placed near the upper and lower surfaces of the girders. The measured strains are plotted against time in Figs. 4.6 and 4.7. Simple comparisons with the mechanically-measured strains plotted in Figs. 4.2 and 4.3 show that there was no consistent correlation between the strains measured with the Carlson meters and those indicated by the Whittemore gage readings.

The plots of strain versus time obtained from both the mechanical and Carlson strain gages appear to be relatively smooth curves and all of the

data points from either type gage are consistent with each other. There is no reasonable basis for determining whether either is correct simply from the strain data.

In order to help determine which of the two gages was giving the correct strain readings, the strains were reduced to curvatures and the curvatures were plotted against mid-span camber in Figs. 4.8 and 4.9. It can be seen that all of the points from the Carlson meter fall relatively close to a straight line, and all of the points from the Whittemore gage fall close to a second straight line. The theoretical relationship between mid-span curvature and deflection is also plotted in the figures, and it can be seen that the curvature values from the Whittemore gage are very close to the theoretically correct values. The line shown is the relationship for the condition of the beam being supported on a 70 ft span as was the case for most of the early life of the beams.

From this it was concluded that the mechanical strain gage readings were correct, and that the readings from the Carlson meters were in all cases too high.

The difficulties with the Carlson meters stemmed from the fact that a modified version of the meter was used in order to increase the available strain range. To illustrate, the profile of a standard gage, which has a 10 in. gage length, and of the modified gage, with a 7.75 in. gage length, are shown in Fig. 4.10. The gage length was shortened by moving the flange at one end of the gage 2.25 in. from its original position. The remainder of the gage body which projected beyond the flange was tapered slightly and then covered with a knitted cotton sleeve in order to break the bond. This measure was not sufficient, however, because the "nose" of the gage was bearing

on the concrete and the effective gage length was longer than the 7.75 in. between the flanges.

Using the strain data from a previously reported auxiliary test of a Carlson meter (1), the effective gage length required to obtain the same results as were obtained from the Whittemore gage is 9.20 in., which is closer to the overall length of the gage than to the distance between the flanges.

All quantitative discussions in this report are based on the strains obtained by use of the mechanical strain gages.

4.3.2. Quarter-Point Strains

The time-strain curves for strain gage lines located at the quarter-points of girders are given in Figs. 4.11 and 4.12, respectively. Strain distributions over the depth of the girders for selected time intervals are plotted in Figs. 4.13 and 4.14.

The strains were approximately the same as at the mid-span section, and exhibited the same general trends. The final curvatures at the quarter-points were approximately the same as those at mid-span of the same beam.

There were significant differences in strains in beam BX-3 and BX-4, but the strain readings consistently followed the same trends within each beam.

4.3.3 Strains Near End of Beam

Time-strain curves are given for Carlson meters, Figs. 4.15 and 4.16, to illustrate that the general form of the curves was similar to those at other sections of the span.

Strains were measured on a relatively large number of Whittemore gage lines located near the south ends of the girders, and the data from the reading are summarized in Figs. 4.17 to 4.26.

Strain distributions over the depth of BX-3 at five sections located near the end of the girder are shown in Figs. 4.17 to 4.21. The indicated distances from the end of the beam are the distances to the centers of the 10 in. gage length considered.

There is a definite distortion of the cross-section, especially very near the end of the beam. This should be expected, however, since the prestressing forces are anchored only near the top and bottom of the section and are not uniformly distributed over the section depth. The strains at the section located 47.5 in. from the end of the beam are much nearer to a linear distribution than are those 7.5 or 17.5 in. from the end of the section, as would be expected.

The very low strains indicated at gage line S61, Fig. 4.17, were undoubtedly greatly influenced by cracking which occurred in the anchorage zone. A crack crossed the end of the beam at the junction of the web and lower flange, less than an inch below the gage points nearest the end of the beam.

There were very large increases in strain at the lowest gage line, with the strains at line S84, for example, increasing from about 510×10^{-6} at release to about $1{,}410 \times 10^{-6}$ at 575 days. These strains were the largest measured in the test structure.

The changes in strain along the length of the member near the ends are of interest since this gives an indication of the distance required to develop the prestressing force, by bond, after the strands have been cut. The strains occurring at release at six different levels in the beams are plotted versus distance from the end of the beams in Figs. 4.22 and 4.23. The transfer length was evidently 20 in. or slightly less. The strand was slightly rusty when used, which accounts for the slightly lower transfer length than reported by other investigators (4,5), but comparable to that found in the Jefferson Co. test structure (1).

The strain distributions along line S8X at various times are plotted versus distance from the end of the beams in Figs. 4.24 and 4.25. While there were marked increases in strain, there was no change in shape of the distribution. This leads to the conclusion that the transfer length could not have changed appreciably with time and that the bond strength did not decay significantly with time.

Vertical strain measurements were made on two sets of gage lines 2.5 in. from the south ends of the beams, Lines S31 measured strains just above the beam centroid, and Lines S51 measured strains just below the beam centroid. These gage lines were accessible for only 182 days after which they were covered by formwork.

Fig. 4.26 shows that both sets of lines have tensile strains which decay with time after 12 days. Line S51 in each beam had one anchorage crack with width of about 0.004 in. crossing it, and shows maximum measured strain of $+500 \times 10^{-6}$ for BX3 and $+700 \times 10^{-6}$ for BX4. No visible anchorage cracks crossed lines S31, and maximum apparent strains are 150×10^{-6} for BX3 and 250×10^{-6} for BX4. The 0.004 in. crack in the 10 in. gage length can account for the differences of about 400×10^{-6} in apparent strain between lines S31 and S51 for each beam.

4.4 Strand Forces

Forces in 12 of the 38 strands were measured during the construction of the girders as was described earlier. The results of these measurements are tabulated in Table 4.1, and may be summarized as follows.

The design prestressing force was 18.9 kips per strand, so the total force was to be 718.2 kips. The forces achieved in each of the 12 strands immediately after that strand had been anchored are listed. The average

force in the straight strands was 18.58 kips while the average force in the draped strands was appreciably lower at 17.66 kips. Slip in the strand grips was responsible for part of the lower-than-desired force, but this loss should not have been large since a 1/4 in. slip in a 210 ft strand causes a change in force of about 0.3 kips.

The draped strands were tensioned in the draped position and apparently considerable force was lost in friction as the strands went through the seven sets of guide rollers required for two beams.

The force measurements taken immediately after all of the strands were stressed, indicated that the remaining prestressing force was about 687 kips, 31 kips lower than the desired value. Part of this deficiency was caused by deflection of the prestressing abutments as successive strands were stressed, part by slip at anchorage, and part by not having enough force in the draped strands to start with.

Immediately after the last strand was tensioned, it was found that the forces at the two ends of the top draped strand differed by 8 1/2 per cent.

A set of prestress readings taken during the steaming indicates a decrease in strand force of about two kips for every strand. About half of the decrease can be attributed to temperature changes caused by the steam curing. Air temperature and strand temperatures were about 50°F at the time of stressing, and reached over 100°F during the steaming cycle. A 50°F temperature increase causes a reduction in strand force of about one kip. There is no apparent explanation for a reduction of two kips. By the time the strands were cut, about 67 hours after the strands were stressed, the total prestressing force had increased from 687 kips to about 695 kips.

This strand force change can probably be attributed to temperature decrease between the times of the two readings. The changes, however, are not entirely consistent since the straight strands show a minor increase while the draped strands show a minor decrease.

The changes in strand force after the release of the prestressing were obtained from the measured strain data. The concrete strain at the level of the centroid of the steel was assumed to be the same as the change in strain of the reinforcement. The stress change was determined by using the average value of Young's Modulus of 28,200 ksi. The estimated total force remaining in the strand is plotted against time for both beams in Figs. 4.27 and 4.28, respectively, and it can be seen that the force remaining after two years is slightly higher than the residual force assumed when the member was designed. The assumed loss was 24.4 per cent of the initial force, and the measured loss was about 24 per cent.

The time-dependent losses in prestressing force after release do not include relaxation in the strand, and there is no direct way of evaluating this loss in a structure with bonded prestressed reinforcement. However, the relaxation losses after release would not be expected to be very large since the yield stress for the strand was very high relative to the applied stress level.

4.5 Cracking

Both test beams developed anchorage cracks in both ends when the prestressing force was released. Altogether, 18 beams for the test bridge were examined, and anchorage zone cracks were found in 35 of the 36 ends. All of the cracks were "spalling" cracks, and no "bursting" cracks were found in any beam.

The most common crack position was in the web, about 6 in. above its junction with the flange. A crack at the web-flange junction was also very common. Similar behavior was also noted in a previous study on similar beams (1).

The measurable cracks in the test beams ranged from 0.003 to 0.007 in. in width, and extended no more than 9 1/2 in. from the end of the beam. Their widths did not change during the interval from six weeks to 5 1/2 months after release of prestress.

5. CREEP AND SHRINKAGE

5.1 Introduction

The data obtained from the creep and shrinkage measurements on the various test specimens are presented in this chapter. Creep and shrinkage strains were measured in 6 by 12 in. cylindrical specimens, and shrinkage strains were also measured in short sections of full-sized girders and in prisms representing the deck, as explained in Sec. 3.7.

The storage conditions of the specimens are described in Sec. 5.2. The ages of the concrete at the time of the initial readings and at the times of loading of the creep specimens also are given.

The shrinkage and creep data are presented in Sec. 5.3.

5.2 Storage Conditions and Times of Loading

The dates of casting of the various test specimens, the dates and ages at initial shrinkage readings, and the dates and ages when the various creep specimens were loaded are tabulated in Table 5.1.

The beam concrete specimens were initially inside the prestressing plant at Rochelle. On 4 January 1969 the laboratory specimens, including cylinders for strength determinations, creep tests, and shrinkage measurements, and the 2 ft long beam specimens, were moved to Urbana where they were placed in a humidity controlled room in the Civil Engineering Building. The humidity control room is intended to maintain a 70°F and 50 per cent relative humidity environment, but some rather large divergences have occurred, especially during early summer of 1970 when the air conditioning was inoperative for two months. The humidity was lower than desired during the early months of 1969 due to other equipment problems.

The field specimens remained with the beams in the storage yard at Rochelle until 28 May 1969. The specimens were relocated on 29 May 1969 to near the test bridge at Tuscola, where they rested on wooden blocking. The two test beams arrived at the bridge site on 3 June 1969. The test specimens were moved to their final location on wooden steps under the south end span of the bridge on 11 July 1969.

The specimens of deck concrete were cast on 5 August 1969. Eight cylinders used for creep and shrinkage measurements, and three 7 by 14 x 28 in. prisms used for shrinkage measurements were made for laboratory storage. An equal number were made for the field.

The laboratory specimens were stored in the Civil Engineering Building along with the laboratory specimens of beam concrete.

The specimens stored at the bridge site are subjected to highly variable environment. The yearly temperature range is from about $-10^{o}F$ to about $100^{o}F$ with relative humidity range of about 30 to 100 per cent. A typical recorder chart is shown in Fig. 3.8. Weekly ranges and averages of temperature and relative humidity are shown in Figs. 5.1 and 5.2, respectively.

The maximum and minimum temperature and relative humidity for each week were read off of the chart by inspection. Approximate average temperature and relative humidity values were determined by averaging the high and low readings of the individual cyclic variations over the whole chart.

It should be noted that the temperature range for the recorder is only from $0^{o}F$ to $100^{o}F$, and temperatures outside this range occurred, but the extreme values could not be determined. The relative humidity sensing element is known to be unreliable at relative humidity values in excess of about 80 per cent, and the off-scale readings must be interpreted as indicating very high humidity.

5.3 Creep and Shrinkage Strains

The creep and shrinkage data from all the cylindrical test specimens are given in Figs. 5.3 to 5.8. Figs. 5.3 and 5.4 contain total strain information for creep cylinders located in the field and the lab, respectively. These curves represent total strain from the time of loading, including elastic strain due to the application of load. No attempt was made in these figures to separate the creep and shrinkage strains.

Shrinkage and creep values for field and laboratory stored beam concrete are given in Figs. 5.5 and 5.6. Each figure contains a shrinkage-time curve and two creep-time curves for specimens loaded to 1,000 psi compressive stress, one at the time of release of prestressing and the other soon after the deck was cast. The values of creep are the resultant of subtracting the elastic and shrinkage strains from each total strain reading.

Shrinkage-time curves and creep-time curves for the deck concrete specimens stored in the field and in the lab are shown in Figs. 5.7 and 5.8, respectively. In these graphs, shrinkage strains measured in both the cylindrical and prismatic test specimens are plotted.

There are two aspects of the measured strains from the field-stored specimens, Figs. 5.3, 5.5, and 5.7, which are quite different from the behavior ordinarily observed under laboratory conditions. First, there are appreciable annual variations in strain which can be attributed to seasonal climatic changes. These changes, which are expansions in the fall and winter and contractions in the spring and summer, occur in both creep and shrinkage specimens. Second, the "final" shrinkage strains for the field-stored specimens are quite small, especially when compared with the laboratory specimens of the same concrete.

The "final" shrinkage strain for the field-stored beam concrete cylinders is almost zero, as can be seen in Fig. 5.5, and the corresponding value for the deck concrete is 50 x 10^{-6} expansion. These represent mid-winter readings when the shrinkage is a minimum. The shrinkage strain for the laboratory-stored beam concrete was about 650 x 10^{-6}, and that of the deck concrete about 300 x 10^{-6}. While comparisons between the shrinkage values for the two storage conditions must be made very carefully, and the conditions that are being compared must be explicitly defined, it is clear that the shrinkage strains in the field-stored specimens were considerably less than one-third those in similar specimens stored in the laboratory.

These small values of shrinkage imply high values of average relative humidity in the field, and on the basis of a report by ACI Committee 435 (7) the shrinkage may be estimated as

$$\epsilon_{sh} = 12.5 \times 10^{-6} (90 - H) \qquad (5.1)$$

where H = average relative humidity in per cent.

If the measured "final" shrinkage is about 125 x 10^{-6}, the implied relative humidity is 80 per cent. Such a value of relative humidity is not inconsistent with records which were obtained from the temperature and humidity recorder located with the field specimens at the test bridge and reported in Fig. 5.2.

Fig. 5.2 clearly shows that the average relative humidity during the winter months is above 90 per cent, which would explain the zero, or slightly expansive, strains found in the last set of readings.

The shrinkage of the prismatic specimens of deck concrete was usually smaller than that of the cylinders. In the laboratory, the shrinkage rate of the prisms was slower than for the cylinders and the final shrinkage value was only three-fourths as large (Fig. 5.8).

The horizontal strain distributions for the 2 ft beam specimens are shown in Figs. 5.9 and 5.10 for various times. All the strain distributions are fairly linear over the depth of the beam, which indicates that bond of the prestressing strands was successfully prevented and the specimens are free from horizontal stress. This conclusion is substantiated by Fig. 5.11, which shows that the horizontal and vertical strain averages are almost identical in an example specimen. All six 2 ft beams showed the same behavior pattern.

Even though there appears to be no prestressing force in the 2 ft beams and the strain distributions are linear, the shrinkage in all the laboratory specimens is larger near the top than at the bottom. The field specimens show a more constant strain distribution over the depth of the beams. The anomaly seems to be caused by the relatively rapid drying out of the top sections of the young laboratory specimens. Moisture was able to flow out of the exposed upper sections of the laboratory beams more quickly than from the more massive lower sections. Even though the specimens were set on blocks, the air circulation near the floor is relatively poor and this may be an additional factor in the lower strains near the bottoms of the specimens.

In contrast, shrinkage in the field stored beams was more uniform. Initially it was much slower, because the environment was very cold and humid for several weeks. The field beams did not begin rapid shrinkage until consistently warm weather arrived after about 100 days.

Average horizontal strains for the three laboratory beams are compared to the average horizontal strains for the three field beams in Fig. 5.12. The lab curve shows rapid initial shrinkage rate which slows down with time, as is expected from theory. The field curve, however, shows a very strong

seasonal variation with strong shrinkage in the summer months and expansion in the winter months.

Comparison of the laboratory curve in Fig. 5.12 with the curve for laboratory shrinkage cylinders in Fig. 5.6 indicates that the 2 ft beam shrinkage occurred at a slower rate, but has now reached almost the same magnitude as the cylinder shrinkage. Comparison of the field curve in Fig. 5.5 shows that the seasonal variations are very similar in shape and magnitude, but the total strains are different because the cylinders had an initial expansive strain of 200×10^{-6}.

Comparison of Figs. 5.3 and 5.4 indicates that the total strain of beam creep cylinders in the field is only about 3/4 of the total strain for the companion cylinders in the lab. The corrected creep strains for field and lab cylinders are compared in Figs. 5.13 and 5.14.

The beam cylinders loaded at the time of release of prestress show almost identical creep strain values in the field and in the lab. The creep values for the beam concrete cylinders loaded at the time the deck was cast are considerably lower than their companion specimens loaded when the prestress was released. This is consistent with the results of other investigations (18), which have shown a strong trend of reducing creep strain with increasing age of concrete when loaded.

While the creep strains of lab and field specimens loaded when the concrete was very young were nearly identical, there are substantial differences between strains in specimens loaded at 220 days. The strains were comparable for about 50 days after loading but after that time the creep strain in the field specimens decreased significantly and has remained lower than in the laboratory specimens. There is no apparent explanation for such a change in behavior, nor do the weather records (Figs. 5.1 and 5.2) provide a suitable explanation.

A comparison of the total strain curve for the first field stored creep rack (Fig. 5.3) with the measured strains at the centroids of BX3 and BX4 (Figs. 4.2 and 4.3, respectively) shows that all three curves are remarkably similar in shape and in magnitude. The final compressive strains shown in all three curves are between 1.1×10^{-3} and 1.2×10^{-3}. This behavior is as expected since the beams themselves represent very large creep tests, though not at constant stress. The average stress in the beams was about 1,100 psi immediately after release of prestress and decreased to about 950 psi after two years.

The stresses at the centroids of the beams soon after release were about 10 per cent higher than in the creep specimens. The creep specimens were subjected to constant stress while the girder stress decayed with time, and this helps to explain why the strains in the creep specimens soon exceeded those in the girders. A second cause of the difference may be found in the effects of specimen size. The Volume/Surface ratio, V/S, for the beams was nearly 4 in., while it was 1.5 in. for the 6 by 12 in. cylinders. While it is not clear that the numerical V/S effects found by Hansen and Mattock (19) are valid for non-constant environments, the trend of decreasing creep with increasing member size is shown by these strain measurements.

There is a generally accepted principle that a specimen stored in a high-humidity environment will undergo less creep than a similar specimen stored in a much dryer environment. In this case there is ample evidence, from the shrinkage strains if from no other source, that the field environment, on the average, is much wetter than the laboratory environment. Under such conditions all design guides, such as Ref 7, would lead one to expect creep strains in the laboratory to be up to twice those in the field. It is important to remember that the creep data which was used in deriving the

relationships given in Ref 7 were from tests at constant environmental conditions. However, there is a growing body of data (1, 8, 9) which indicates that while the average humidity is important in determining the final value of shrinkage, any movement of moisture into or out of a specimen increases the creep strain.

Since a highway bridge structure is completely open to every change in the weather, on both daily and annual cycles, it is probably never in moisture equilibrium with the surrounding air. This will lead to larger values of creep strain than were anticipated by the designer, and it would appear that major changes in the methods used to estimate the long-term strains in a bridge structure are necessary.

The creep strains in the cylinders loaded at the time of release of prestress are nearly identical for any given time, regardless of whether the specimens were stored in the laboratory or in the field (Figs. 5.5 and 5.6).

The strains in the beam creep specimens which were loaded at 220 days were also nearly identical for the first 60 days after loading. After that time the strains in the field-stored cylinders decreased significantly, and the final creep strains in the field-stored specimens were about 2/3 those in the laboratory. Similar trends may be noted in the deck concrete creep strains (Figs. 5.7 and 5.8), and in both cases the decrease in strains occurred about the time of the first wintry weather. The temperature records show this decrease corresponding reasonably well with the cooling of the weather in the fall season.

The field specimens loaded at release also show a recovery of creep strains in the fall, but the recovery of 50×10^{-6} strain out of 650×10^{-6} does not represent a very noticeable change in the trend of the curve. The recovery

in the specimens loaded at 220 days was about 70×10^{-6} out of 200×10^{-6}, which is a relatively much more visible change. The recoveries of 50 and 70×10^{-6} must be viewed as essentially identical since the sensitivity of the mechanical strain gage used is about 10×10^{-6}.

The recovery appears to have been caused by the seasonal environmental changes, but a mechanism to explain such a large recovery of creep strain has not been found.

6. DISCUSSION OF RESULTS OF OBSERVATIONS

6.1 Introduction

Various aspects of the observed behavior of the test structures are discussed in this chapter, with comparisons of observed, design, and theoretical values being made in the following sections. The changes in camber and deflections are discussed in Sec. 6.2, and the loss of prestress with time in Sec. 6.3. The strains measured in the girders are discussed in Sec. 6.4, and the cracking observed is discussed briefly in Sec. 6.5. The calculated strength of the test structure is discussed in Sec. 6.6.

6.2 Camber and Deflection

The observed changes in camber in the beams are plotted against time in Fig. 4.1. The initial camber values accompanying release of prestress are 0.97 and 0.89 in. for beams BX-3 and BX-4, respectively. The calculated value of initial camber was 1.04 in., using Young's Modulus of 3.4×10^6 psi for the concrete at the time of release and using the 65 ft span between the temporary supports.

After release of the prestress, the camber in the two beams increased at the same rates to respective values of 1.73 and 1.62 in. at 193 days when formwork for the deck was begun.

The construction of the deck formwork and placement of the deck reinforcement caused a deflection of about 0.08 in., and the weight of the deck concrete caused a deflection of about 0.40 in., for a total deflection of 0.48 in. in each beam due to the weight of the deck.

The camber allowance for dead load indicated on the bridge plans was 5/8 in., while the computed deflection, using the measured value of Young's Modulus of 4.7×10^6 psi (Table 2.3) at 219 days, was 0.505 in. The computed

and measured values are in good agreement, but both are lower than the design value.

The design value apparently was larger than the computed value because of at least two factors. First, the Young's Modulus for the concrete was assumed as 4.3×10^6 psi, corresponding to f'_c = 5,000 psi, instead of the measured 4.7×10^6 psi. Second, the full beam length of 72 ft 9 in. was apparently used instead of the span of 71 ft 8 in. center-to-center of bearings. The second factor may appear to be small, but it acquires importance since the computed deflection varies as the span to the fourth power. Finally, the calculated value may have been rounded to the nearest 1/8 in.

After the deck was cast, the changes in deflection were very small, as would be expected. Under the full dead load, the stress distribution in the girder at mid-span was approximately uniform over the depth of the girder and under such stress conditions the tendency to deflect either up or down is very small.

An unexpected facet of the long-term deflections is the small increase in camber which has continued to take place during the second year. After the deck was cast there were small movements corresponding to about the measuring precision, but after about 290 days the camber started to increase again.

Such an increase in camber is consistent with the movements expected to be caused by forces caused by differential shrinkage between girder and deck concrete. If the deck shrinkage exceeds the beam shrinkage, downward movements are induced in a simply supported beam. However, on the basis of an elastic analysis, the interior span of a structure containing three equal spans moves upward as a result of the continuity forces induced by the differential shrinkage. The upward movement is 0.2 times the downward movement in

a simply-supported span, so the small upward movements are consistent with the predicted values. Since the differential shrinkage values were small, only small movements would be expected, and these would be modified by the time-dependent effects in the concrete. Similar upward movement was observed in the structure described in Ref 1.

A general method of analysis of camber changes, such as is outlined in Ref 10, could be used. The amount of computation required is large and requires a computer solution similar to one of those described in Refs 10, 11, and 12, but with the additional capability of taking the changing span conditions and continuity into account. Such a program is being developed and will be described in a later report.

The approximate method of analysis of camber changes which is given in Ref 7 might be satisfactory for use in this case. It gives a net upward deflection of 0.94 in. at release, and 2.06 in. after 185 days. The agreement with observed camber is very good at release, but is about 20 per cent too high at 185 days.

The calculation leading to a predicted camber of 2.06 in. at 185 days was done using creep and shrinkage data from the 6 by 12 in. cylindrical specimens stored in the field. The initial value of Young's Modulus was 3.42×10^6 psi, the creep coefficient was 2.0, and the shrinkage strain was 40×10^{-6}.

The strains in the girder were probably less than those in the small test specimens (19) because of various size effects, and a reasonable estimate of this effect is that the creep and shrinkage strains in specimens the same size as the girders would be about 3/4 those in the cylinders.

Reducing the creep coefficient and shrinkage strains to 75 per cent of the values obtained from the 6 by 12 in. cylinders leads to a calculated camber of 1.91 in., which is somewhat closer to the measured values.

The calculations were done assuming the beam to be simply supported on a span of 71 ft 7 in. at all times. The method is not strictly applicable after the deck is cast because of the major changes in stress accompanying addition of the dead load of the deck.

Temperature gradients within beams can have a significant influence on the deflection measured at a particular time. The following calculation shows the effect of a $10^{\circ}F$ temperature gradient across the 48 in. depth of a 70 ft long beam:

$$\Delta\epsilon = \Delta T \times \alpha = 10^{\circ}F \times 6.5 \times 10^{-6} \text{ in/in/}^{\circ}F = 6.5 \times 10^{-5} \text{ in/in}$$

$$\Delta\varphi = \frac{\Delta\epsilon}{d} = \frac{6.5 \times 10^{-5} \text{ in/in}}{48 \text{ in.}} = 1.35 \times 10^{-6} \text{ in}^{-1}$$

$$\delta = \frac{\Delta\varphi \ell^2}{8} = \frac{(1.35 \times 10^{-6} \text{ in}^{-1})(70 \times 12)^2 \text{in}^2}{8} = 0.12 \text{ in.}$$

Temperature differentials in the beams were determined by comparing Carlson meter readings obtained from instruments in the top and bottom flanges at mid-span. Temperature gradients of $10^{\circ}F$, $8^{\circ}F$, and $9^{\circ}F$ were measured at 12, 32 and 103 days, respectively. In each case the top of the beam was warmer than the bottom, resulting in upward deflection.

The readings for these three days show higher camber (Fig. 4.1) than readings taken when a smaller temperature gradient was present. In all cases, both beams had very similar temperature gradients, differing by only one to two degrees, as is evident in Fig. 4.1 by the very parallel nature of the two camber time plots.

After the deck was finished, the deflection measurements were nearly always taken about the same time of the day, between 9:00 and 10:00 a.m., and this has probably minimized errors due to different temperature distributions. In addition, the completed structure is continuous over three spans and any tendency to deflect due to temperature differentials is largely counteracted by restraint forces.

6.3 Loss of Prestress

The initial value of the prestressing force was slightly lower than the design value, as was discussed in Sec. 4.4, and this in turn must lead to lower losses of prestress with time than would otherwise be expected. The design calculations were made on the basis of an assumed loss of prestress, including both elastic losses at release and long-term losses due to creep, shrinkage, and relaxation, of about 24 per cent of the force before release. There was no direct calculation in the design process of the stress conditions immediately after release of the prestressing, although the possible importance of tensile stresses at this stage was recognized in that minimum span limits were placed on each strand configuration used with the 48 in. deep beams.

The force immediately before release was 695 kips, or 168 ksi, as shown in Table 4.1. The calculated force at mid-span immediately after release was 634 kips including the effects of the dead load of the girder, and 622 kips ignoring the dead load. This calculation was made on the basis of $E_c = 3.4 \times 10^6$ psi, and assuming the beam to be supported on a 64 ft 3 in. span. The measured forces immediately after release were 642 kips in BX-3 and 633 kips in BX-4, which are nearly the same as the theoretical value.

The variation of the prestressing force with time in beams BX-3 and BX-4 is shown in Figs. 4.27 and 4.28, respectively. It can be seen that there were

large losses during the first six months of the life of the structure, and that there have been annual cycles of force variation since that time.

The prestressing force remaining in BX-3 after more than two years is about 556 kips, or 135 ksi, which is 12 kips above the design value. The corresponding prestressing force in BX-4 is 566 kips, or 137 ksi, which is 22 kips above the design value. These measured prestressing forces do not include any relaxation losses that have occurred.

However, it is not believed that stress-relaxation was significant in this structure, as is discussed in the following paragraph, so the force values shown in Figs. 4.27 and 4.28 are essentially correct.

According to the analysis of stress relaxation reported in Ref 6, the stress at any time t can be predicted on the basis of the following equation for strand at constant strain:

$$f_s = f_{si}\left[1 - \frac{\log t}{10}\left(\frac{f_{si}}{f_y} - 0.55\right)\right]$$

where f_{si} = initial stress

t = time in hours

f_y = yield stress at 0.001 offset strain

f_s = stress at time t.

For the steel used, f_y = 247 ksi and f_{si}, taken as the stress just after release, was 152 ksi in BX-4. For a time of 100 days, the stress is calculated as $f_s = 152\left[1 - \frac{3.38}{10}\left(\frac{152}{247} - 0.55\right)\right] = 149$ ksi, giving a very small loss. In the bridge girders, the stresses were also reduced because of creep and shrinkage, and the stress relaxation losses would be expected to be reduced below those calculated.

It is generally not possible to make a completely reasonable estimate of the losses on any theoretical basis because of the lack of reliable creep data for the concrete in a specific structure under field conditions. However, there are relatively standard methods of estimating the losses which are used in design. The 1954 Bureau of Public Roads Criteria for Prestressed Concrete Bridges (13) contained the following equation for loss of prestress:

$$\text{Loss (in psi)} = 6{,}000 + 16\, f_{cgs} + 0.04\, f'_{si}$$

where f_{cgs} = compressive stress in concrete at center of gravity of prestressed reinforcement due to the dead load moment and the prestressing force before release, and

f'_{si} = initial stress in prestressed reinforcement (before release).

The 6,000 psi loss corresponds to a shrinkage strain of about 0.0002, the second term is the elastic shortening plus creep loss of about the same magnitude as the elastic shortening at release, and the third term is stress relaxation of the reinforcement.

Application of this equation to the experimental bridge structure gives a calculated loss of 43.9 ksi, or 181 kips, which is considerably higher than the average measured loss of 134 kips for the two beams. However, the computed loss includes about 6.7 ksi due to relaxation, and if this is ignored as was stated in Sec. 4.4, the computed loss becomes 150.7 kips, about 12 per cent larger than the measured loss. In any event, the equation predicts a loss which is somewhat too large.

The 1969 AASHO Specifications (14) state simply that the loss in prestress from all sources in a pretensioned member shall be taken as 35 ksi unless better information is available. Although this is commonly used as the time-dependent loss after release of prestress, the original source of this value, ACI-ASCE

Joint Committee 323 (15), makes it quite clear that this loss includes the elastic loss accompanying release of the prestressing force.

Since the measured loss of prestress from before release to 782 days averaged 134 kips, or 32.4 ksi, for the two beams, the agreement between the current nominal AASHO design value and the measured value is quite acceptable.

Both of the above methods of obtaining design values have a common drawback, although it must be noted that both are to be used only if nothing better is available. The problem is that the loss value suggested is in no way tied to the environmental conditions, and while the values are not unreasonable for conditions in the central portions of the United States, they are likely to substantially underestimate the losses occurring in a very dry region, such as the desert regions of the southwest. A dry environment leads to higher shrinkage and creep values than were anticipated in the derivation of the design recommendations, and blind application of these values could lead to much greater losses than anticipated. This will not affect the strength of the structures to any appreciable amount, but will reduce the cracking load and may cause deflection problems. On the other hand, an overestimation of the prestressing losses may lead to excessive camber and the attendant problems.

The 1970 AASHO Interim Specifications for Highway Bridges (20) makes an attempt to include some effects of environmental conditions. It divides the loss of prestress into four factors:

$$\Delta f_s = SH + ES + CR_c + CR_s$$

where

Δf_s = total prestress loss

SH = concrete shrinkage loss based on average ambient relative humidity

ES = elastic shortening loss = 7 f_{cr}

where f_{cr} = concrete stress at the level of prestressing steel at the time of release. We have assumed f_{cr} to be the stress after elastic losses accompanying release.

CR_c = loss due to concrete creep = 16 f_{cd}

where f_{cd} = average compressive stress in concrete at the level of prestressing steel under full dead load.

CR_s = loss due to relaxation of prestressing steel = 20 ksi - $0.125(SH + ES + CR_c)$.

When this formula is applied to the test beams using a 71 ft 7 in. effective span, the following prestress loss is predicted:

$$\Delta f_s = 4.0 + 12.0 + 18.65 + 15.67 = 50.32 \text{ ksi}$$

This value is far larger the maximum measured losses which average 35.2 ksi after 600 days. Neglecting steel relaxation gives a predicted loss of 34.65 ksi which is very close to the measured value, which also neglects relaxation.

This last value does not, however, represent the true conditions present in the beam. The deck was not cast on the beams until they were about 220 days old. Prior to that time, the dead load was less than half that used in the above calculation, and the actual losses should be somewhat larger than those calculated using the full dead load of the beam plus deck. If only the beam dead load is used in the calculation, the predicted loss of prestress is 57.95 ksi, or 43.4 ksi if relaxation is neglected.

While use of the 1970 AASHO provisions for calculating loss of prestress gave a reasonable result (neglecting relaxation), the inclusion of the full dead load is clearly unreasonable since it simply was not present during the

most critical time of the life of the member. The more reasonable assumption of including only the girder dead load results in a calculated loss of prestress about 23 per cent greater than measured maximum loss.

The report of ACI Committee 435 (7) was concerned primarily with the prediction of long-term camber changes, but almost all the information needed for estimating the loss of prestress is developed while finding camber. Using the approximate method developed in the reference, the predicted loss at 185 days was 38.6 ksi neglecting relaxation, while the measured average loss was 34.0 ksi. As it has turned out, the losses at 185 days were about the maximum observed (Figs. 4.27 and 4.28), so the estimated loss is in good agreement with the measured value and is also a good estimate of the final loss value.

6.4 Measured Strain in the Beams

The results of the strain measurements, which were presented in Sec. 4.3, are useful in defining the behavior of the bridge structure in a number of ways. The strain measurements were used in obtaining the prestressing loss data which were discussed in the preceding section.

The strain-time curves plotted in Figs. 4.2, 4.3, 4.11, and 4.12 show that there were very large increases in strain with time until the deck was cast, and that the general trend thereafter is for the strain to increase at a low but continual rate, with a large seasonal cyclic variation superimposed on the trend. The strain-time curves for the top, centroid, and bottom gage lines have been similar for both beams. This indicates that the beams are straining axially, but are maintaining a constant camber. This interpretation agrees with the direct camber measurements shown in Fig. 4.1, where it is obvious that there has been almost no camber change since the deck was cast at 218 days.

Measurements on 1/8 scale models of this bridge in the laboratory also showed no camber changes in the center span after the deck was cast. They did, however, have rather large camber changes in the end spans.

The end spans provide very effective restraint against movement of the center span, but are relatively free to move since they each have one free end. No camber measurements were made on the end spans of this test bridge, and so comparison with the laboratory observation of end span deflections was not possible.

The annual cyclical strain variations are very pronounced in both the beams and the test specimens.

Even though the shrinkage and creep specimens were stored under the end span of the bridge, the exposure conditions for the girders and for the specimens were not quite the same. The girders in which the strains were measured are the center girders in a six-girder bridge and consequently are never rained on directly. The test specimens can be wetted by rain whenever a NW or NE wind accompanies the rain, and measurements have been made when the specimens were dripping wet, but the bridge girders were dry to touch. On at least one occasion, the girder surfaces were wet as a result of condensation on the cold concrete during a short period of warm, foggy weather.

The shortening of the bottom fiber of a beam is of interest since this movement should be taken into account when designing the bearing devices. The final average value of compressive strain at the bottom of the beam is about 0.00115, as can be seen by examination of the various strain-time curves and strain distributions, and this corresponds to a beam shortening of slightly over one inch. About half of this strain occurred at release, which leaves about one-half inch of movement to be taken care of by the bearing devices in addition to the movements caused by temperature variations, if the beam is placed on its final bearing devices soon after the release of the prestressing.

In this bridge this was no problem since the girders were about six months old when they were moved to the bridge site, and by that time almost all of the time-dependent shortening had already taken place.

The most difficult factor in making meaningful strain measurements in a field investigation is providing adequate temperature compensation for the mechanical strain gages. The procedure followed, as explained in Sec. 3.3.2, was to use a steel bar which was placed on the concrete, but not in the sunshine, and allowed to reach temperature equilibrium before readings were made. The standard bar temperature always stabilized closer to the air temperature than to the concrete temperature. If the readings are taken early enough in the day, and before noon may be early enough, the readings seem to be consistent. However, on the day the deck was cast readings were taken quite early in the day and again in late afternoon. That the temperature compensation was not able to properly handle the change in temperature is evident in that a strain change was measured at the centroid of the section during the day the deck was cast, as can be seen in Figs. 4.2, 4.3, 4.11, and 4.12.

A second problem with temperature compensation is that steel has a coefficient of thermal expansion that is 1 to 1.5 x 10^{-6} in./in./F^{o} larger than that of the concrete. Such a difference is hardly significant if the temperature range is $10^{o}F$, but readings over a temperature range of about $80^{o}F$ (beam temperatures from 91^{o} to $8^{o}F$) were made, with the initial zero readings taken at the high end of the temperature range.

The use of the steel standard bar over-compensates for the temperature movements, and when the strain is compressive, a temperature decrease results in an indicated strain that is too low. For a temperature reduction of $50^{o}F$ and a differential in coefficients of expansion of 1.5 x 10^{-6}, the strain

will be 0.000,075 too low. This could be cited to explain the reductions in strain observed during the first two winters, but evidence reported in Ref 1 indicates that it is not valid since no strain reductions were recorded in a similar situation after the first two winters.

The error introduced by the temperature compensation problem is not as serious as might be implied from the last paragraph. The most important reason for this is that only two sets of readings were made in which the beam concrete temperature was below 20°F. Most of the wintertime readings were made when the concrete temperatures were 30°F or higher, and most of the summer readings were made at temperatures below 85°F.

The principle lesson to be learned from the discussion is that the temperature effects must be carefully considered, and that information needed for adequate compensation includes the temperature of the concrete, of the standard bar, and of the surrounding air.

An error in temperature compensation does not lead to an error in curvatures calculated from the strains. All strains are affected by the same numerical quantity, and the differences which are used in determining curvatures are not changed from their correct values.

Deck concrete temperatures were as much as 10°F higher than the beam temperatures during the summer, but no strain readings were taken on the deck, and so compensation was not a problem.

6.5 Anchorage Zone Cracking

The anchorage zone cracking found in the girders was described and discussed in Sec. 4.5. Since the possibility of this cracking had been taken into account during the design process, sufficient vertical reinforcement was provided at the ends of the girders to limit the cracks to acceptable

widths. This reinforcement apparently was proportioned on the basis of a report by Gergely, et al. (16), and three short double-legged stirrups of #5 reinforcing bar were provided near the end of each beam as can be seen in Fig. 2.3. An analysis of the beams using Gergely's analysis indicates that about 1.3 in^2 of reinforcement working at 20 ksi is required. This analysis is conservative in that it ignores the contribution of the tensile strength of the concrete.

The work by Welsh and Sozen (17) indicates that the tensile strength of the concrete makes an important contribution in limiting the crack size and in reducing the amount of reinforcement required. It would appear that some reduction in the amount of reinforcement could be made and still maintain acceptable crack widths.

The most important observation about the anchorage zone cracking is that the cracks apparently nearly always occur in I-beams, but that only a small amount of reinforcement is required to keep the crack within reasonable width limitations.

6.6 Strength of the Bridge

The strength of structure was evaluated on a limit analysis basis while the design calculations were being studied and checked. The structure met the design conditions in effect in 1966 when it was designed almost exactly, with very little excess capacity existing on the basis of the allowable stresses used. The negative moment continuity was taken into account in proportioning the positive moment sections.

The interior span will theoretically support, at collapse, loads equivalent to 21.7 HS-20 trucks, assuming all beams to resist equal loads. This load includes impact, the dead load of the bridge, and the effects of continuity. The end spans would support 17.5 HS-20 trucks. These loads

were calculated using the design strengths of the materials and not the actual strengths, which were appreciably higher.

The shear strength of the girders was more than adequate for such loads. The strength of the deck was not evaluated.

The strength appears much higher than would be required for safety. The design was based on $3\sqrt{f'_c}$ tensile stress at the bottom of the girders under full live load plus impact, and the negative moment continuity for live loads was taken into account. The ratio of ultimate moment to the limiting working load moment was somewhat higher than necessary. The ultimate positive moment requirement for each beam, based on 1.5 x Dead Load Moment plus 2.5 x Live Load Moment (including impact) was 3,615 kip ft, while the available ultimate positive moment was about 3,940 kip ft.

The excessive load factor would be reduced somewhat by reducing the conflicts between the working load stress requirements and the ultimate moment requirements. The change to an allowable tension of $6\sqrt{f'_c}$ rather than $3\sqrt{f'_c}$ is of some help in this regard.

The piecemeal approach to bridge design used in connection with the AASHO Specifications is responsible for much of the overdesign, since the total design live load for the six-beam structure is determined by using the expression:

$$\left(\frac{\text{Lane Load}}{2} \times \frac{S}{5.5}\right) \times \text{No. of Beams}$$

$$= \left(\frac{\text{Lane Load}}{2} \times \frac{7.21}{5.5}\right) 6 = 3.93 \text{ Lane Loads.}$$

The 3.93 Lane Loads are applied to a three-lane structure, resulting in 31 per cent excess moment capacity for the structure as a whole.

Another factor entering is the high dead load of the structure, about 500 kips per span, relative to the weight of three HS-20 trucks weighing

a total of 216 kips, plus impact. The requirement of an ultimate moment capacity of 1.5 x Dead Load Moment plus 2.5 x Live Load Moment should perhaps be modified to either reduce the dead load factor when dead load predominates, as is done in the AREA Manual (21), Sec. 8-17-G, or reduce the live load factor.

In the interests of producing more economical structures, some method should be found and used for reducing the excessive load capacity of the prestressed concrete bridges such as the one described in this report.

7. SUMMARY AND CONCLUSIONS

This report describes the results of measurements of strain, camber, and material properties made over a period of two years on a three-span highway bridge constructed using prestressed, precast girders and a cast-in-place deck.

The construction of the bridge is discussed in detail in Chapter 2, as are the strengths of the concretes at various times and the properties of the reinforcement. The details of the bridge superstructure are given.

The instrumentation used in making the measurements of strain, camber, and temperature are described in Chapter 3. The locations and installation of the deflection reference points, the 228 mechanical strain gage lines and the 18 Carlson strain meters are given in detail.

The concrete test specimens used for strength determinations, and creep and shrinkage measurements are also described in Chapter 3.

The results of the observations on the bridge structure are presented in Chapter 4, and the results and discussion of the creep and shrinkage measurements in Chapter 5. Discussion of the results, in terms of comparisons of measured values of camber, strain in the girders, and curvatures, is contained in Chapter 6.

The initial camber values in the 72 ft 9 in. beams were each about one in., and these values increased by about 75 per cent in the 200 days before weight from deck formwork was applied. The deflection due to the weight of the deck was 0.48 in., which is somewhat lower than the design value, of 0.625 in., largely because the concrete strength and Young's Modulus values were substantially above the design values.

The strain data obtained from the mechanical strain gages, whether considered directly or converted to curvatures, were consistent with the camber measurements. Additional information on the cyclic seasonal shortening of the beam which did not affect the camber readings was also obtained. The electrical strain gages did not give satisfactory results, and a probable reason for this error is reported.

The strain data obtained near one end of the beams indicates that the anchorage length for the prestressing strand is probably on the order of 18 in., and does not appear to increase appreciably with time. The strain distributions indicated that the strains near the end of the beam are not linearly distributed over the depth of the beam until a section approximately the beam depth from the end of the beam is reached.

All 18 girders of the bridge were examined for anchorage zone cracks, and cracks were found in 35 of the 36 ends. The reinforcement provided was adequate to restrain the widths of the cracks to acceptable values.

The prestressing force eventually decayed to a value slightly greater than that anticipated in the design process even though the inttial force just before release was lower than specified. The actual losses were less than those considered in the design.

The shrinkage strain values measured in the field were much lower than those measured in the laboratory, but the creep values were comparable. This implies that a major revision in the methods of predicting creep strains is necessary so that the fluctuations in environmental conditions can be taken into account along with the average value of relative humidity. This change will affect the calculation of the camber and losses of prestress, both of which affect the serviceability but not the strength of the structure.

8. REFERENCES

1. Gamble, W. L., "Field Investigation of a Continuous Composite Prestressed I-Beam Highway Bridge Located in Jefferson County, Illinois," Civil Engineering Studies Structural Research Series No. 360, Department of Civil Engineering, University of Illinois, Urbana, 1970.
2. Reynolds, R. J. and W. L. Gamble, "Field Investigation of Prestressed Concrete Highway Bridges--Instrumentation for Long-Term Field Investigation," Civil Engineering Studies, Structural Research Series No. 327, Department of Civil Engineering, University of Illinois, Urbana, 1967.
3. Carlson, R. W., "Five Years' Improvement of the Elastic Wire Strain Meter," Engineering News Record, V. 114, May 16, 1935, p. 696.
4. Kaar, P. H., R. W. LaFraugh, and M. A. Mass, "Influence of Concrete Strength on Strand Transfer Length," Journal Prestressed Concrete Institute, Vol. 8, No. 5, Oct. 1963, pp. 47-67.
5. Stocker, M. F. and M. A. Sozen, "Investigation of Prestressed Reinforced Concrete for Highway Bridges, Part VI: Bond Characteristics of Prestressing Strand," Engineering Experiment Station Bulletin No. 503, College of Engineering, University of Illinois, Urbana, 1969.
6. Magura, D. D., M. A. Sozen, and C. P. Siess, "A Study of Stress Relaxation in Prestressing Reinforcement," Journal Prestressed Concrete Institute, Vol. 9, No. 2, April 1964, pp. 13-57.
7. ACI Committee 435, "Deflections of Prestressed Concrete Members," Journal American Concrete Institute, Proc. Vol. 60, Dec. 1963, pp. 1697-1728.
8. Hansen, Torben C., "Creep and Stress Relaxation of Concrete," Proc. Nr. 31, Swedish Cement and Concrete Research Institute, Royal Institute of Technology, Stockholm, 1960.

9. Wallo, E. M. and C. E. Kesler, "Prediction of Creep in Structural Concrete," University of Illinois, Engineering Experiment Station Bulletin No. 498, Urbana, 1968.

10. Corley, W. G., M. A. Sozen, and C. P. Siess, "Time-Dependent Deflections of Prestressed Concrete Beams," Bulletin No. 307, Highway Research Board, 1961, pp. 1-25.

11. Branson, D. E. and A. M. Ozell, "Camber of Prestressed Concrete Beams," Journal American Concrete Institute, Proc. Vol. 57, No. 12, June 1961, pp. 1549-1574.

12. Sinno, R. and H. L. Furr, "Hyperbolic Functions for Prestress Loss and Camber," Proc. ASCE, Journal of the Structural Division, Vol. 96, No. ST4, April 1970, pp. 803-821.

13. "Criteria for Prestressed Concrete Bridges," U. S. Department of Commerce, Bureau of Public Roads, Washington, D. C., 1954.

14. "Standard Specifications for Highway Bridges," American Association of State Highway Officials, Washington, D. C., Tenth Edition, 1969.

15. ACI ASCE Joint Committee 323, "Tentative Recommendations for Prestressed Concrete," Journal American Concrete Institute, Vol. 54, No. 7, January 1958, pp. 545-578.

16. Gergely, P., M. A. Sozen, and C. P. Siess, "The Effect of Reinforcement on Anchorage Zone Cracks in Prestressed Concrete Members," Civil Engineering Studies, Structural Research Series No. 271, Department of Civil Engineering, University of Illinois, Urbana, 1963.

17. Welsh, W. A., Jr., and M. A. Sozen, "Investigation of Prestressed Concrete for Highway Bridges, Part V: Analysis and Control of Anchorage-Zone Cracking in Prestressed Concrete," University of Illinois, Engineering Experiment Station, Bulletin No. 497, Urbana, 1968.

18. Troxell, G. D., J. M. Raphael, and R. E. Davis, "Long Time Creep and Shrinkage Tests in Plain and Reinforced Concrete," Proc. ASTM, Vol. 58, 1958, pp. 1102-1120.

19. Hansen, T. C. and A. H. Mattock, "Influence of Size and Shape of Member on the Shrinkage and Creep of Concrete," J. ACI, Feb. 1966, pp. 267-290, Proc. Vol. 63; Also PCA Dev. Dept. Bulletin D103.

20. "Interim Specification-Prestressed Concrete, Section 6, "American Association of State Highway Officials, Effective: November, 1970.

21. American Railway Engineering Association, "Manual," 1961, Chicago.

Table 2.1 CHRONOLOGY OF GIRDER CONSTRUCTION

Time	Elapsed Time hours; min.	Task
27 Dec 68		
7:00pm	0:00	Bed clean, bulkheads and holddowns set
7:30	0:30	Start stringing strands
9:30	2:30	Finish stringing strands
9:35	2:35	Start stressing strands
10:05	3:05	Finish stressing strands
28 Dec 68		
12:10am	5:10	Start placing forms
1:15	6:15	Finish placing forms
2:03	7:02	Start placing concrete
4:15	9:15	Finish casting
6:00	11:00	Start steam curing
7:00pm	24:00	Remove forms
8:15	25:15	Start installing gage points
29 Dec 68		
		Install Gage points
30 Dec 68		
8:15am	61:15	Finish installing gage points
1:00pm	66:00	Start zero readings
3:30	68:30	Finish zero readings
4:00	69:00	Start cutting strands
6:15	71:15	Finish cutting strands

Table 2.2 CONSTRUCTION OF BRIDGE AND LOCATIONS OF GIRDERS AT VARIOUS TIMES

28 December 1968	Cast beams BX-3, BX-4
30 December 1968	Release prestress and move beams off of prestress beds
31 December 1968	Move beams outside of plant
4 June 1969	Set beams on piers at bridge site
5 August 1969	Cast deck

Table 2.3 GIRDER CONCRETE PROPERTIES

Age Days After Casting	Field Stored f'_c ksi	Field Stored E_i ksix10^3	Laboratory Stored f'_c ksi	Laboratory Stored E ksix10^3	Age Days After Release of Prestress
2.5	4.94	3.40	-	-	0
16	4.93	3.45	5.51	3.37	14
28	5.14	3.37	6.13	3.63	26
90	5.91	3.24	7.05	3.62	88
219	7.85	4.73	6.84	4.19	217
420	6.92	4.57	5.63	3.85	420

Values are average of three cylinders.

Table 2.4 DECK CONCRETE PROPERTIES

Age Days After Casting	Field Stored f'_c ksi	Field Stored E_i ksi x 10^3	Laboratory Stored f'_c ksi	Laboratory Stored E_i ksi x 10^3	Age Days After Release of Prestress
29	6.56	5.50	6.20	4.83	247
202	5.82	4.66	5.40	4.55	420
364	7.05	4.90			582
367			6.31	4.53	585

Values are averages of three cylinders.

Table 2.5 STEEL STRENGTH DATA

Bar Size	Deck			Girder		
	f_y ksi	f_{ult} ksi	ϵ_{ult} % in 8"	f_y ksi	f_{ult} ksi	ϵ_{ult} % in 8"
3	-	-	-	59.5	94.2	8
4	65.5	117.5	13	-	-	-
5	*70.5	128.0	9	44.5	72.7	25
6	48.5	82.0	19	51.2	82.2	21
7	61.3	111.7	14	-	-	-
8	64.5	122	11	-	-	-

Values listed are the average for two tests.
ϵ_{ult} values are given for nearest whole percent.

*No. 5 bars used in the deck showed evidence of laminations, that is, longitudinal defects or cracks apparently caused by lack of rewelding of material folded over itself during the hot rolling process. This has no affect on the tensile strength of the bar.

Table 4.1 PRESTRESSING FORCE DATA

Dyn. No.	Design Force Kips	Immediately After Prestressing ** 2-1/2 to 3 hr	All Strands Stressed 3 hr	During Steam 49 hr	At Release 70 hr
2	18.9	17.63	17.29	15.49	17.76
6	"	17.92	17.44	15.46	17.77
7	"	18.85	18.50	16.32	18.98
12	"	18.32	17.93	15.71	18.12
13	"	19.26	18.97	16.75	19.36
16	"	18.67	18.34	15.98	18.38
21	"	18.90	18.61	16.60	19.00
23	"	19.22	18.93	16.57	19.13
24	"	18.48	18.19	16.22	18.38
26	"	17.77	17.77	15.66	17.63
27	"	17.38	17.38	15.74	17.62
28	"	17.82	17.77	15.55	17.53
29*	"	19.36	19.36	17.00	19.22
Average Bottom	18.9	18.58	18.24	16.12	18.54
Average Top	18.9	17.66	17.64	15.65	17.59
Projected Total Force	718.20	696.84	687.12	607.86	695.02

Note: *Dynamometer No. 29 is at the far end and is not included in averaging the prestressing force.
**Time elapsed, see Table 2.1.

Table 5.1 TIMES OF INITIAL SHRINKAGE READINGS AND LOADING OF CREEP RACKS

Activity	Field Stored	Lab Stored
Beam Specimens Cast	28 December 1968	28 December 1968
Zero Shrinkage Readings	30 December 1968	30 December 1968
First Creep Rack Loaded	30 December 1968	30 December 1968
Second Creep Rack Loaded	7 August 1969	7 August 1969
Deck Specimens Cast	5 August 1969	5 August 1969
Zero Shrinkage Readings	12 August 1969	12 August 1969
Creep Rack Loaded	2 September 1969	2 September 1969

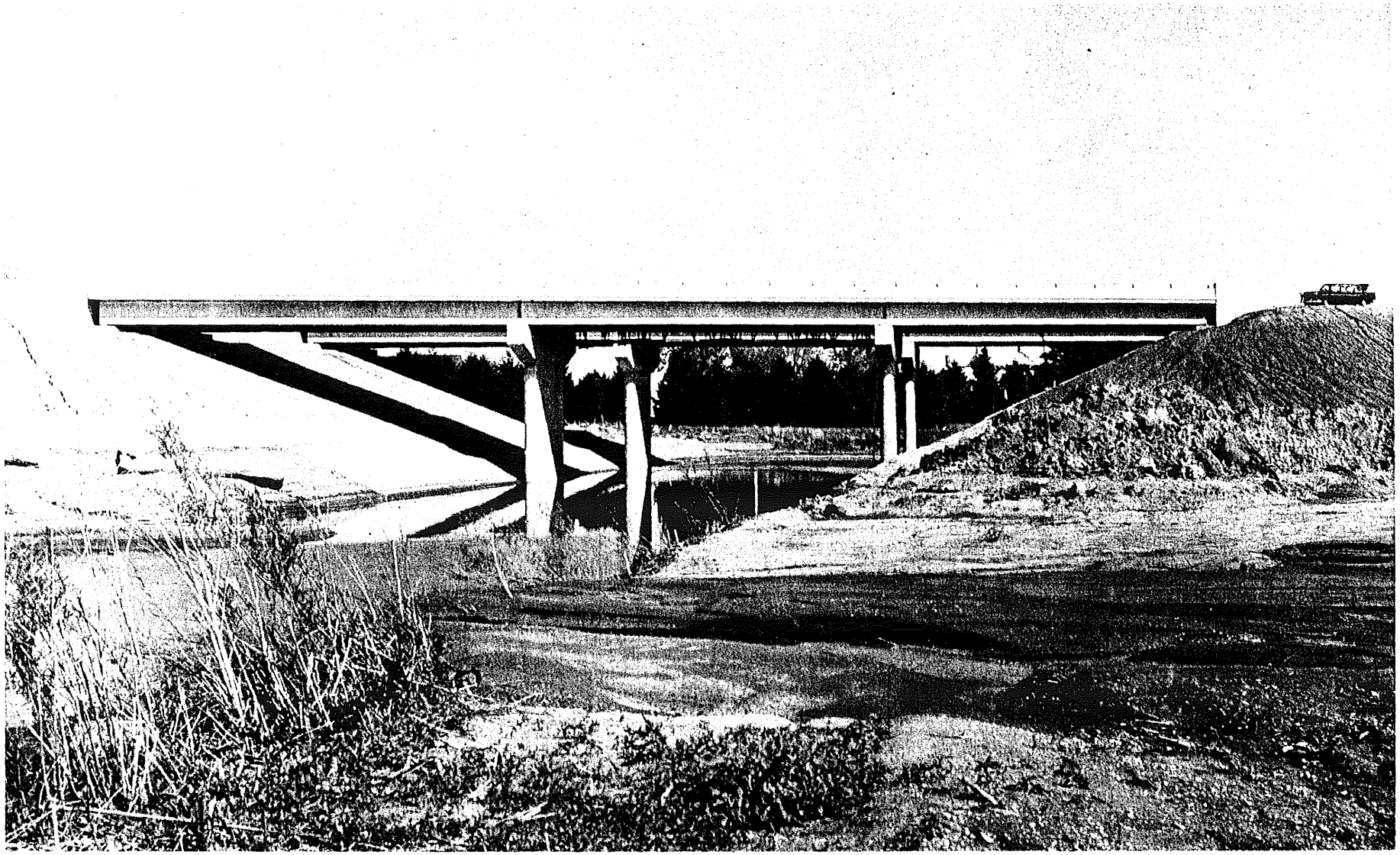

FIG. 2.1 TEST BRIDGE VIEWED FROM THE WEST

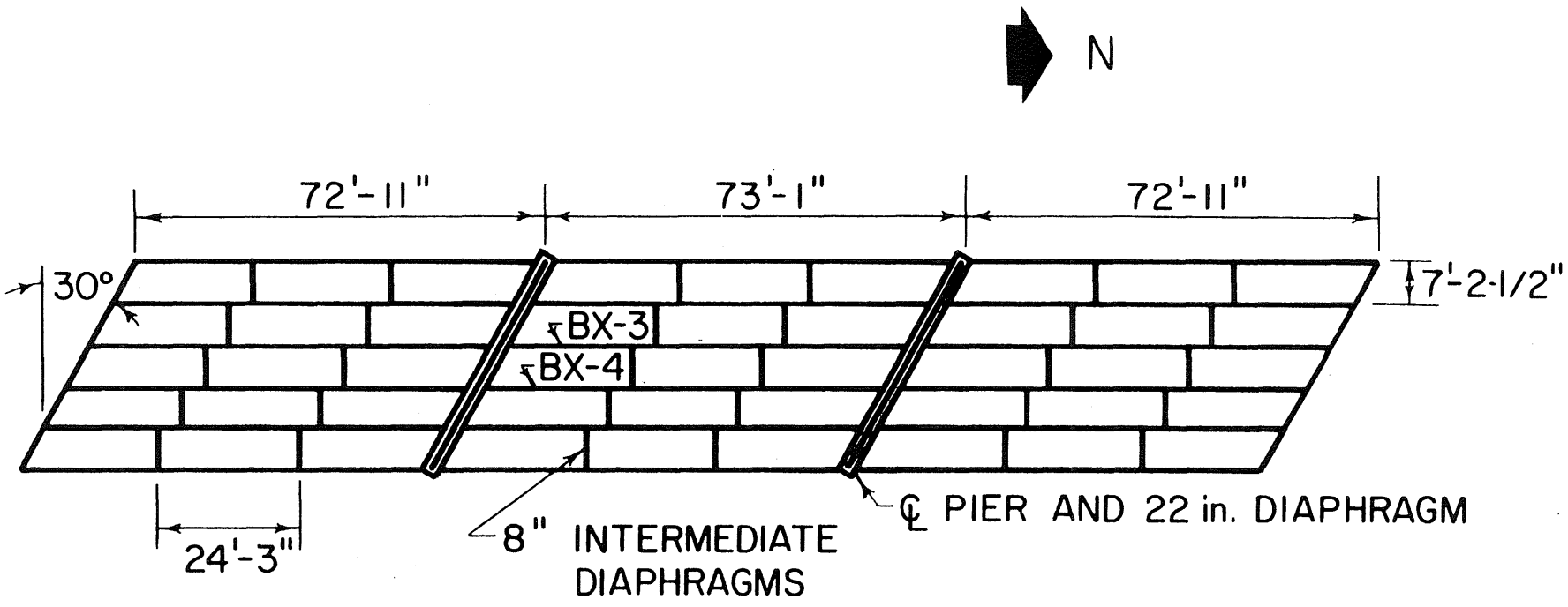

FIG. 2.2 PLAN OF BRIDGE SHOWING GIRDER AND DIAPHRAGM PLACEMENT

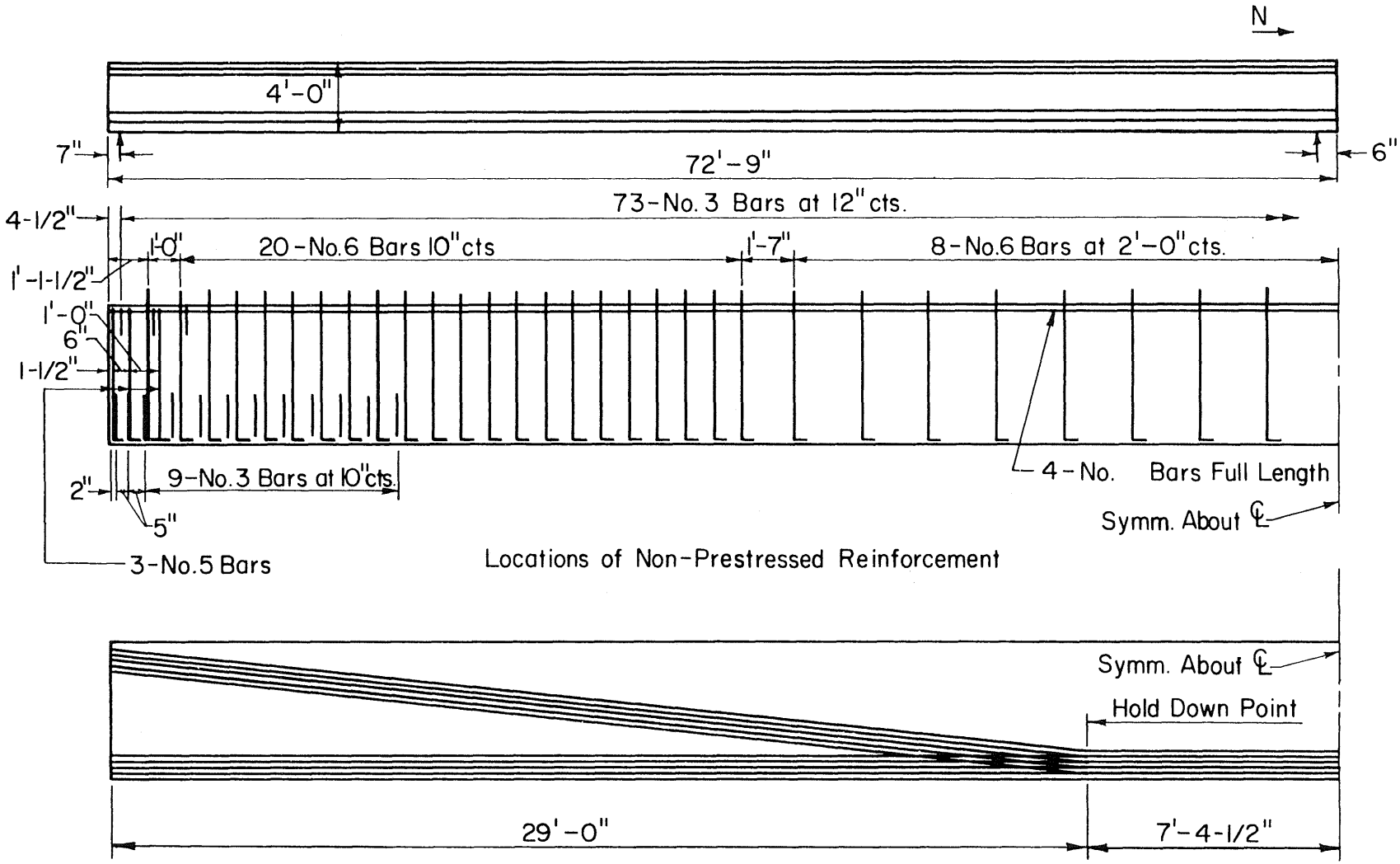

FIG. 2.3 DETAILS OF GIRDERS

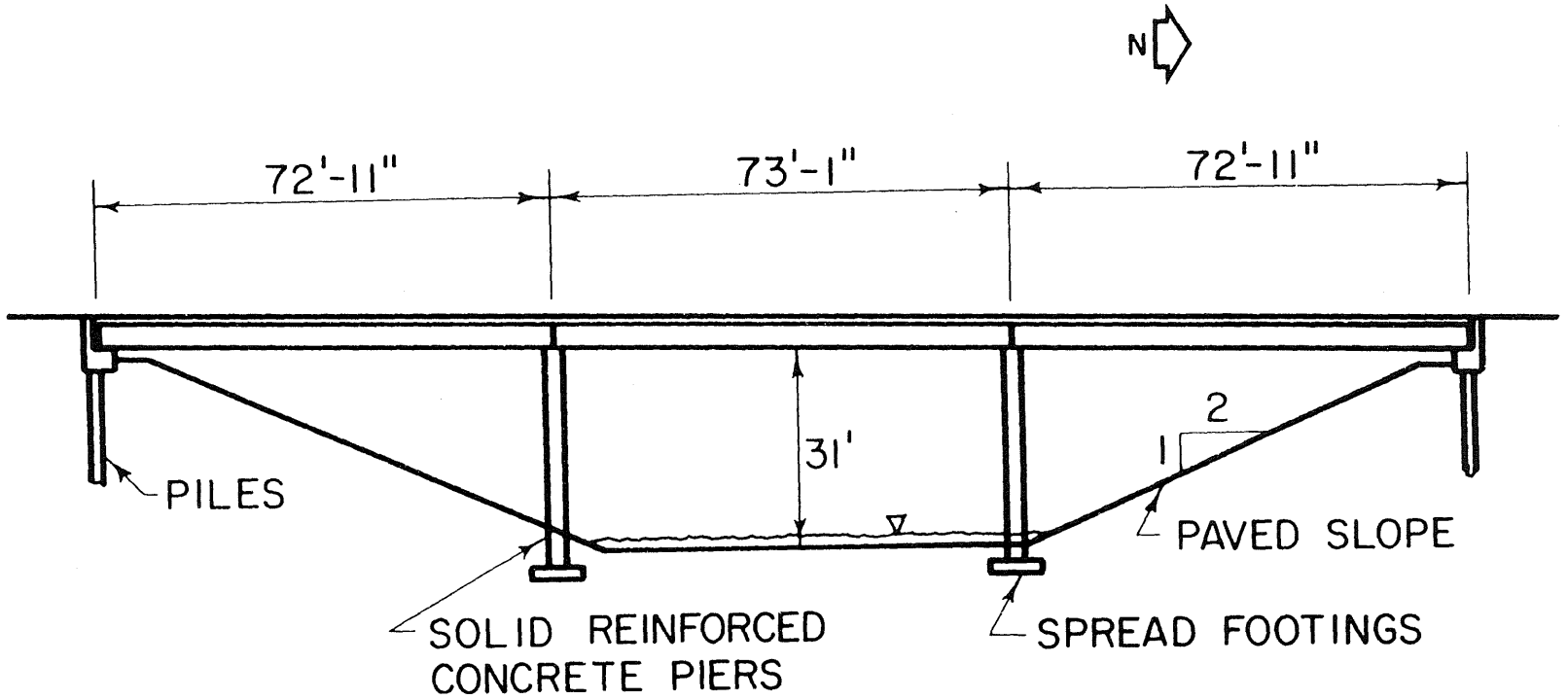

FIG. 2.4 ELEVATION OF BRIDGE

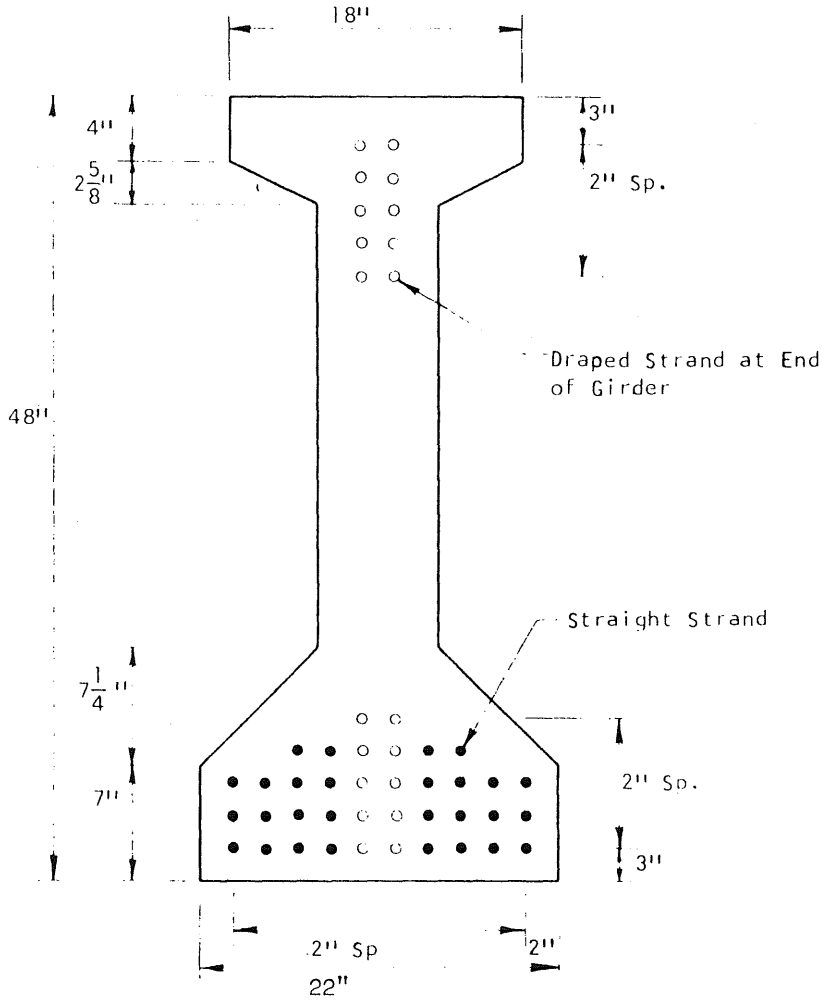

a. Strand Placement

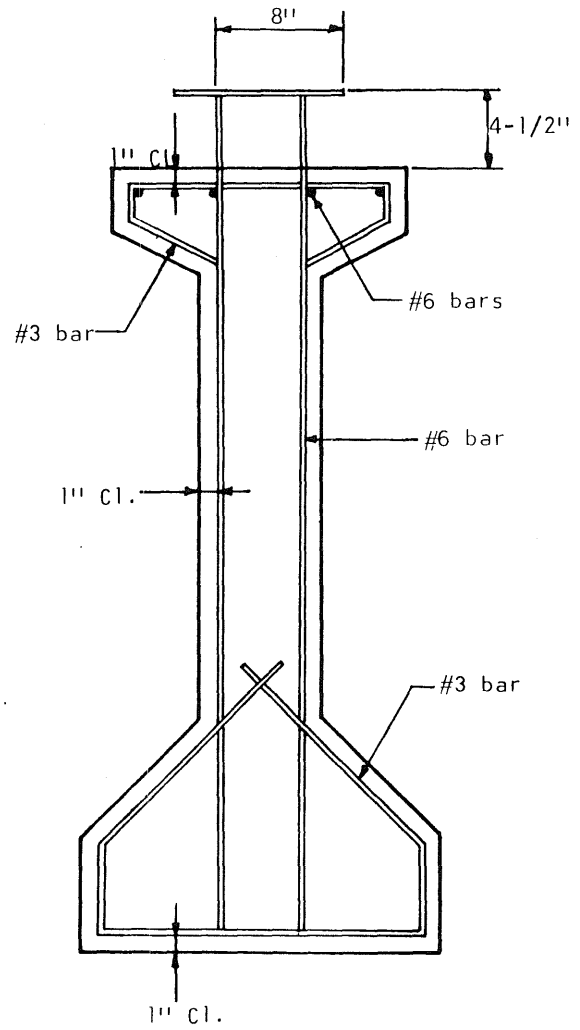

b. Reinforcement

Fig. 2.5 GIRDER CROSS SECTION

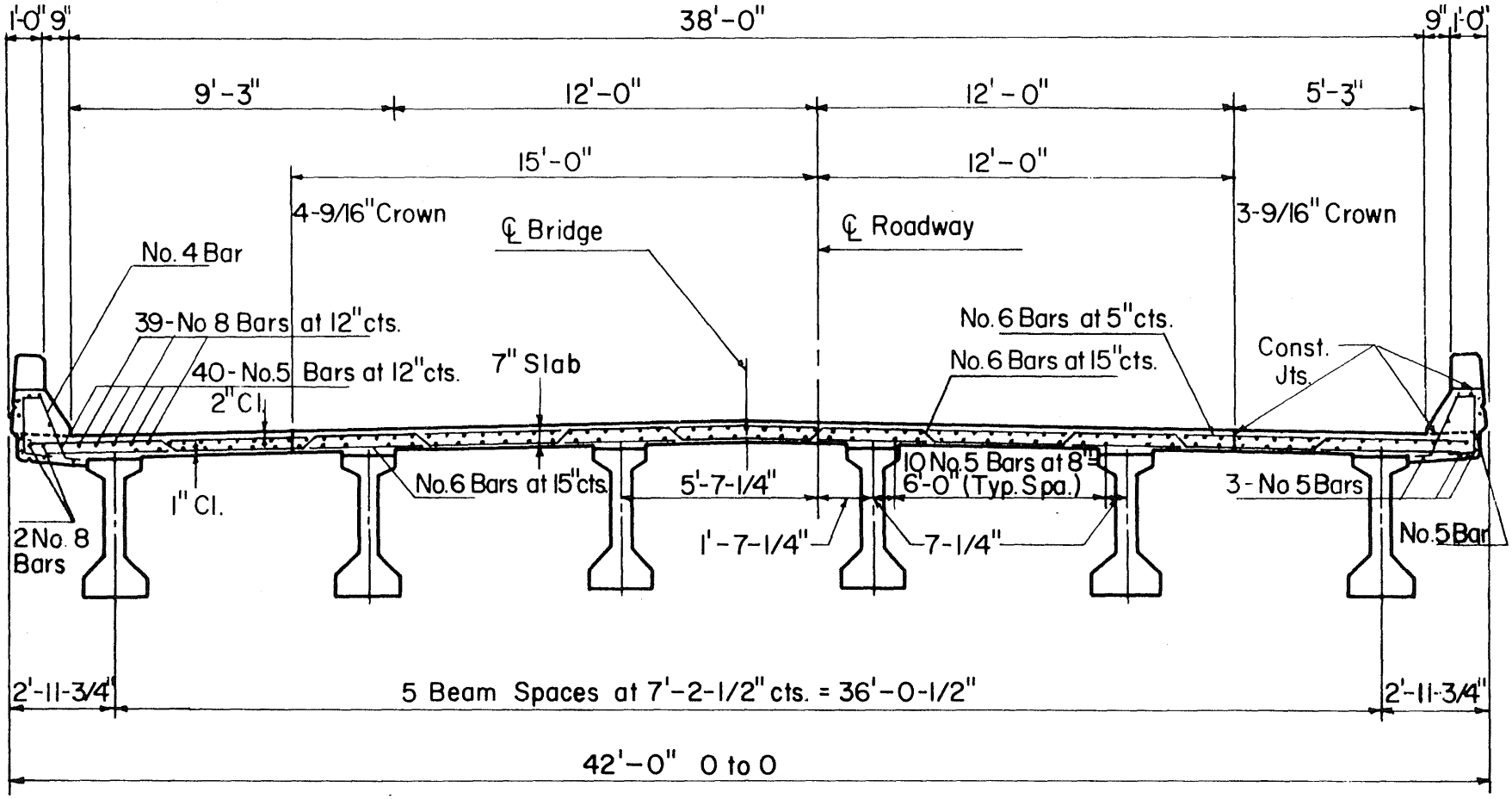

FIG. 2.6 BRIDGE CROSS-SECTION NEAR PIERS

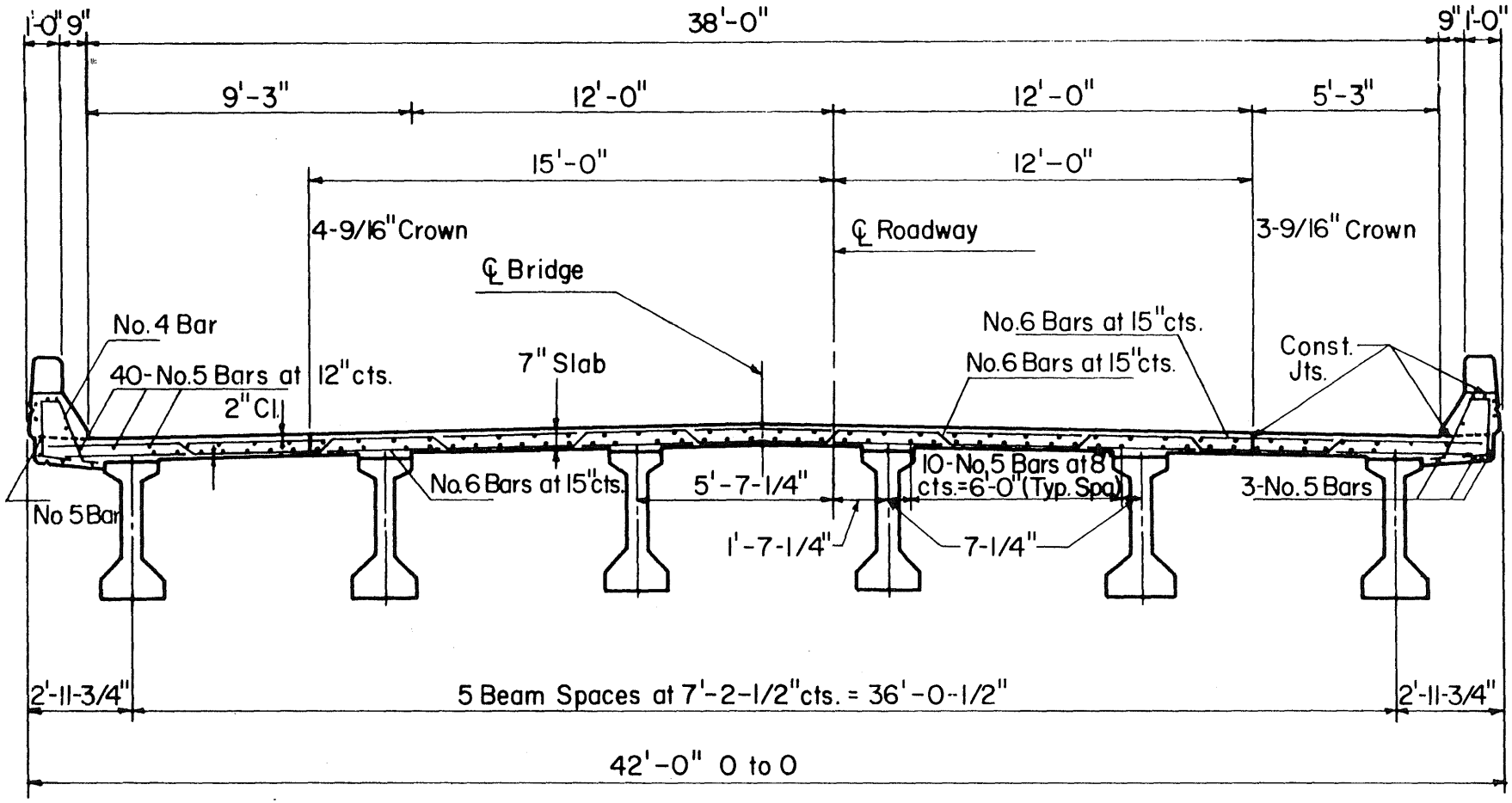

FIG. 2.7 BRIDGE CROSS-SECTION NEAR MIDSPAN

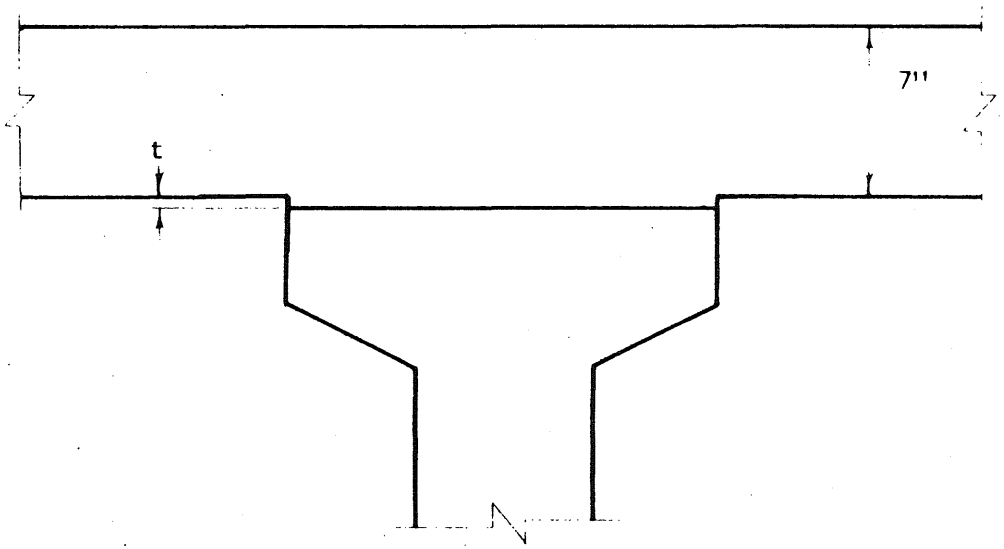

Note: Dimension "t" is adjusted to compensate for measured excess or deficient camber of girder so that final deck elevation is on the proper vertical alignment.

FIG. 2.8 DETAILS OF FILLET AT SLAB-DECK JOINT

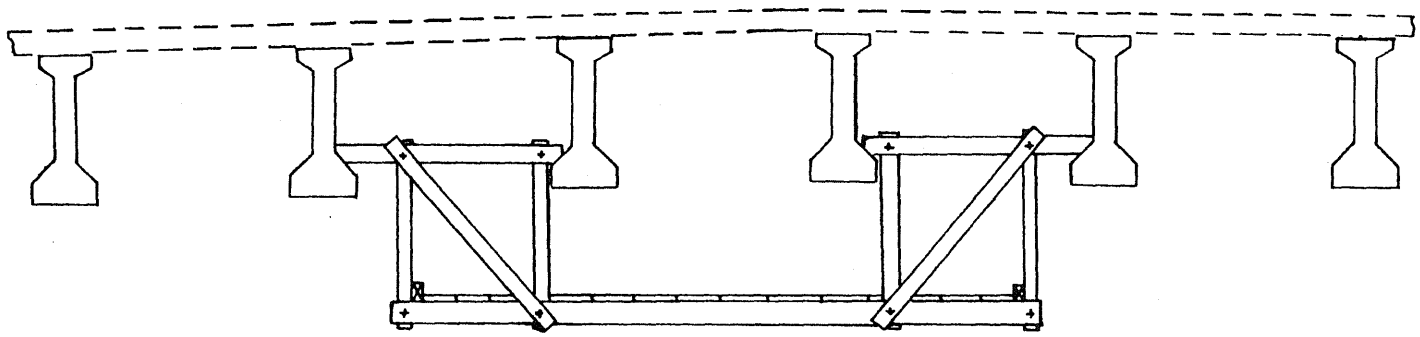

Fig. 2.9 LOCATION OF WOODEN SCAFFOLDING

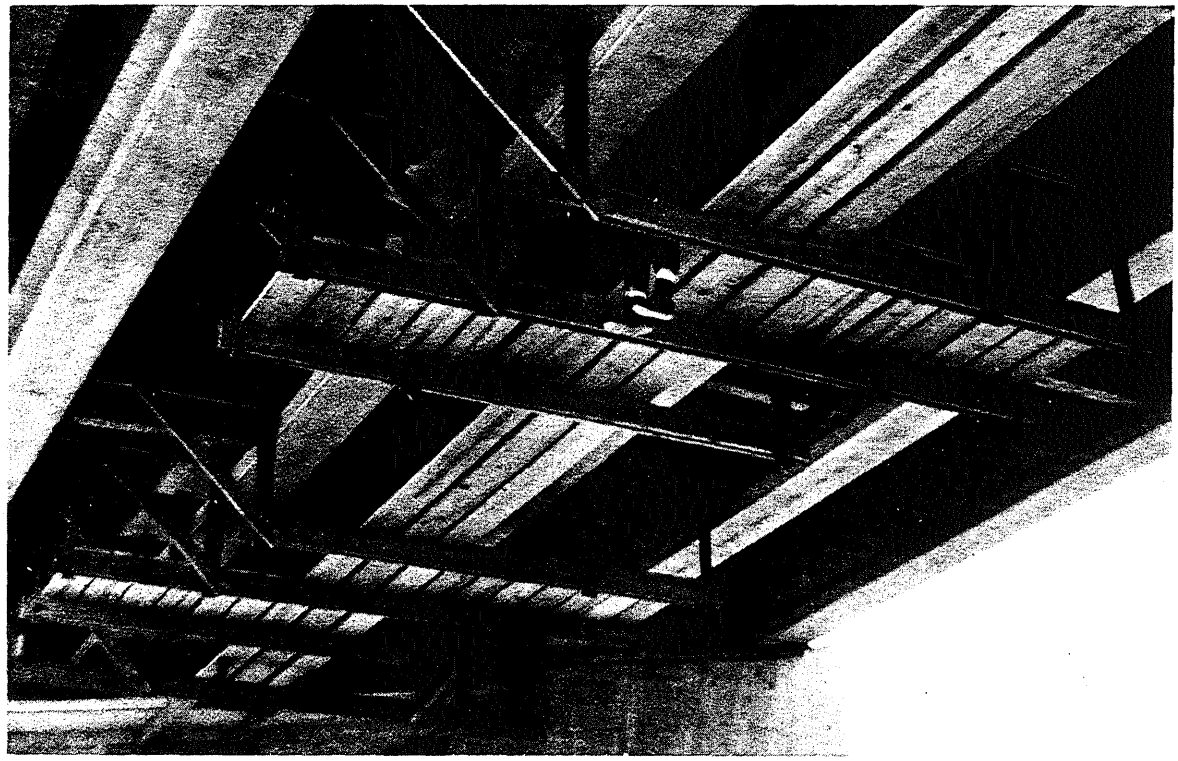

FIG. 2.10 WOODEN SCAFFOLDING

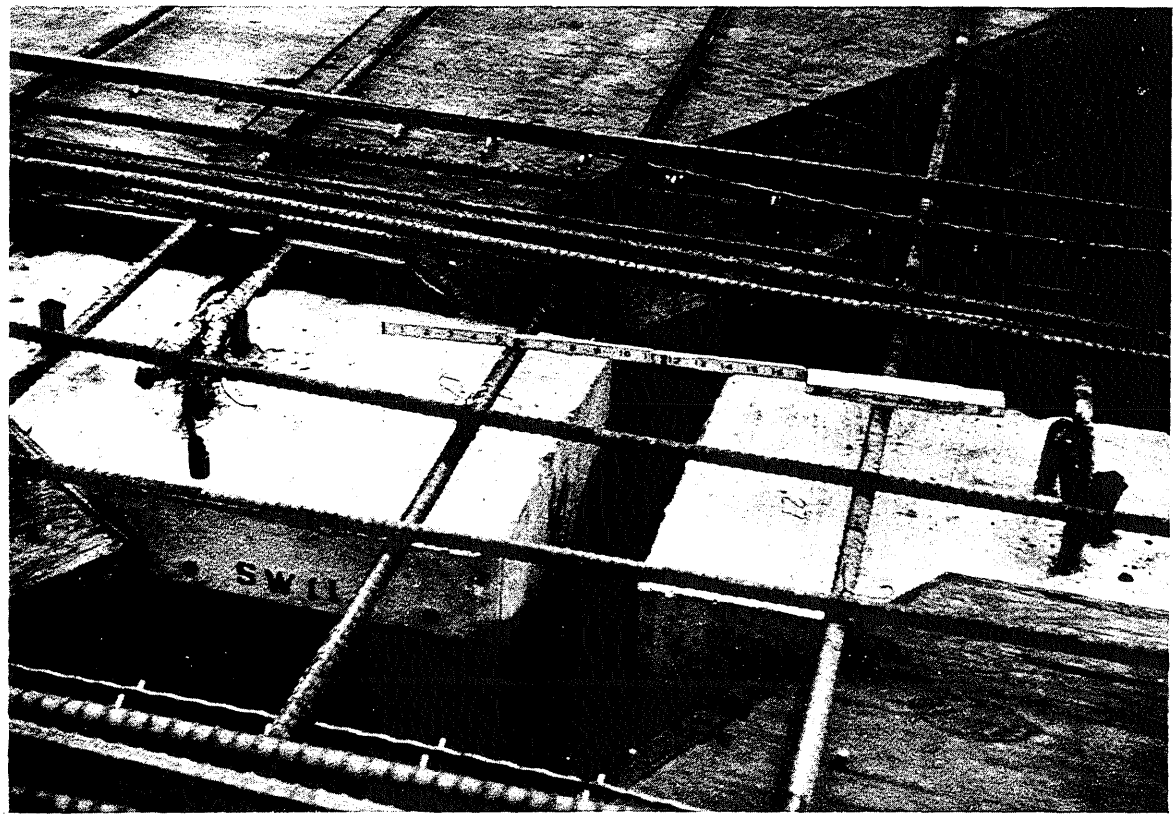

FIG. 2.11 FORMWORK OVER INTERIOR PIER

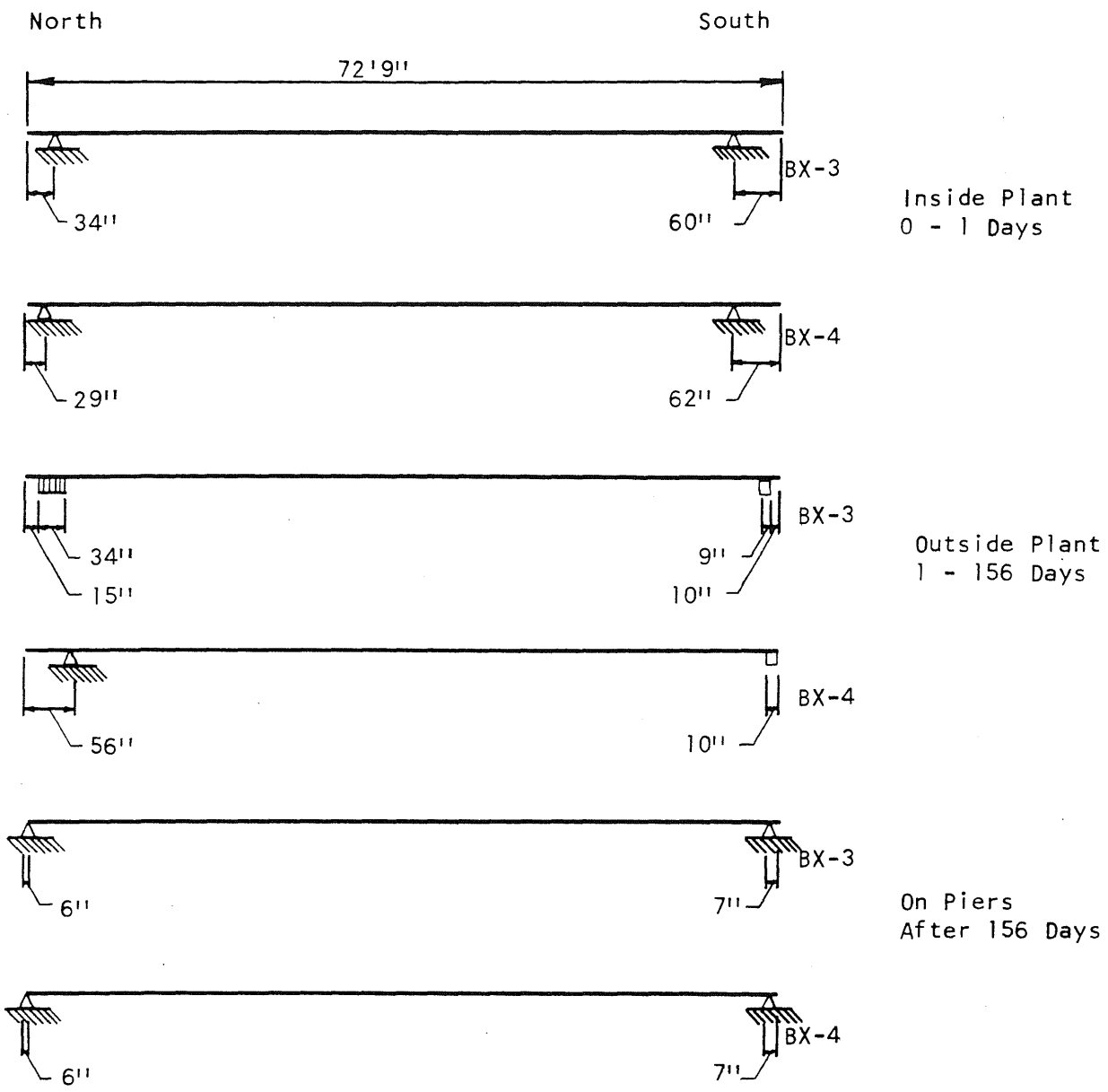

Fig. 2.12 LOCATIONS OF BEAM SUPPORTS AT VARIOUS TIMES

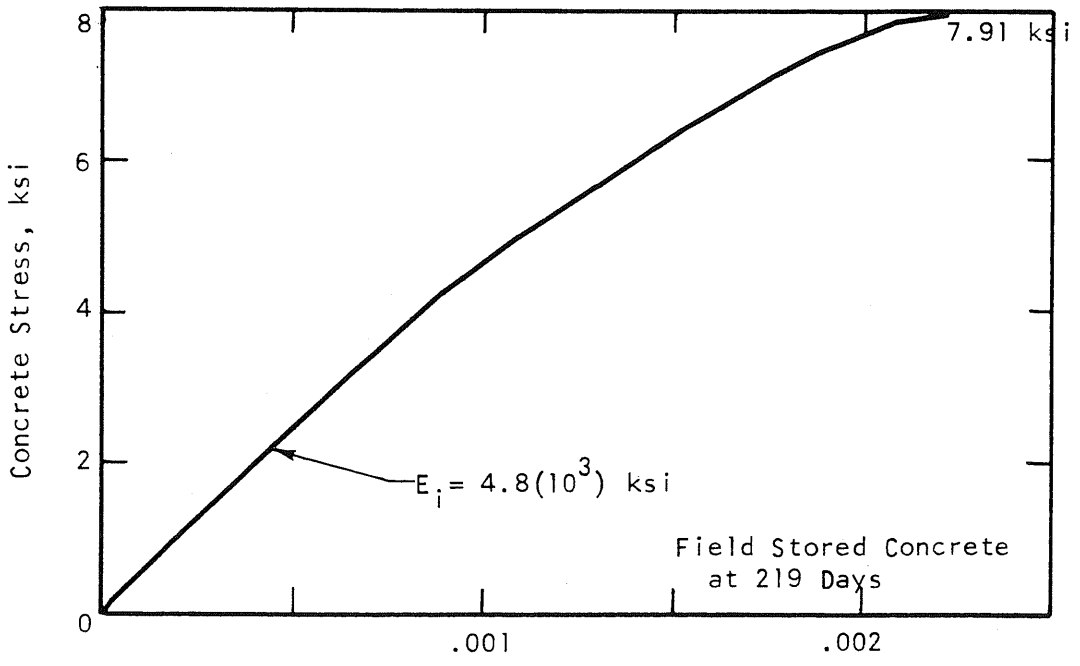

a) Girder Concrete

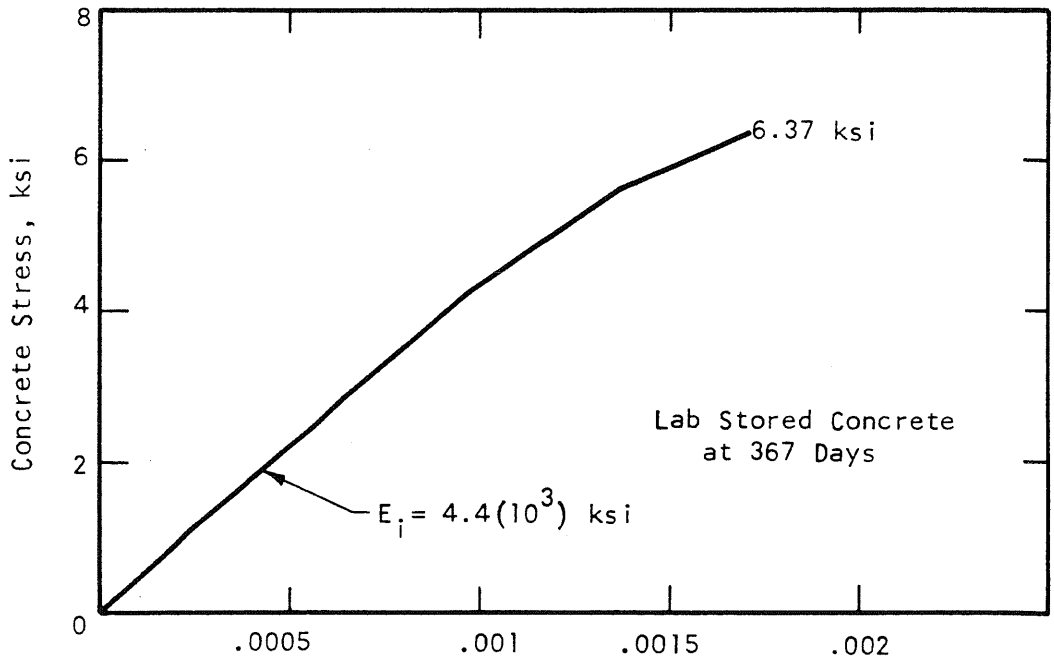

b) Deck Concrete

Fig. 2.13 TYPICAL STRESS-STRAIN CURVES FOR CONCRETE

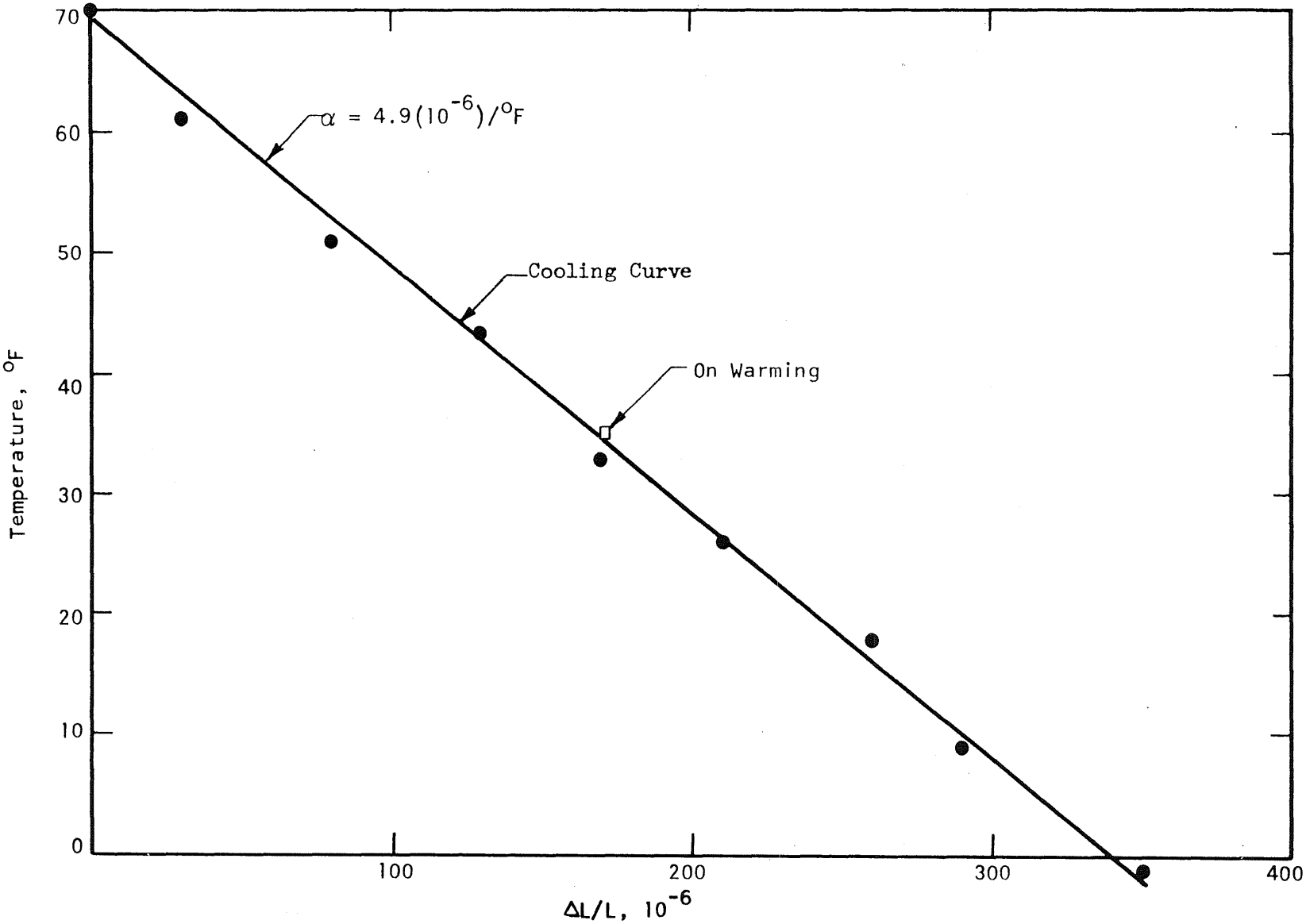

Fig. 2.14 THERMAL COEFFICIENT FOR BEAM CONCRETE

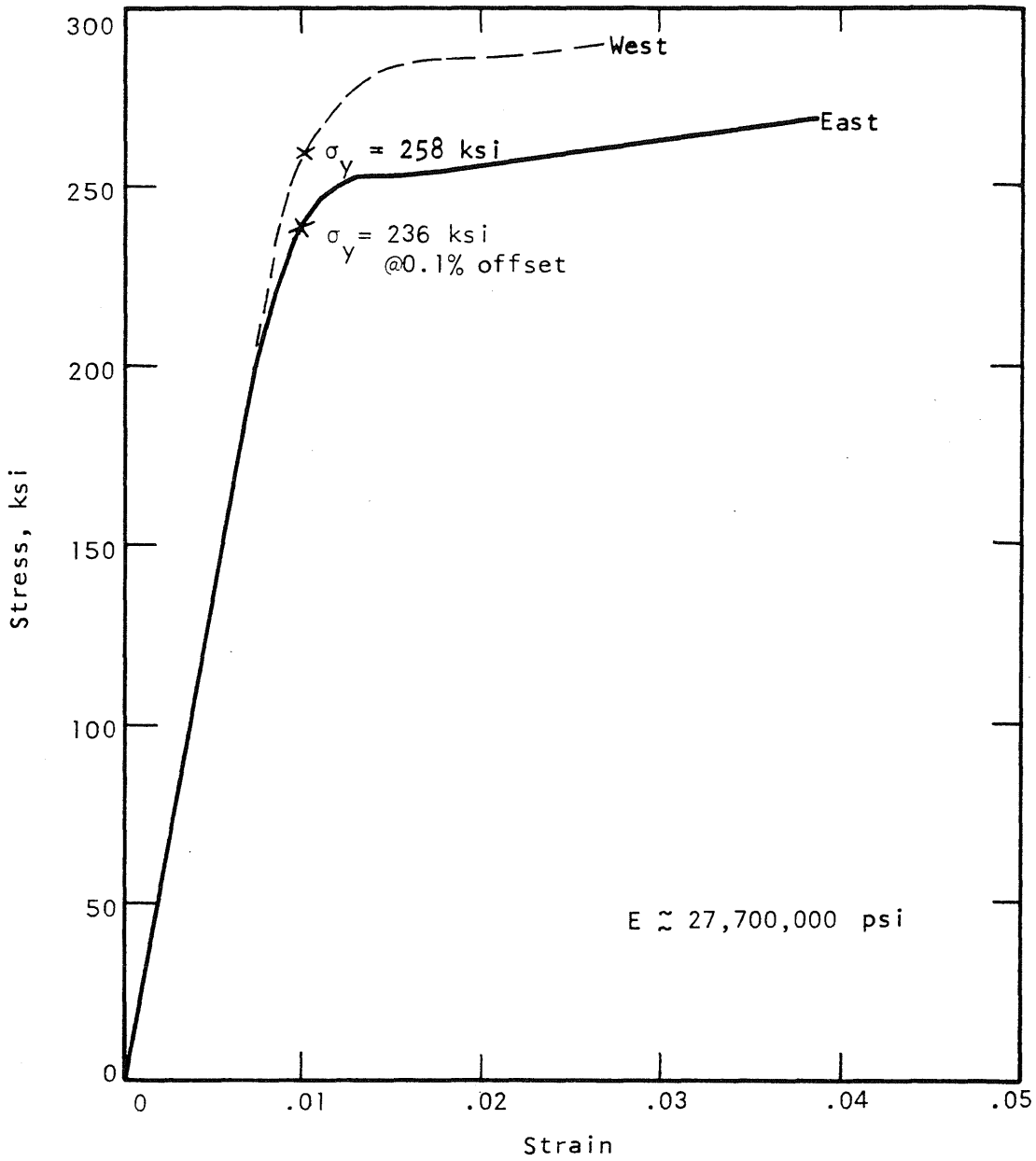

Fig. 2.15 STRESS STRAIN CURVE FOR TYPICAL PRESTRESSING CABLE

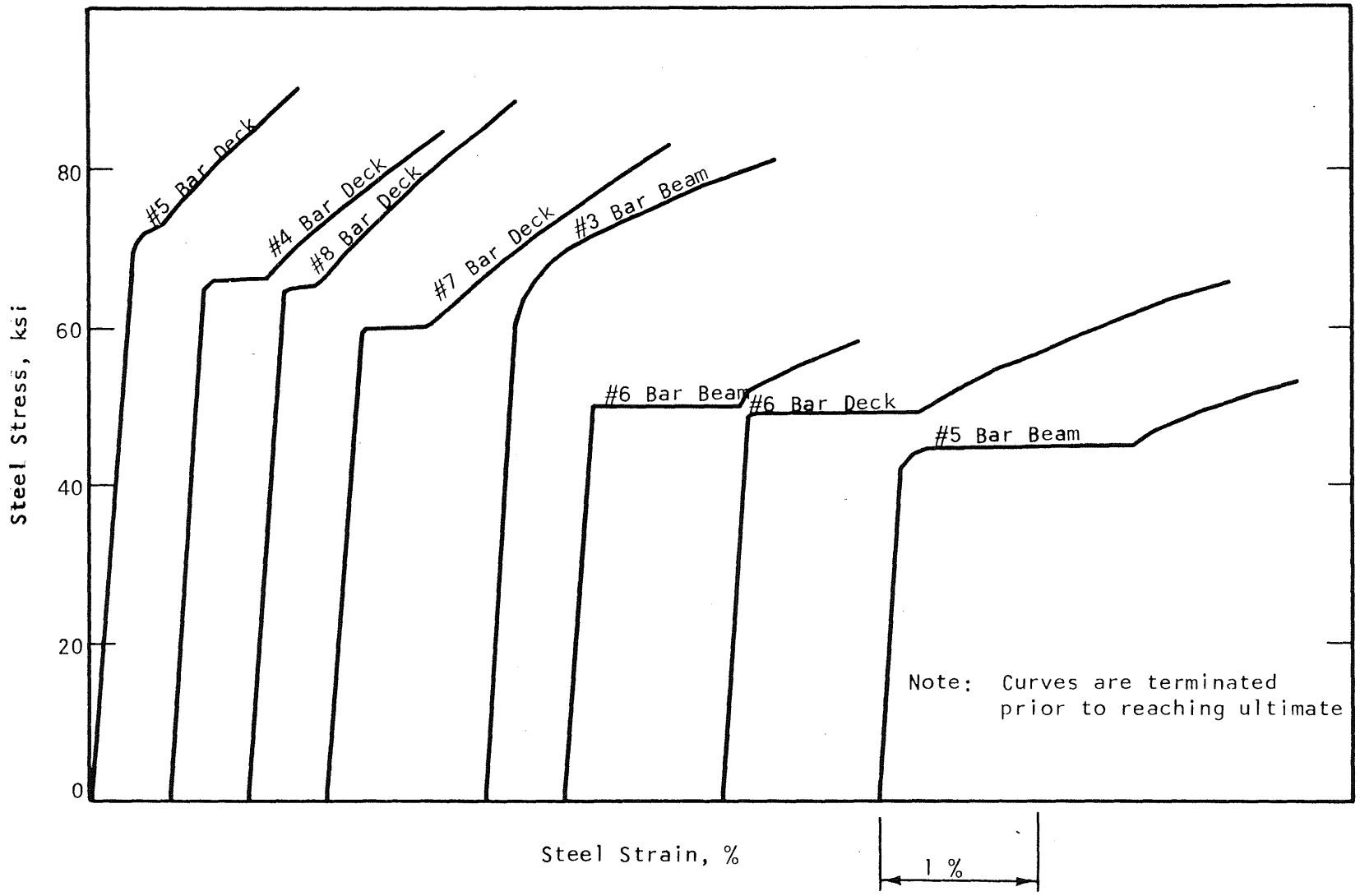

Fig. 2.16 TYPICAL STRESS-STRAIN CURVES FOR STEEL

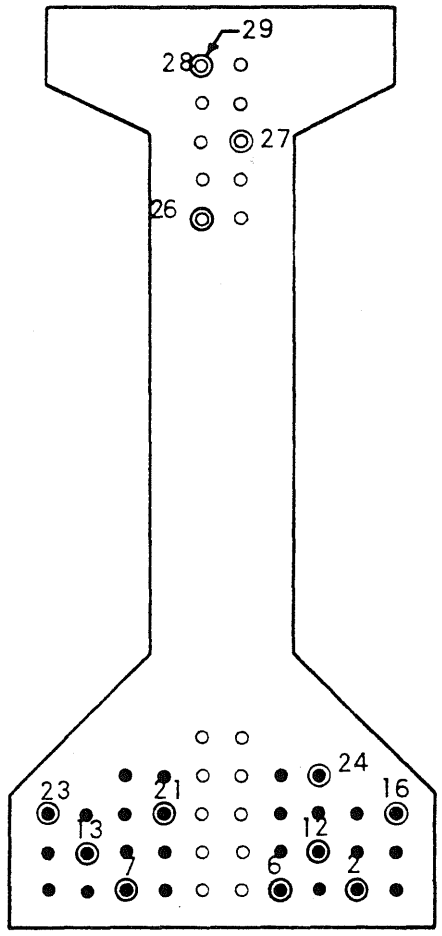

West end as cast

Note: All dynamometers except #29 were at the anchorage end of the prestressing bed.

Fig. 3.1 LOCATIONS & DESIGNATIONS OF STRAND FORCE DYNAMOMETERS

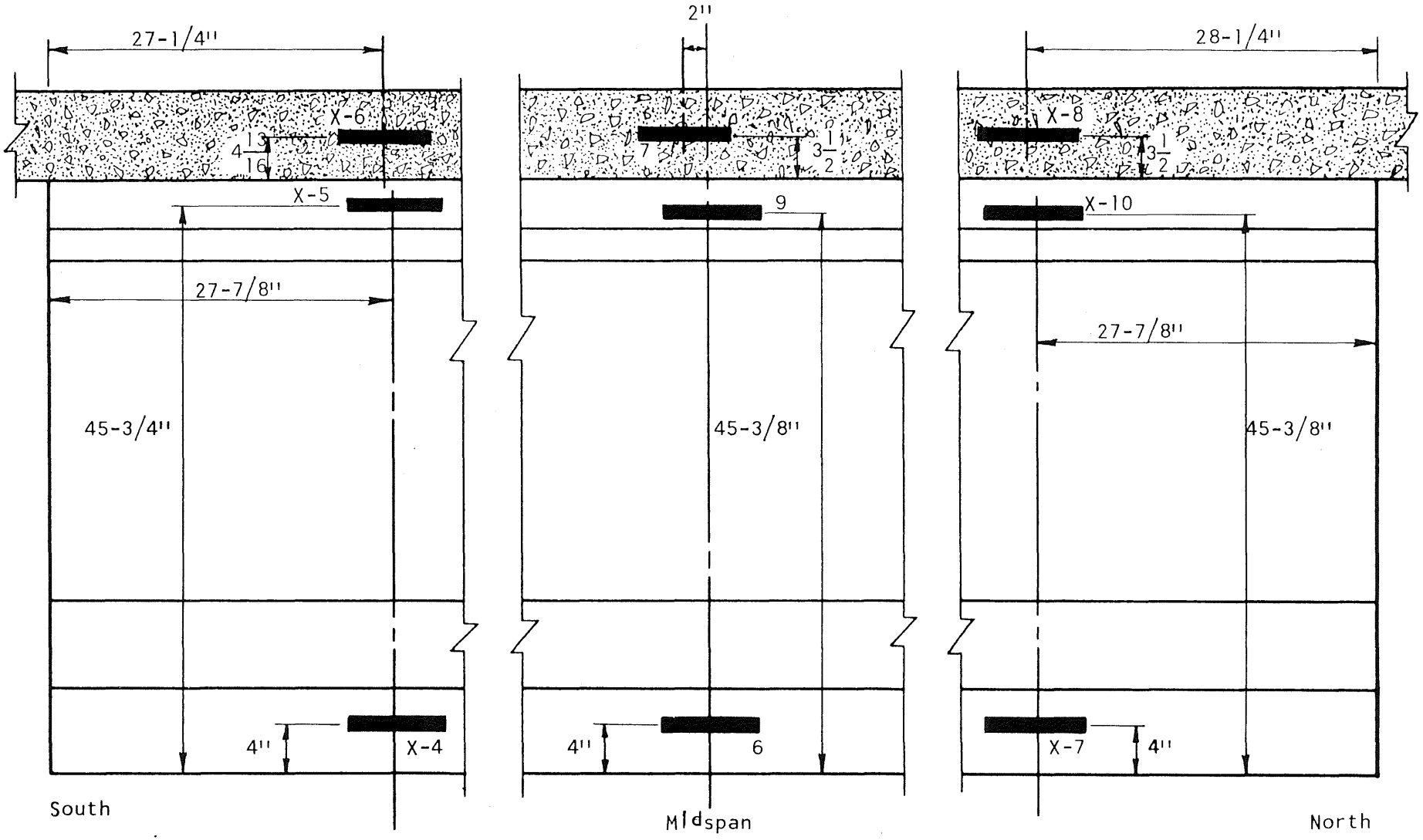

Fig. 3.2 LOCATION AND DESIGNATION OF CARLSON STRAIN METERS IN BEAM BX-3

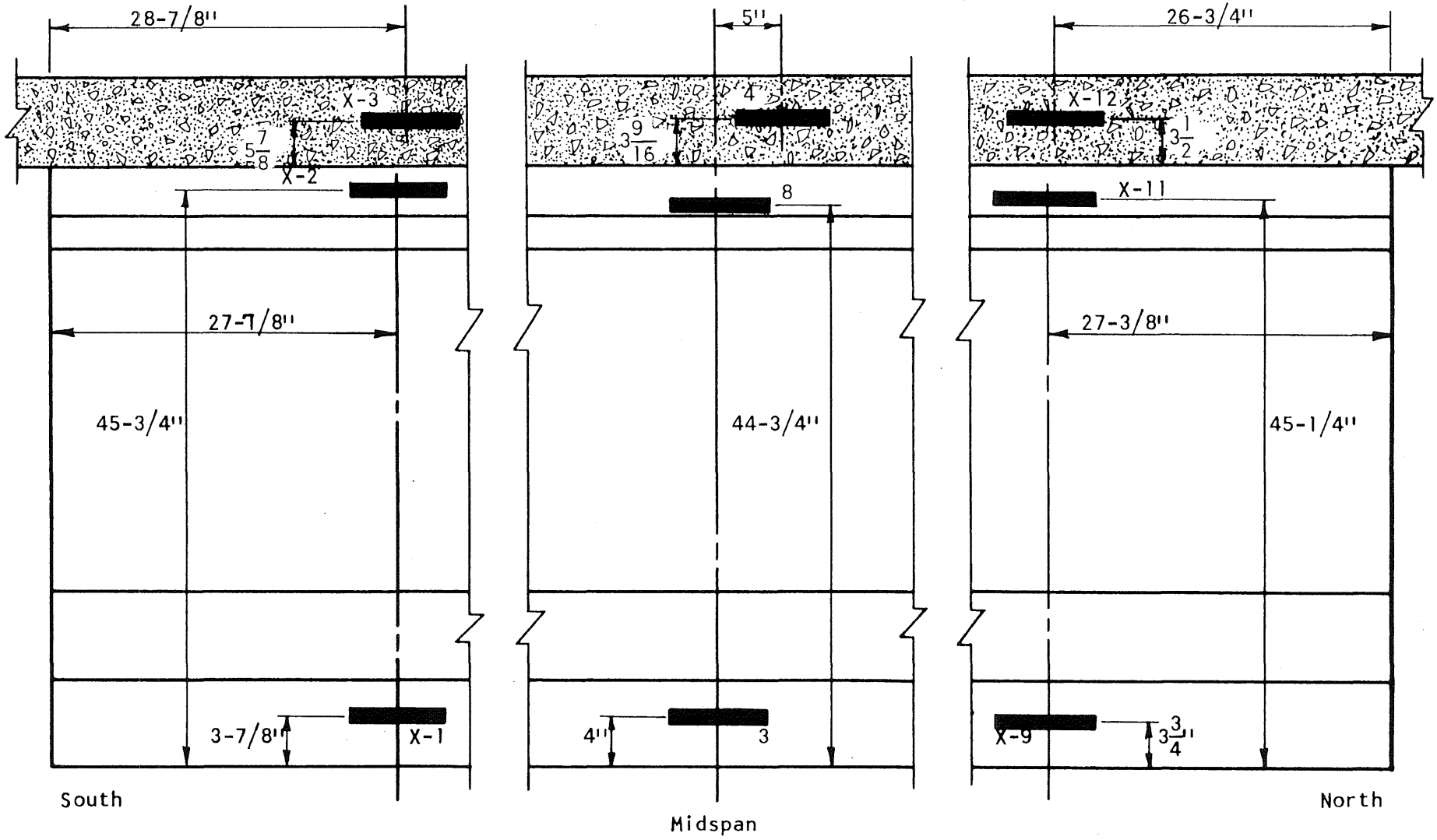

Fig. 3.3 LOCATION AND DESIGNATION OF CARLSON STRAIN METERS IN BEAM BX-4

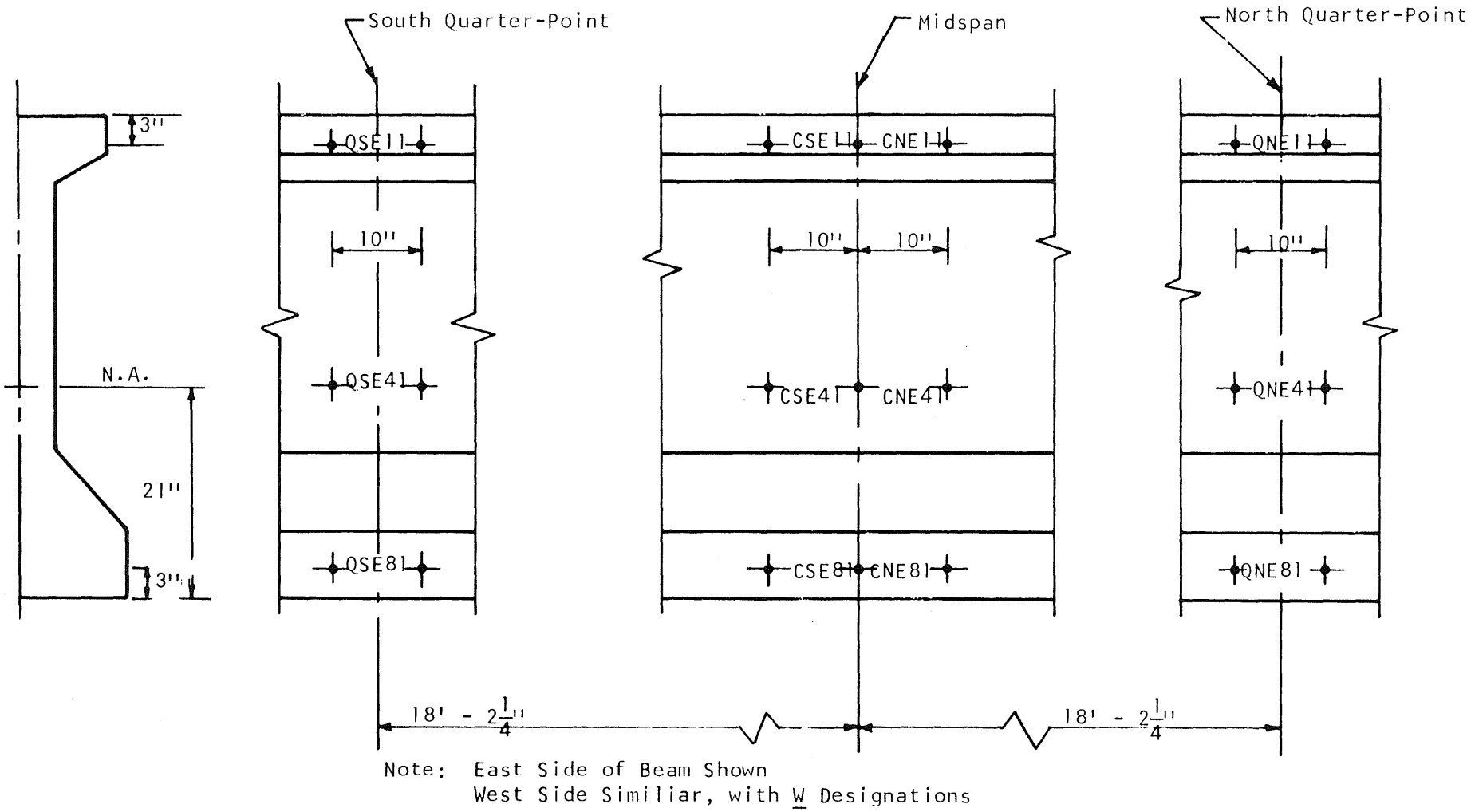

Fig. 3.4 LOCATIONS AND DESIGNATIONS OF MECHANICAL STRAIN GAGE LINES AT MID-SPAN AND QUARTER-POINTS, BEAM BX-4

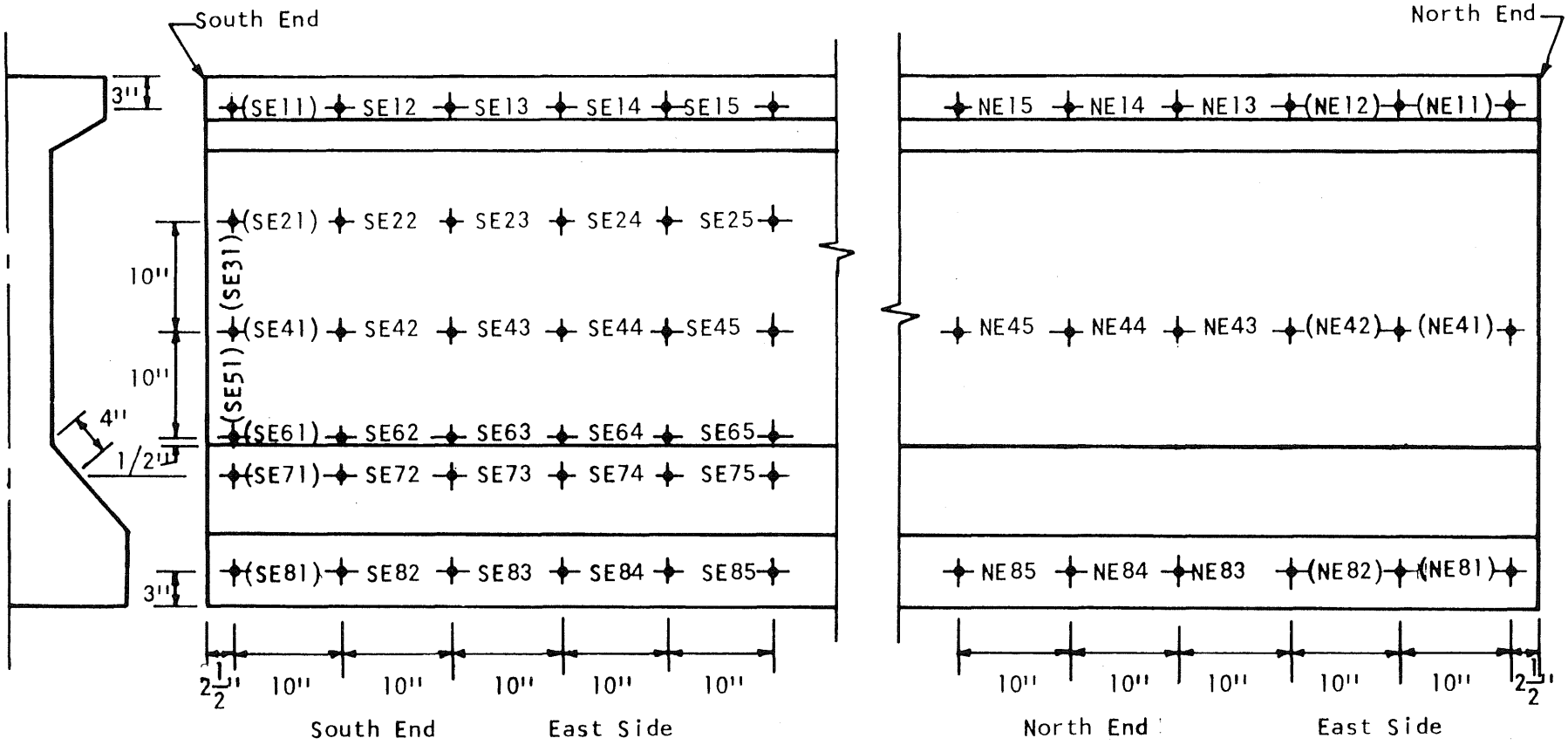

Numbers in Parentheses indicate gage line was lost

Fig. 3.5 LOCATIONS AND DESIGNATIONS OF MECHANICAL STRAIN GAGE LINES ON EAST SIDE OF BEAM BX-4

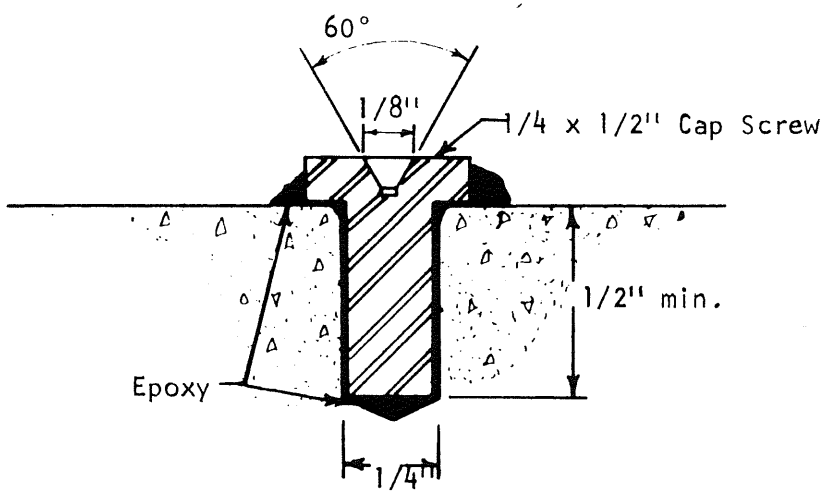

Epoxy-Fixed Gage Point

Fig. 3.6 CROSS-SECTION OF STRAIN GAGE POINT

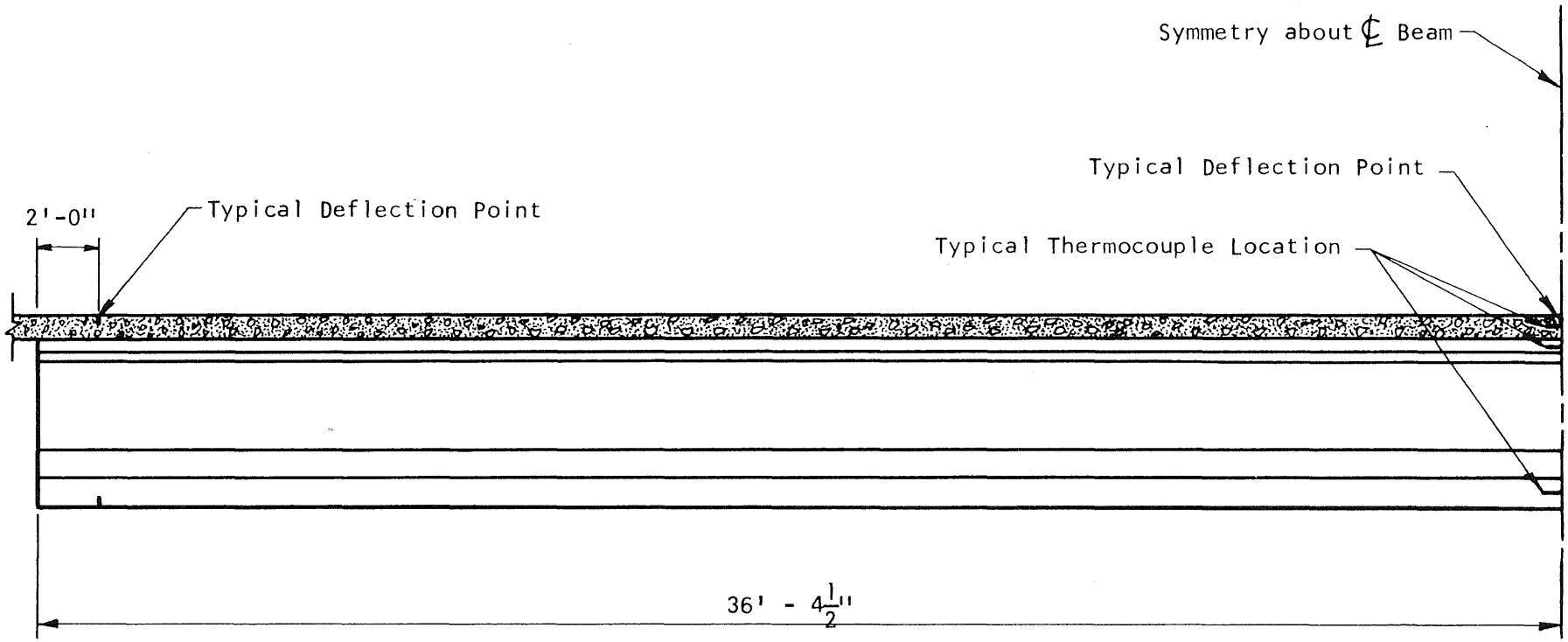

Fig. 3.7 LOCATIONS OF DEFLECTION MEASURING POINTS AND THERMOCOUPLES

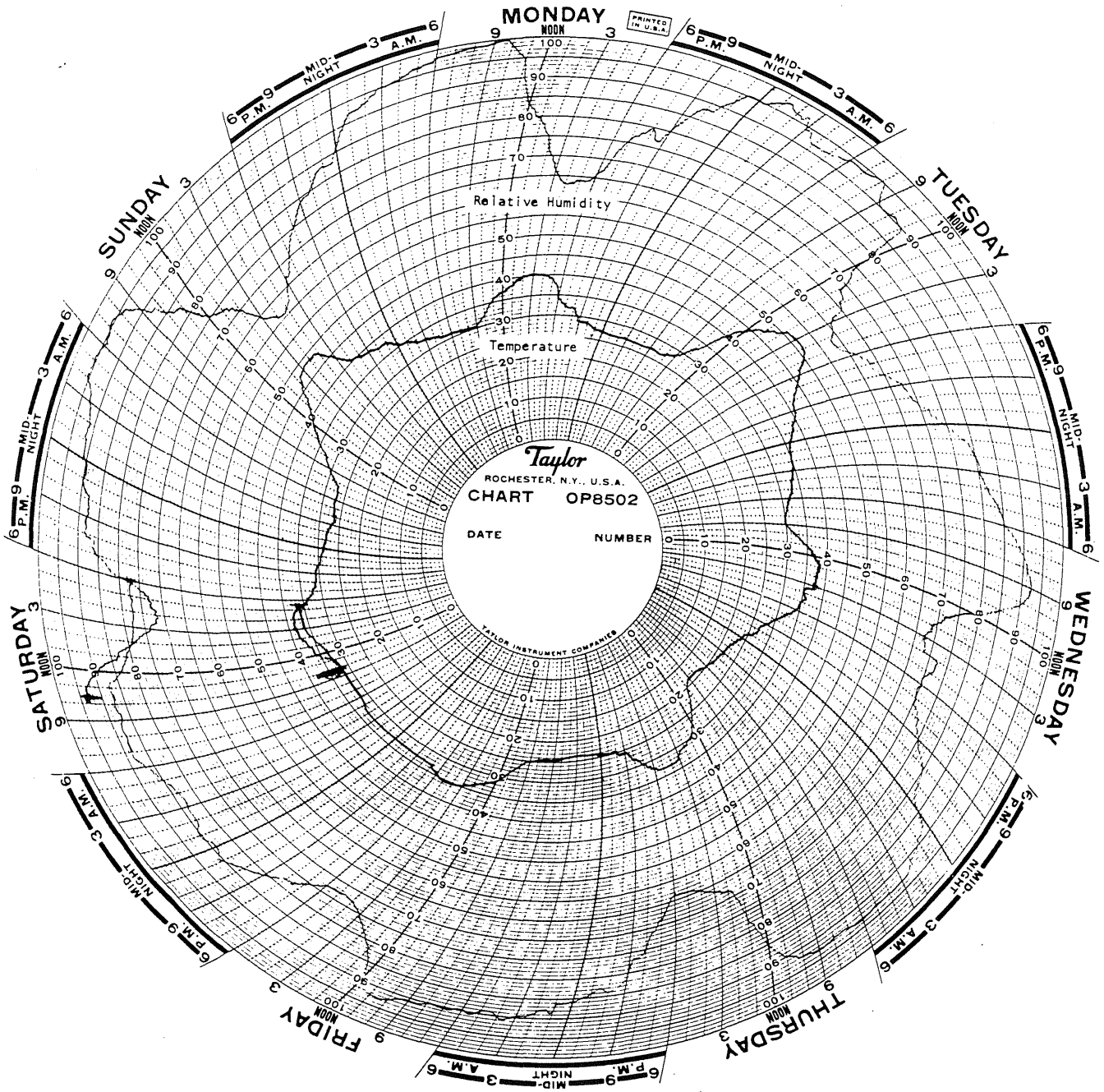

Fig. 3.8 SPECIMEN TEMPERATURE - HUMIDITY CHART
29 Nov. to 6 Dec. 1969

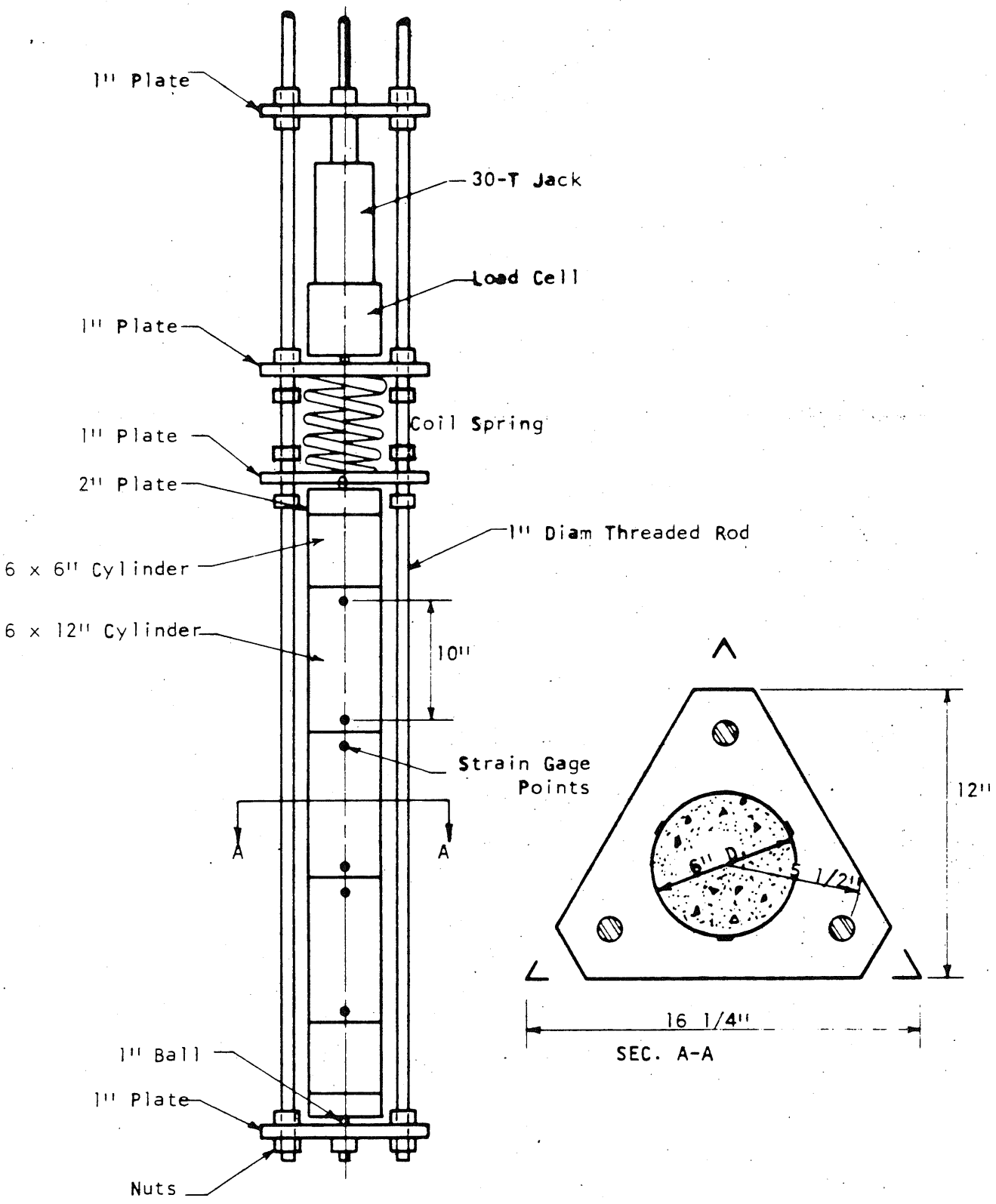

FIG. 3.9 CREEP RACK AND INSTRUMENTATION

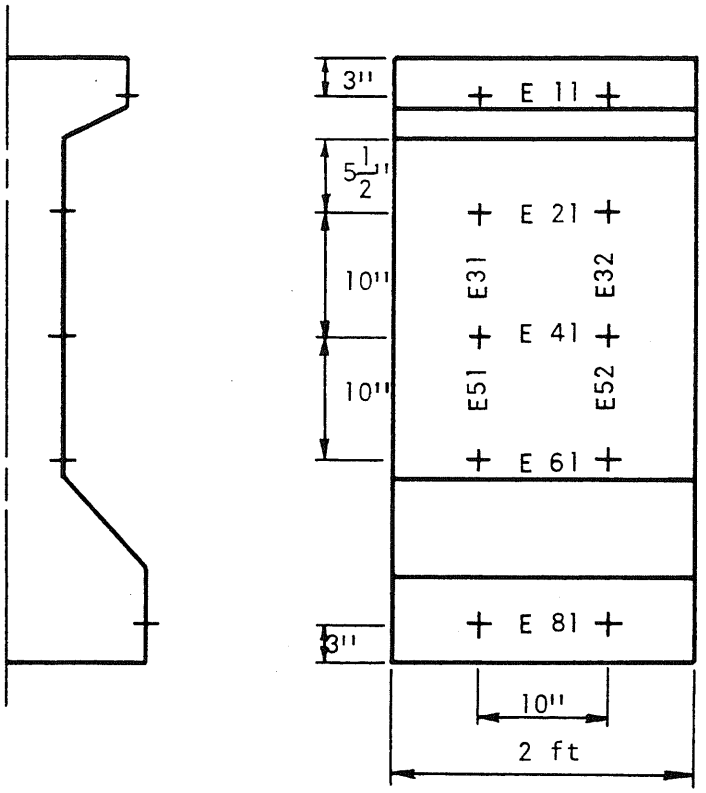

Fig. 3.10 GAGE LINES FOR TWO-FT LONG BEAM SPECIMENS

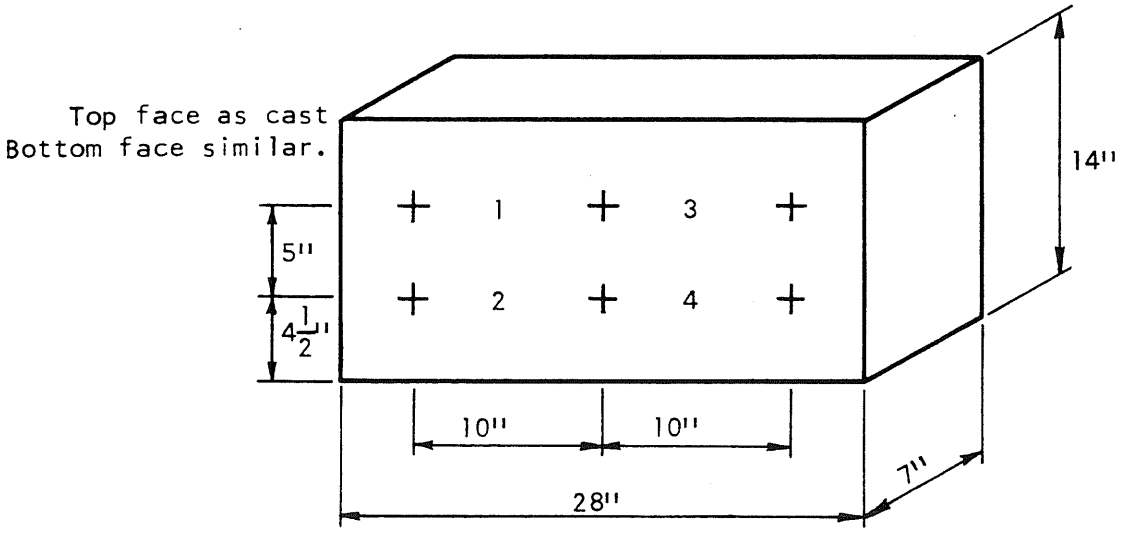

Fig. 3.11 GAGE LINES FOR DECK PRISM SPECIMENS

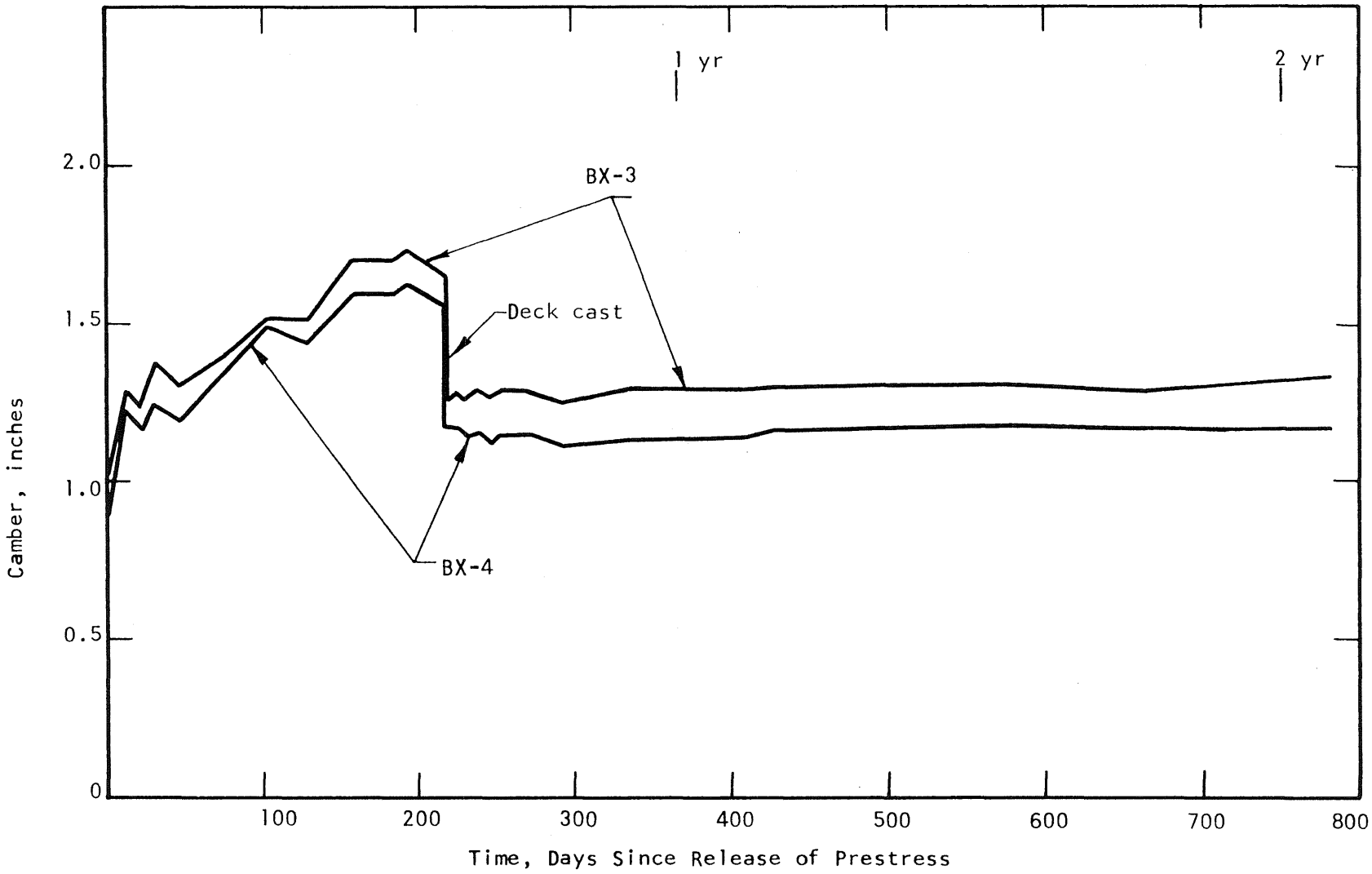

Fig. 4.1 MIDSPAN CAMBER-TIME CURVES

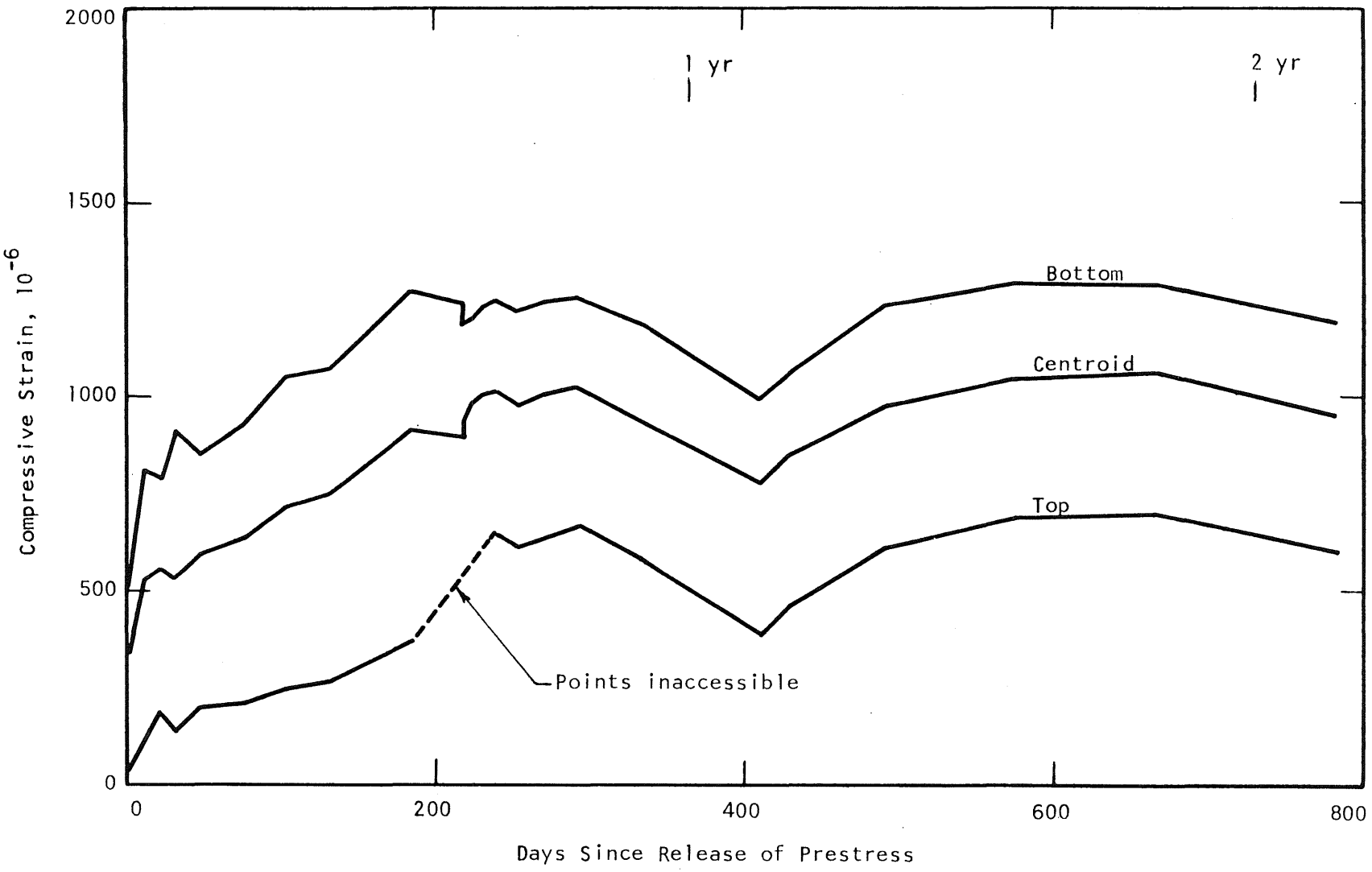

Fig. 4.2 MIDSPAN STRAIN-TIME CURVES, BX-3, WHITTEMORE GAGE

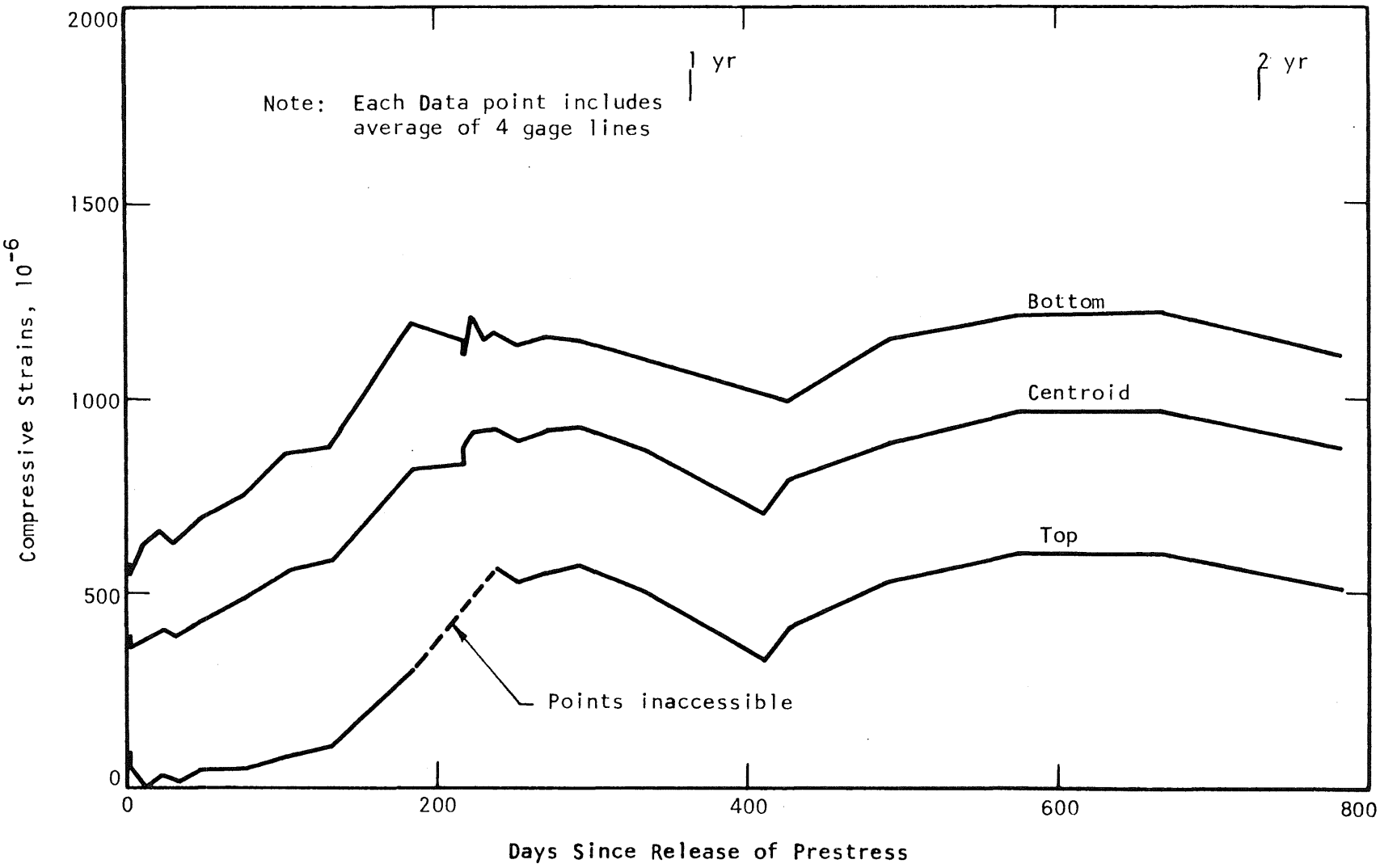

Fig. 4.3 MID-SPAN STRAIN-TIME CURVES, BX-4, WHITTEMORE GAGE

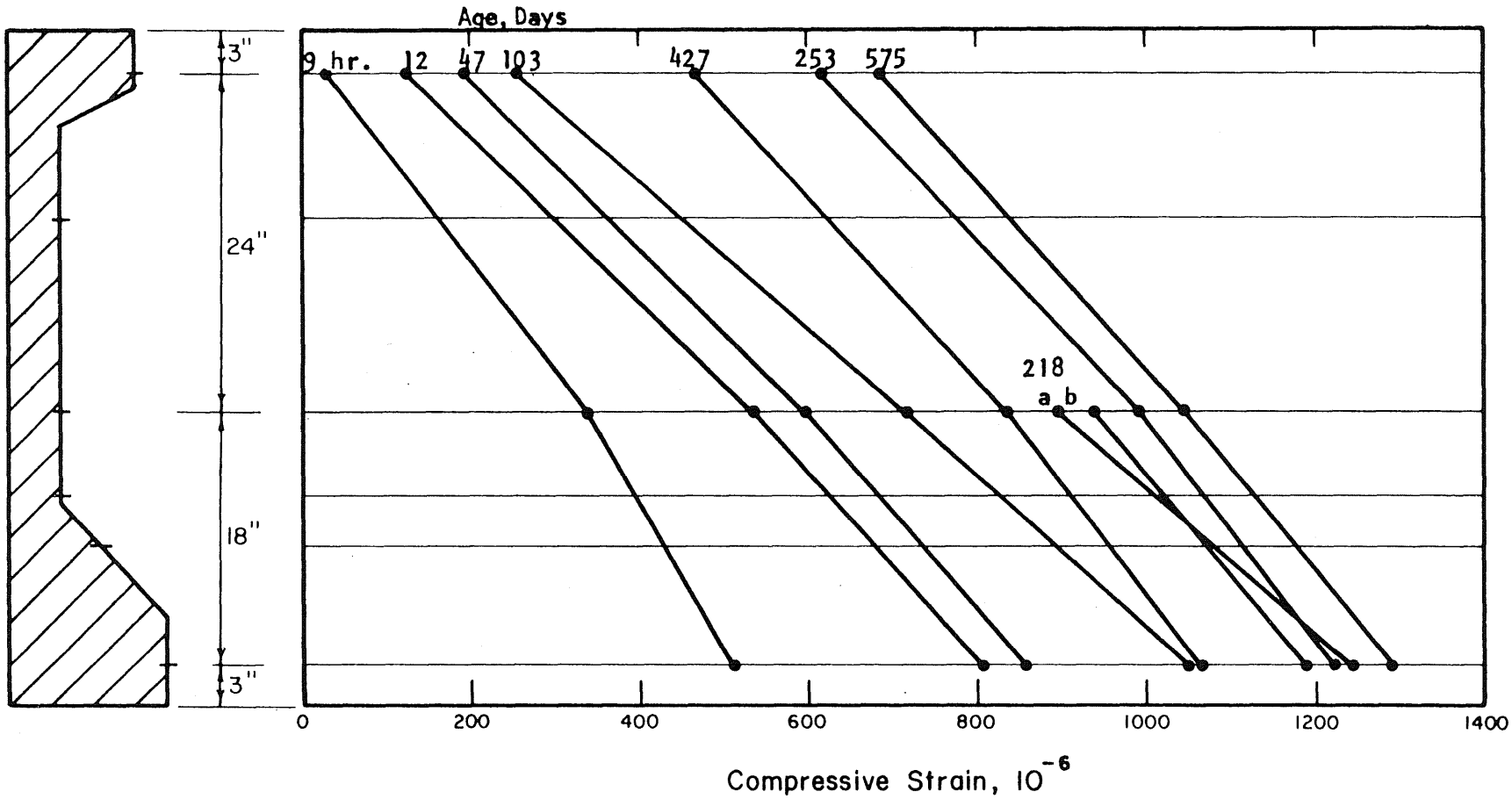

Fig. 4.4 BX-3 MIDSPAN STRAIN DISTRIBUTION

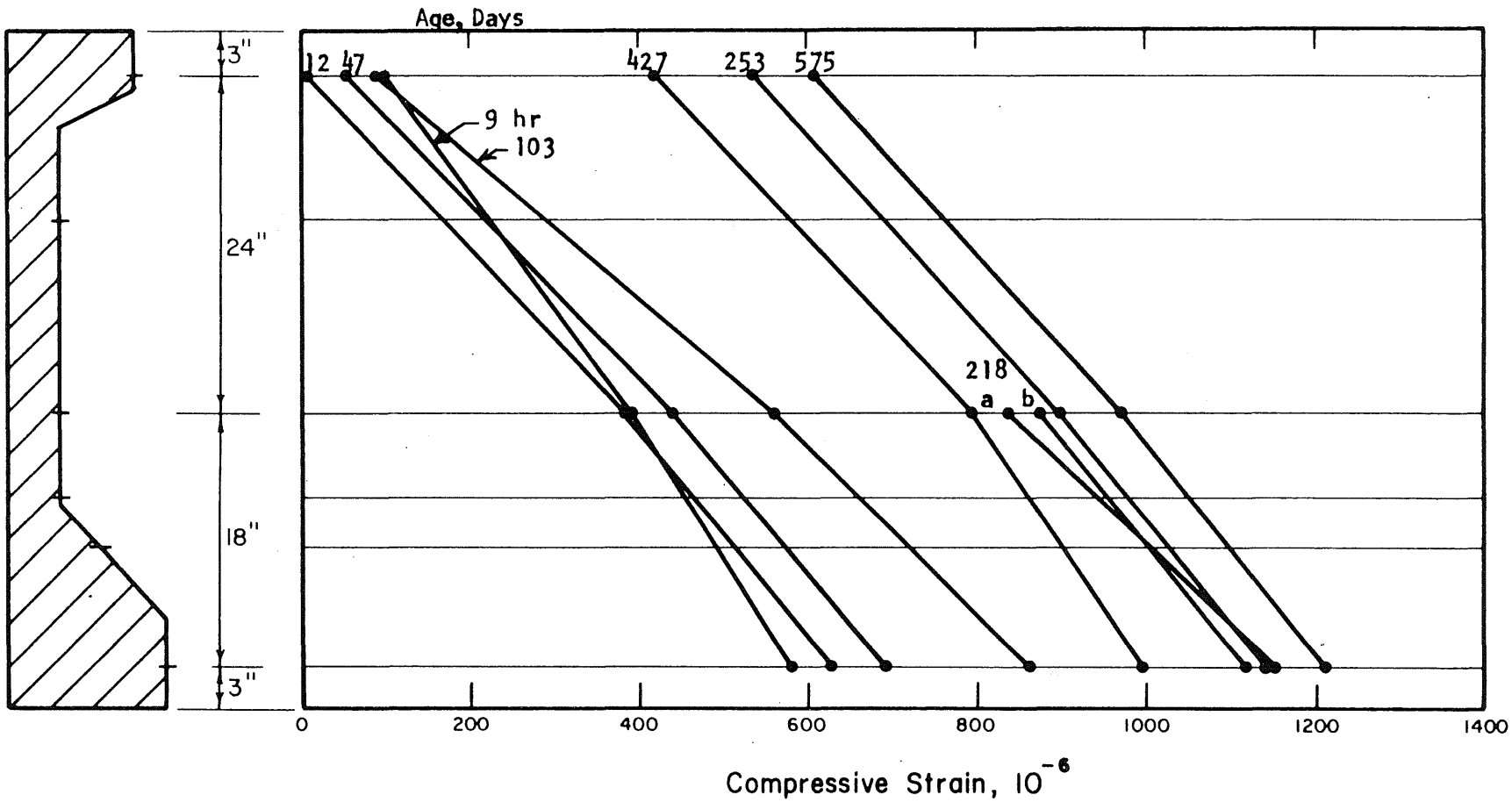

Fig. 4.5 BX-4 MIDSPAN STRAIN DISTRIBUTION

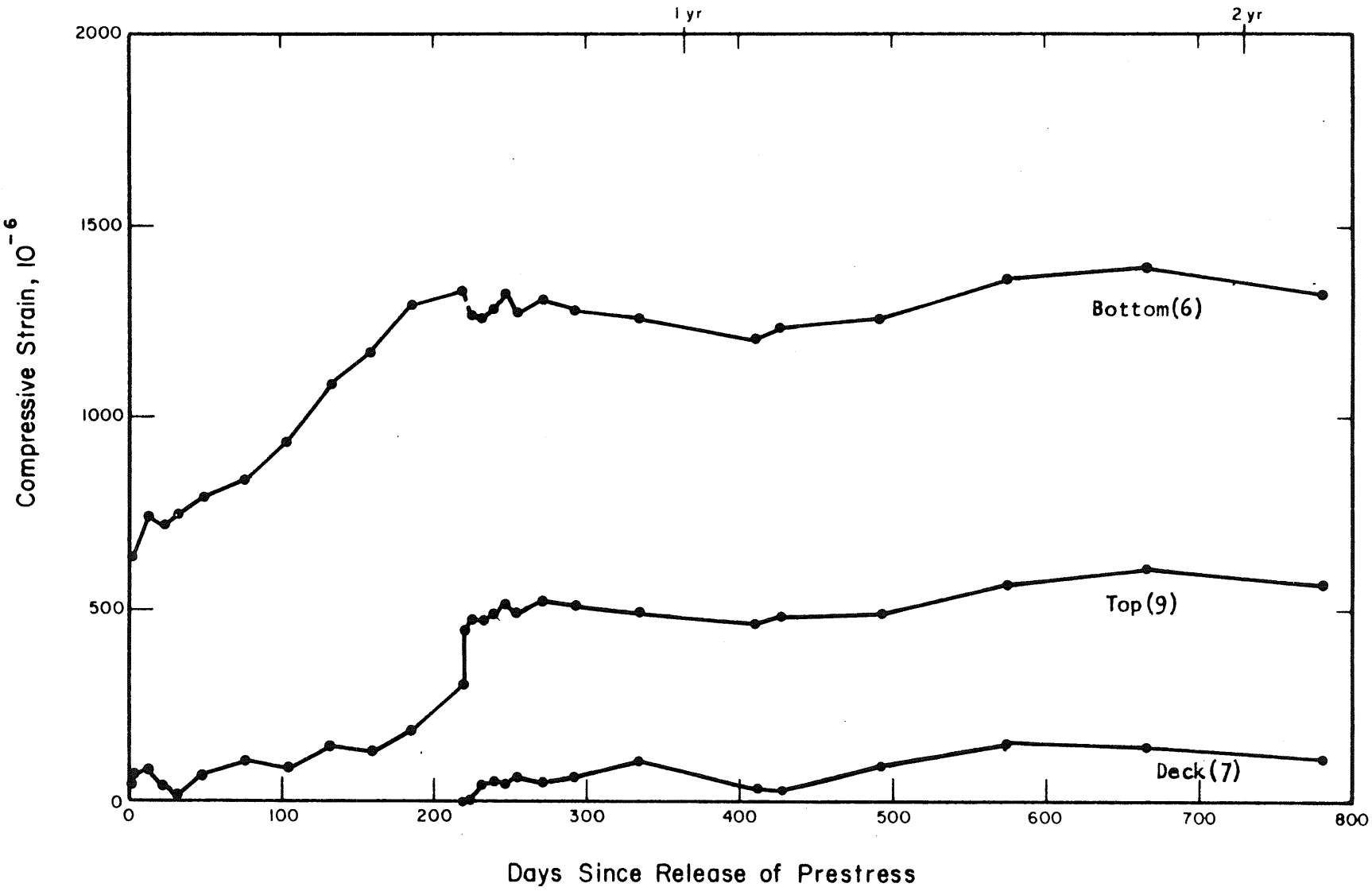

Fig. 4.6 MIDSPAN STRAIN-TIME CURVES FROM CARLSON METERS, BX-3

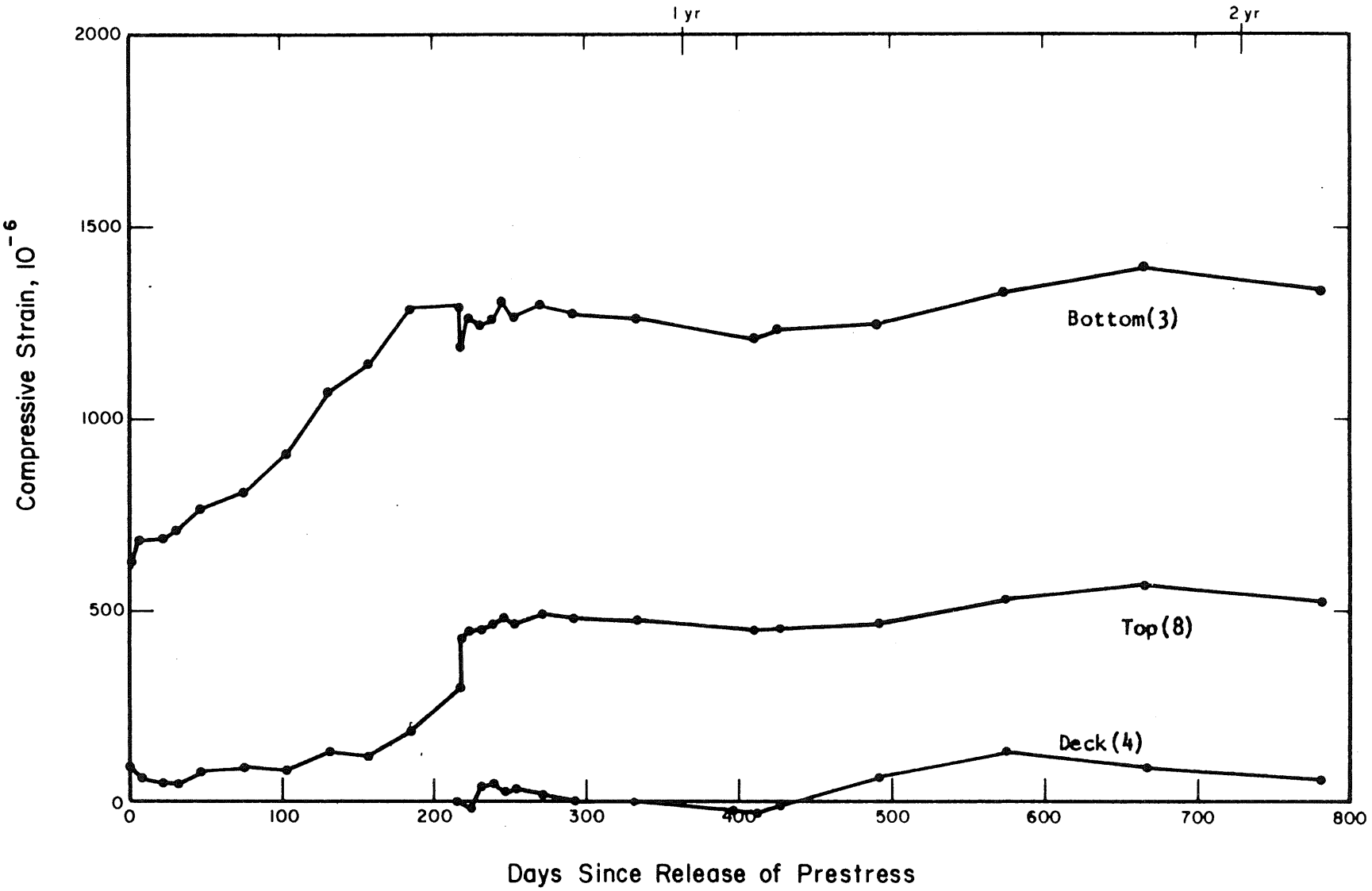

Fig. 4.7 MIDSPAN STRAIN-TIME CURVES FROM CARLSON METERS, BX-4

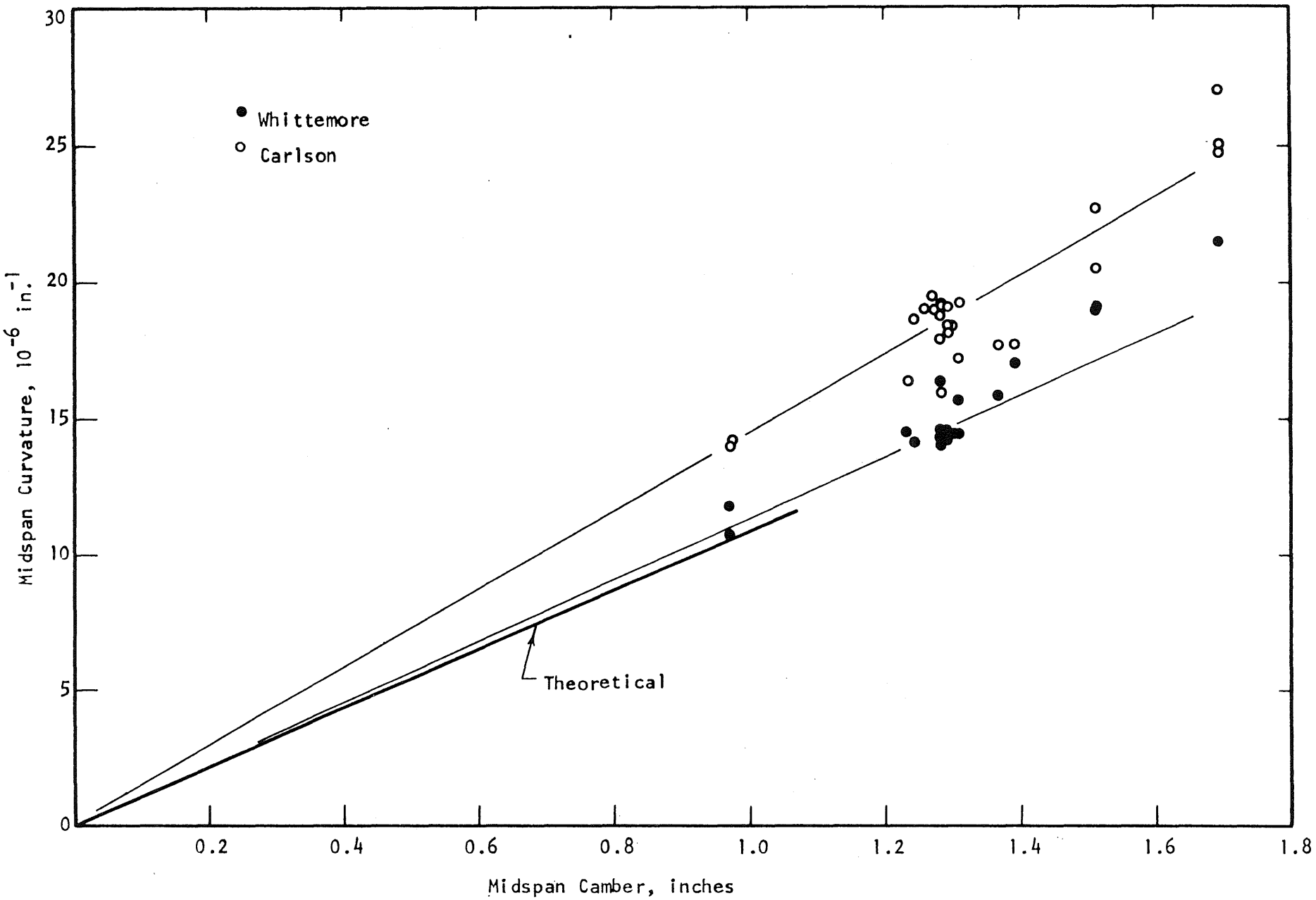

Fig. 4.8 MEASURED CURVATURES VS CAMBER AT MIDSPAN OF BX-3

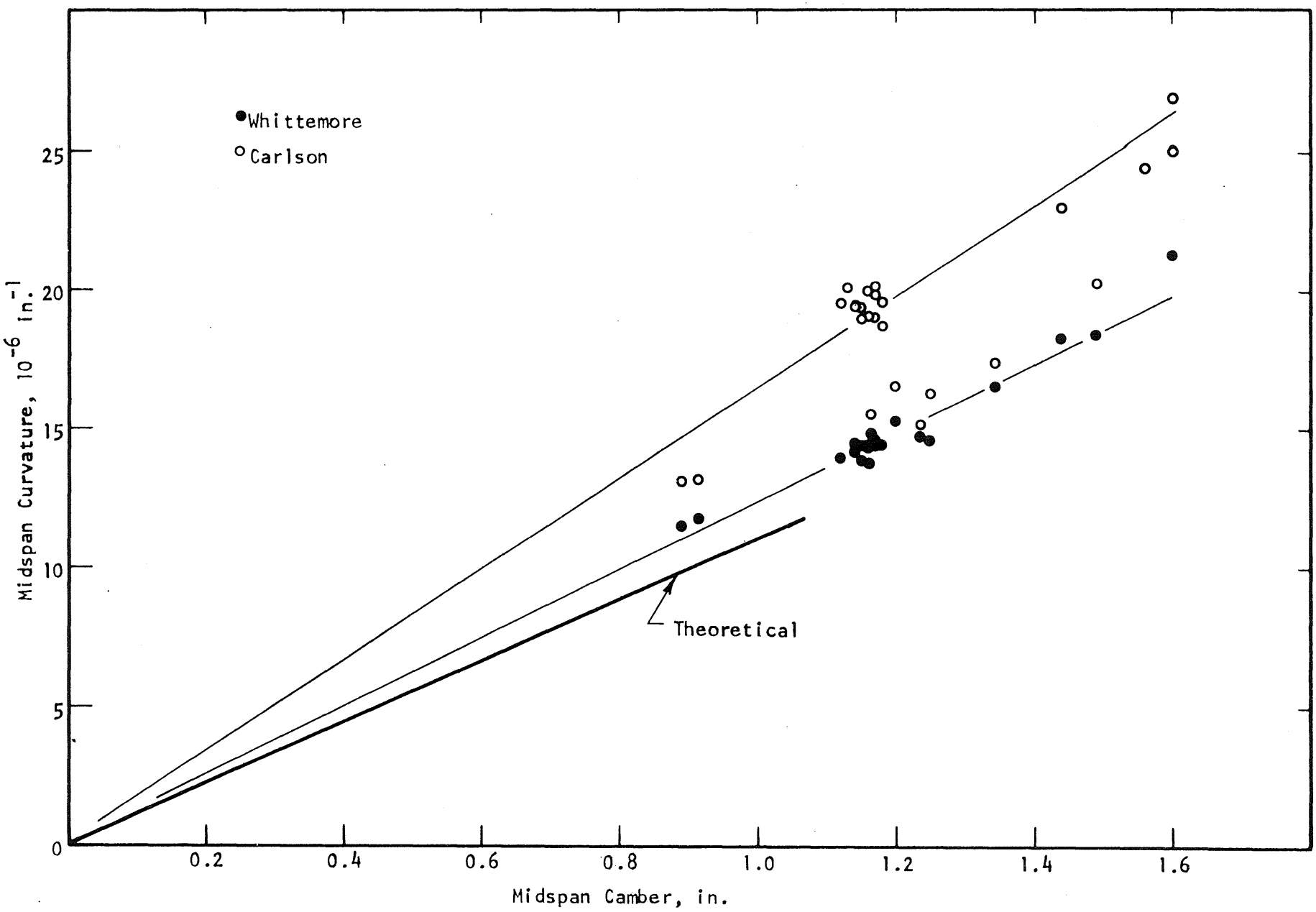

Fig. 4.9 MEASURED CURVATURES VS CAMBER AT MIDSPAN OF BX-4

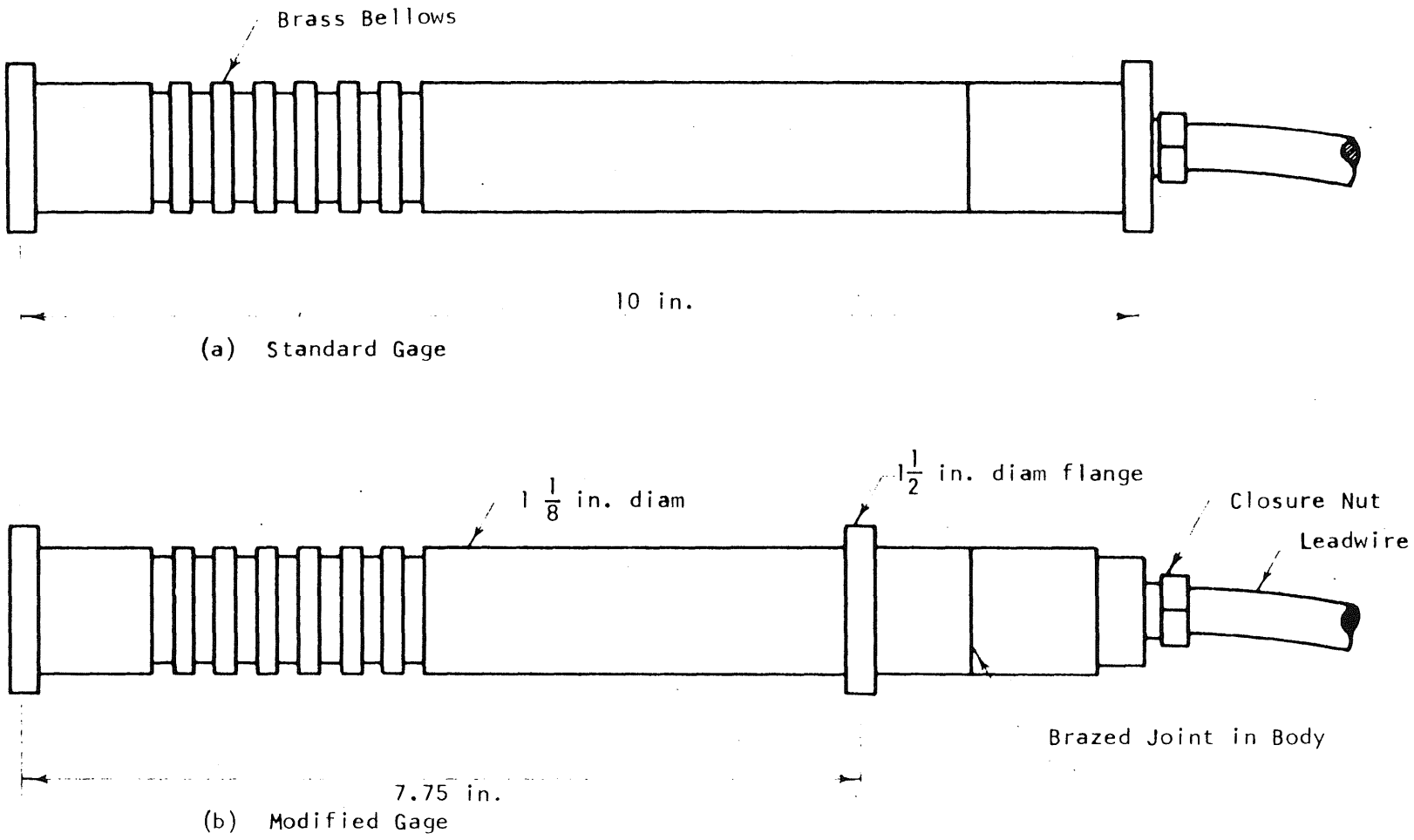

FIG. 4.10 PROFILES OF STANDARD AND MODIFIED CARLSON STRAIN METERS

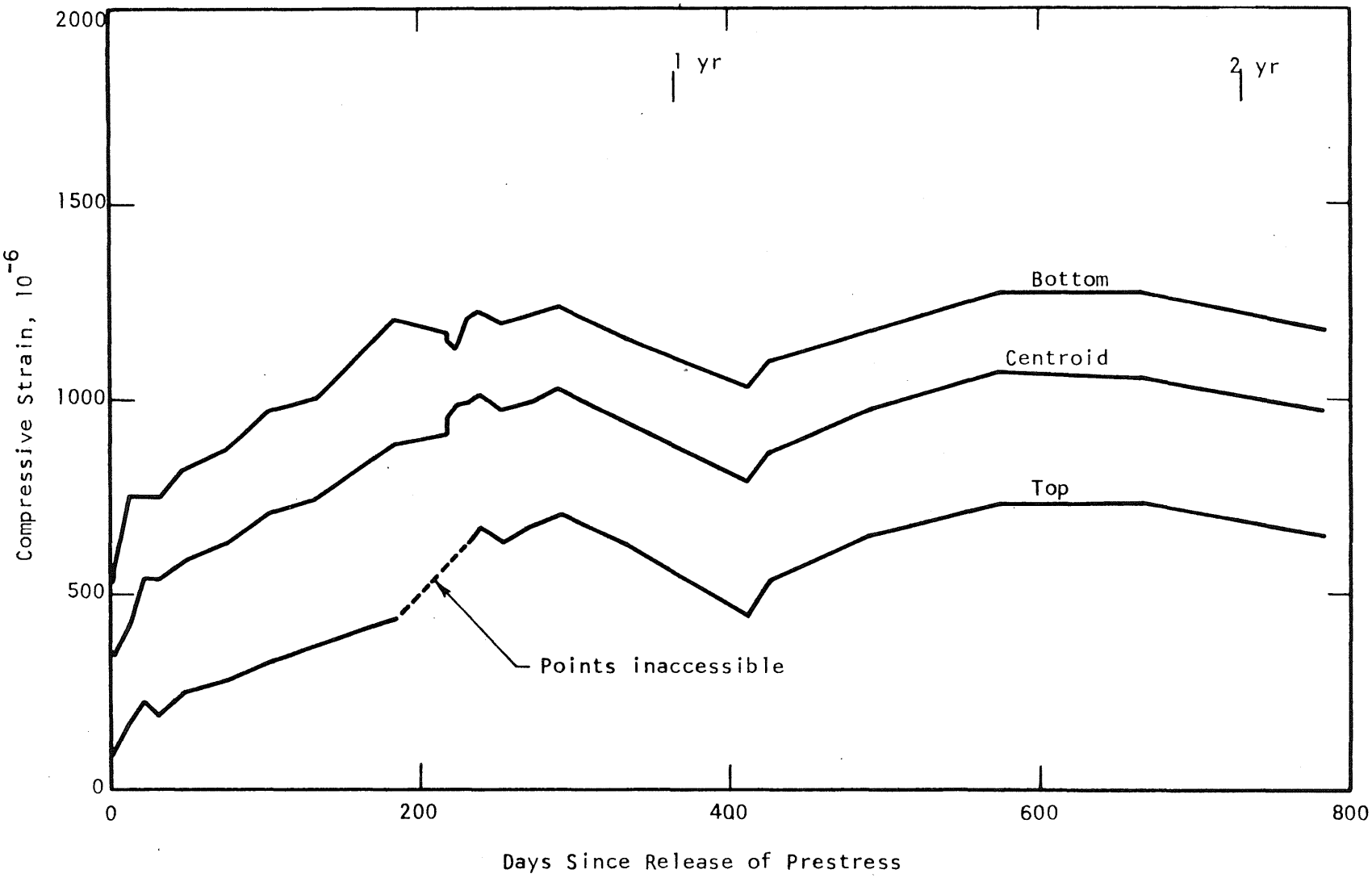

Fig. 4.11 QUARTER-POINT STRAIN-TIME CURVES, BX-3, WHITTEMORE GAGE

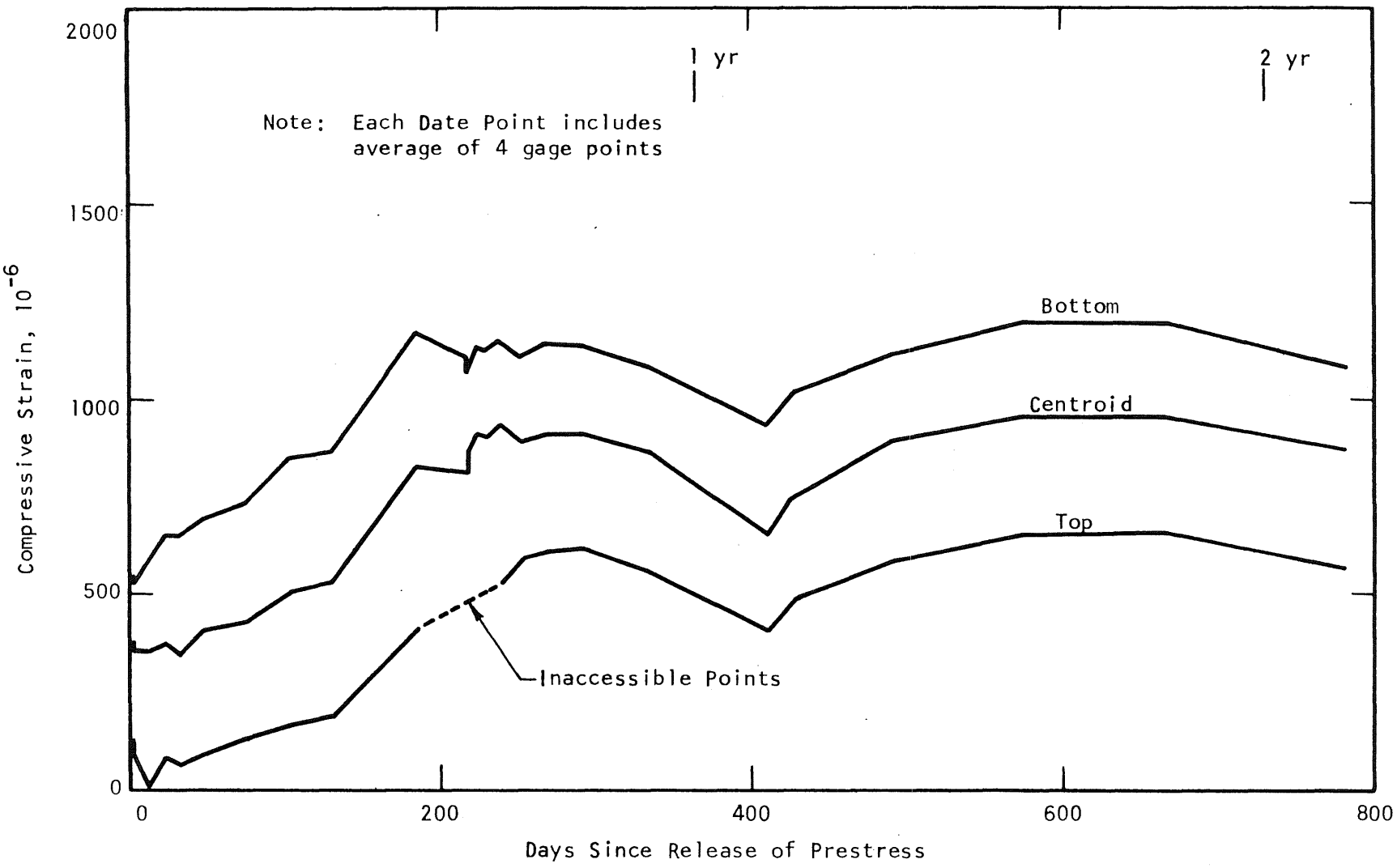

Fig. 4.12 QUARTER-POINT STRAIN-TIME CURVES, BX-4, WHITTEMORE GAGE

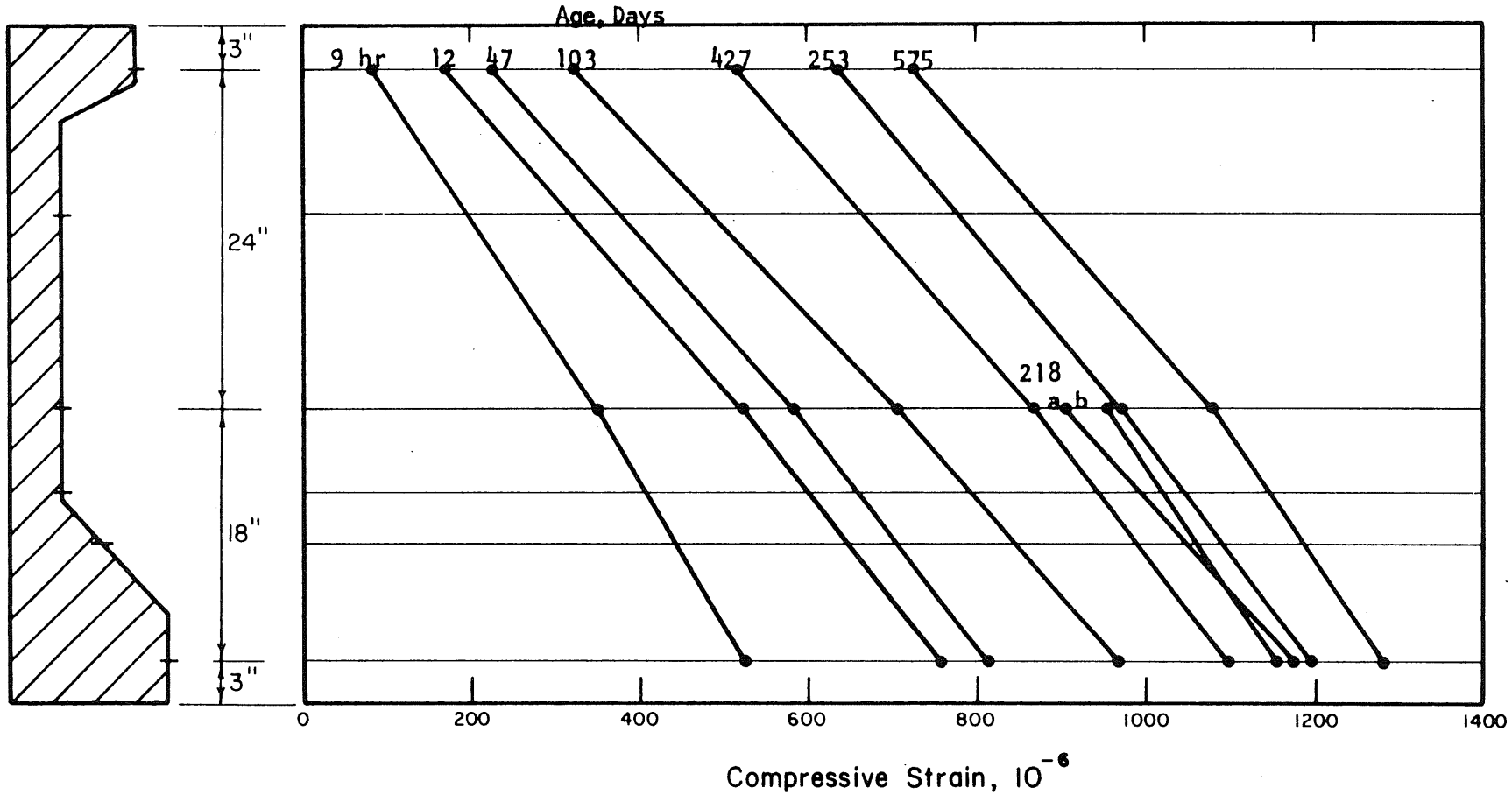

Fig. 4.13 BX-3 QUARTER POINT STRAIN DISTRIBUTION

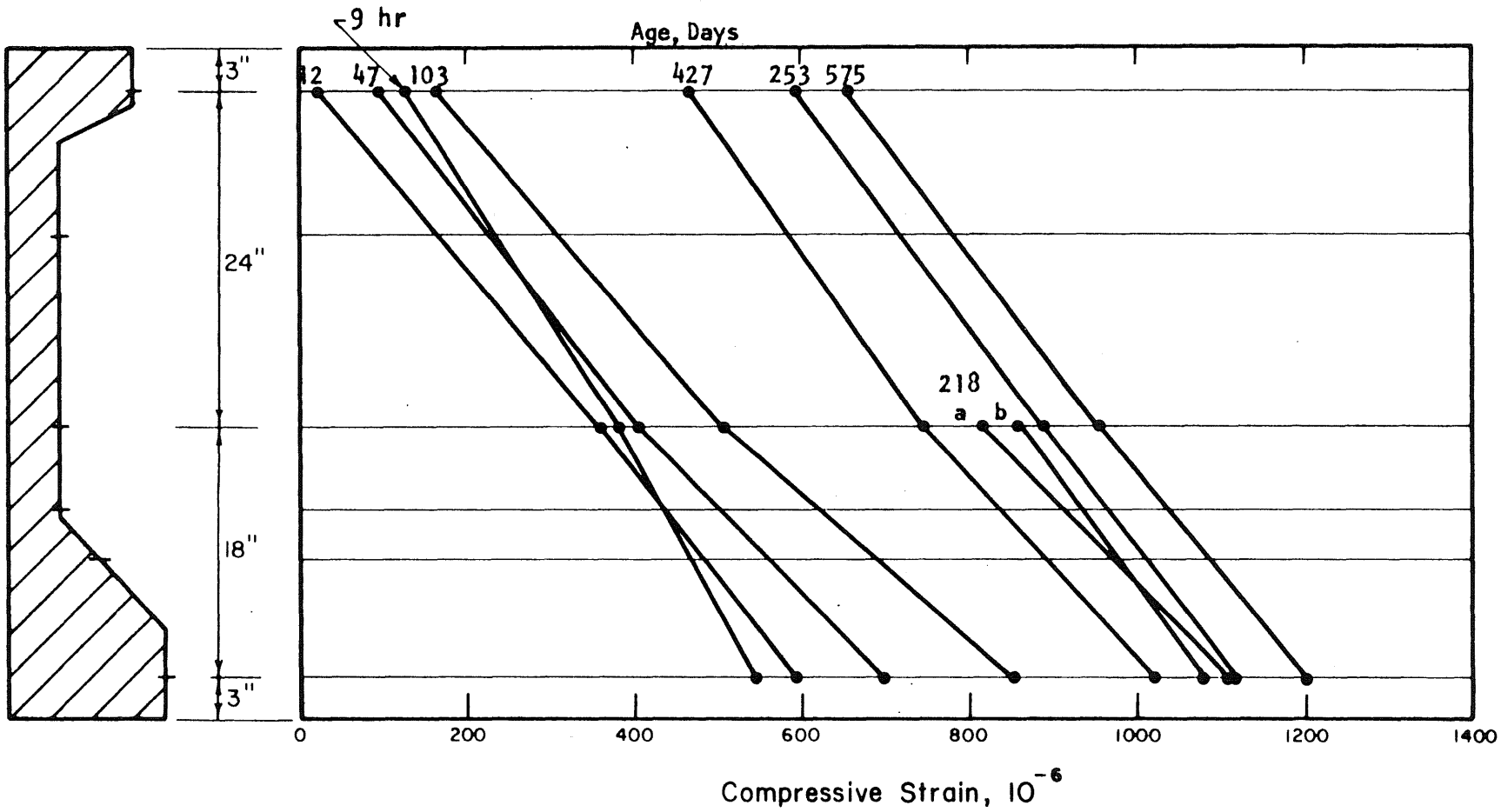

Fig. 4.14 BX-4 QUARTER POINT STRAIN DISTRIBUTION

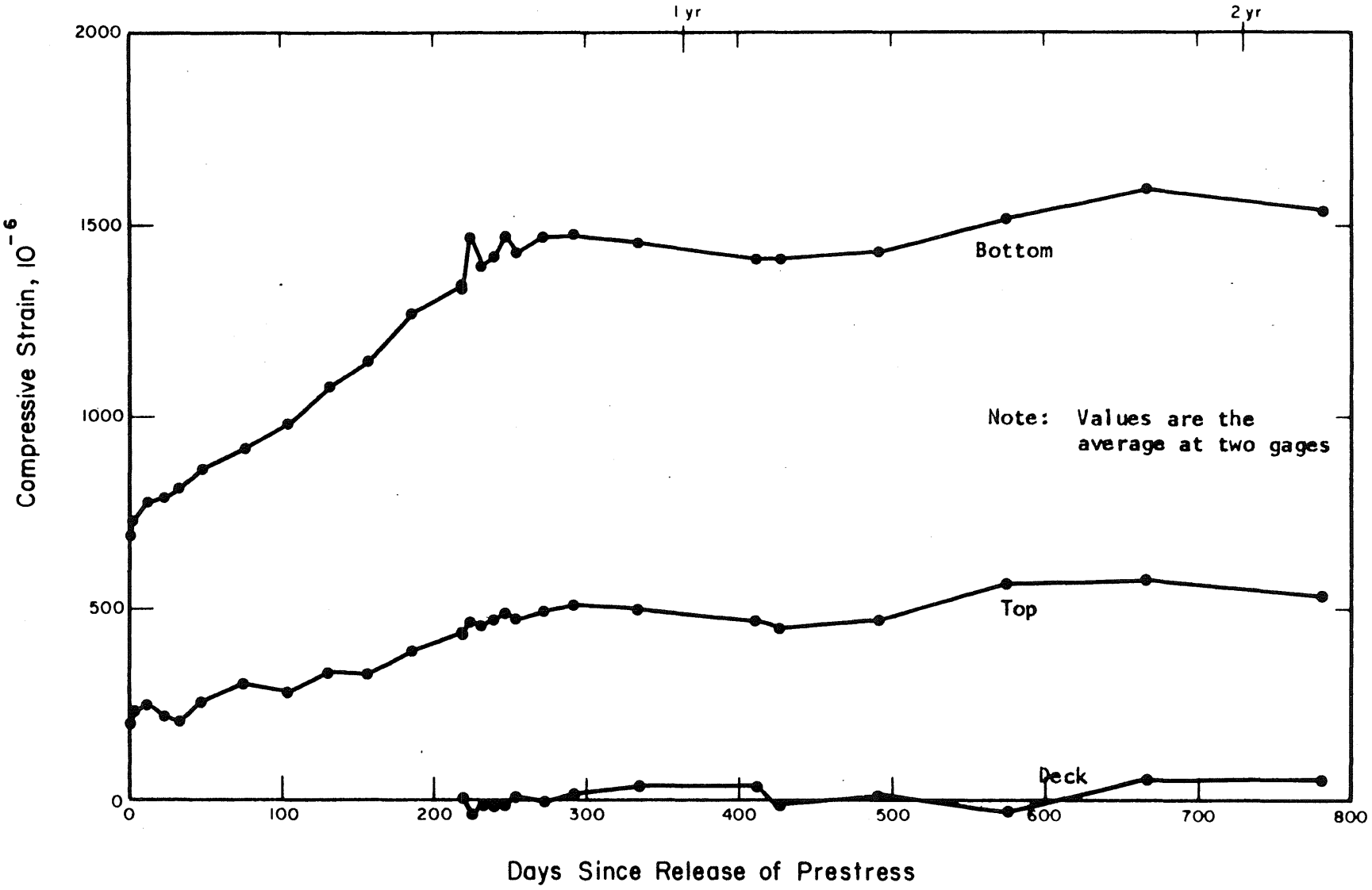

Fig. 4.15 STRAIN-TIME CURVES FROM CARLSON METERS NEAR ENDS OF BEAM BX-3

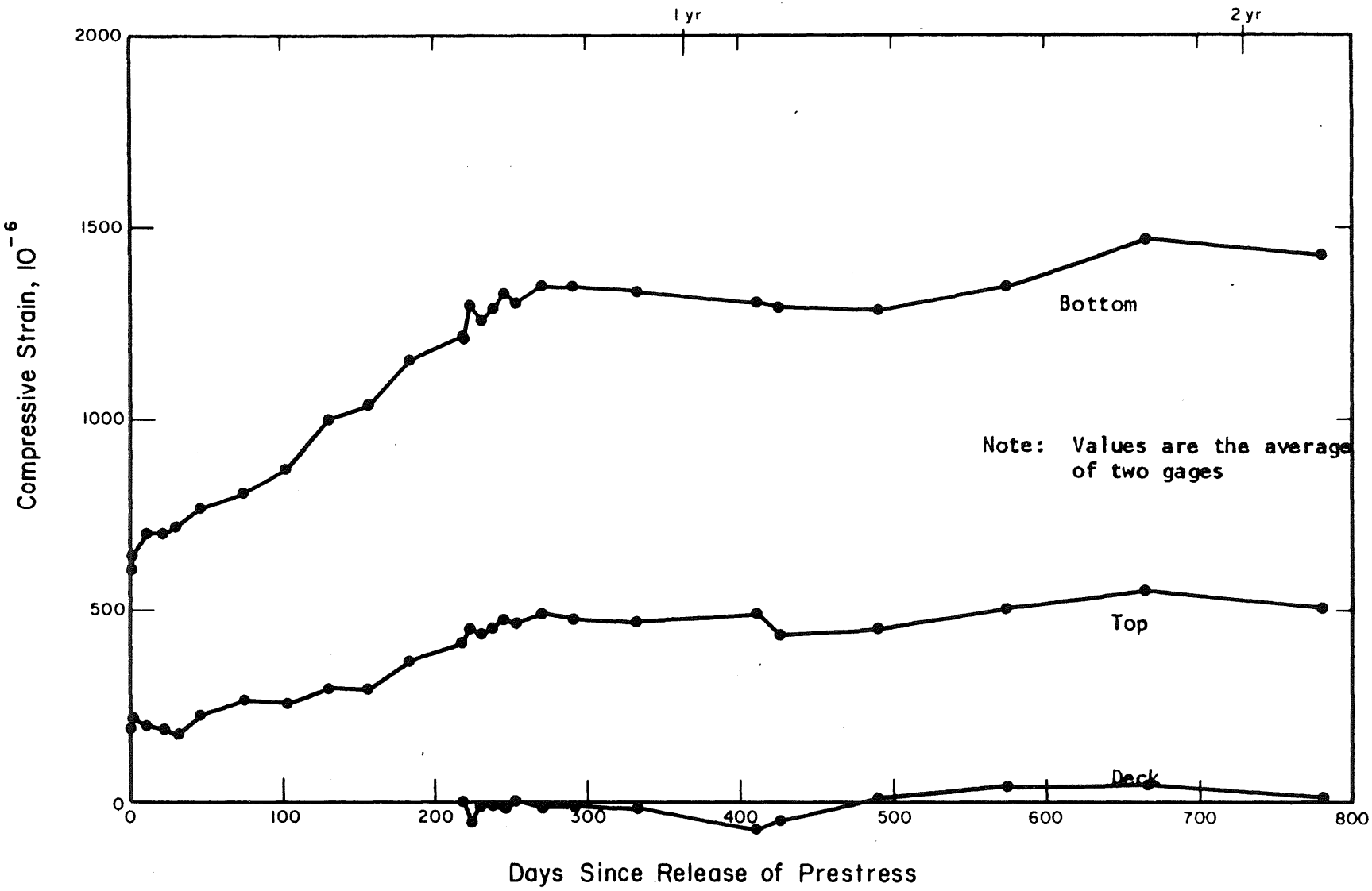

Fig. 4.16 STRAIN-TIME CURVES FROM CARLSON METERS NEAR ENDS OF BEAM BX-4

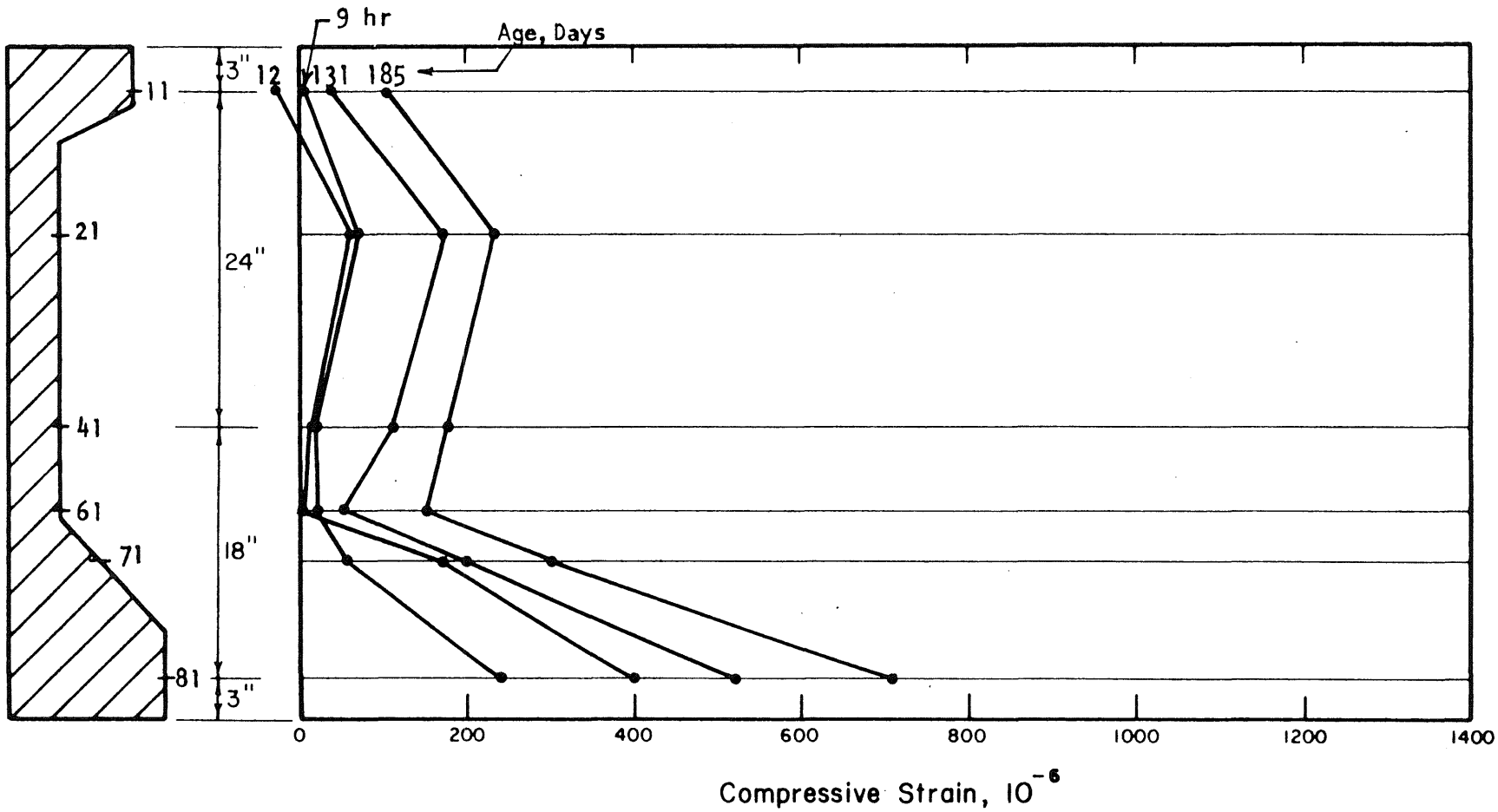

Fig. 4.17 STRAIN DISTRIBUTION AT SECTION 7.5 in. FROM SOUTH END OF BX-3

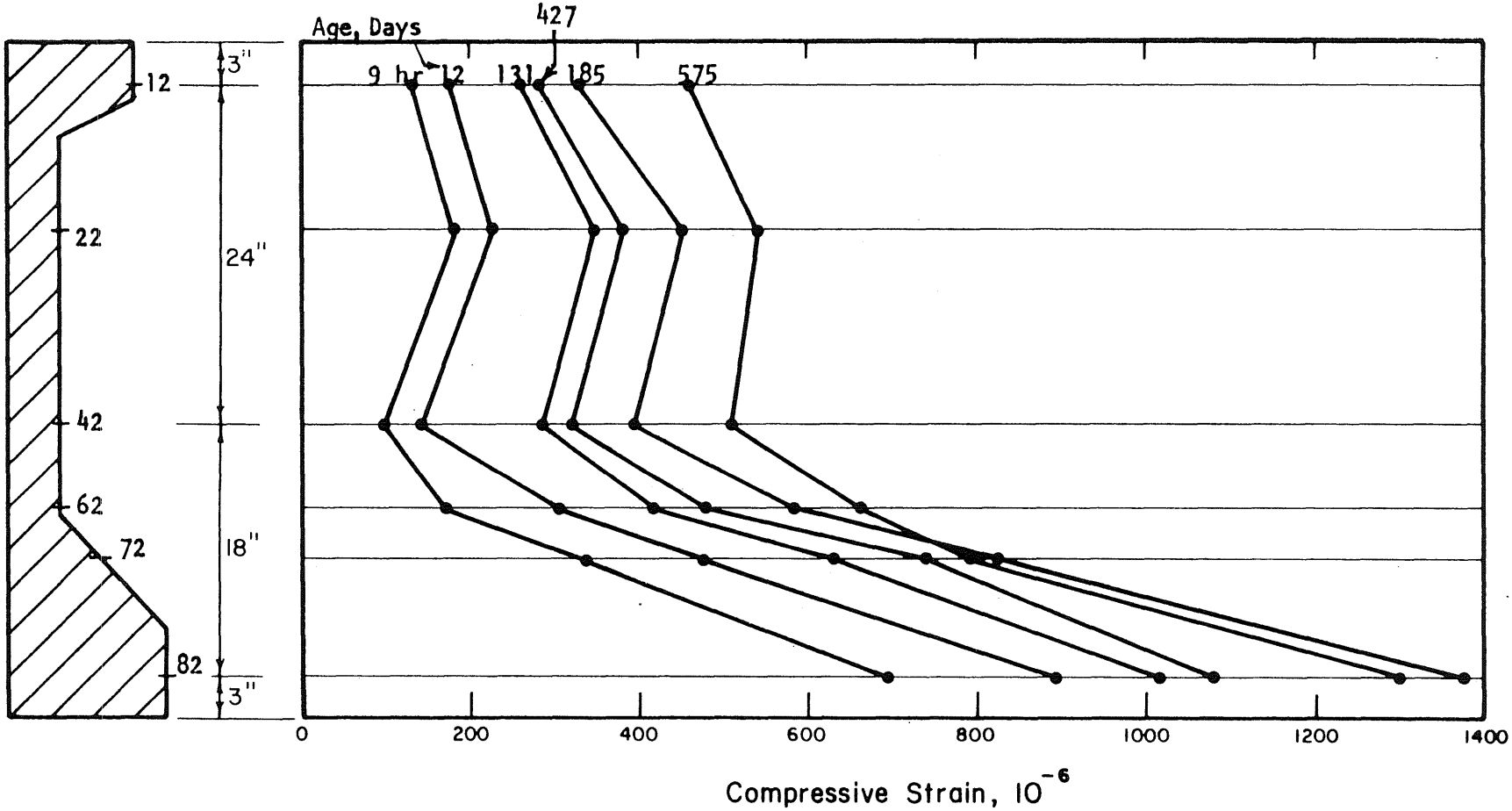

Fig. 4.18 STRAIN DISTRIBUTION AT SECTION 17.5 In. FROM SOUTH END OF BX-3

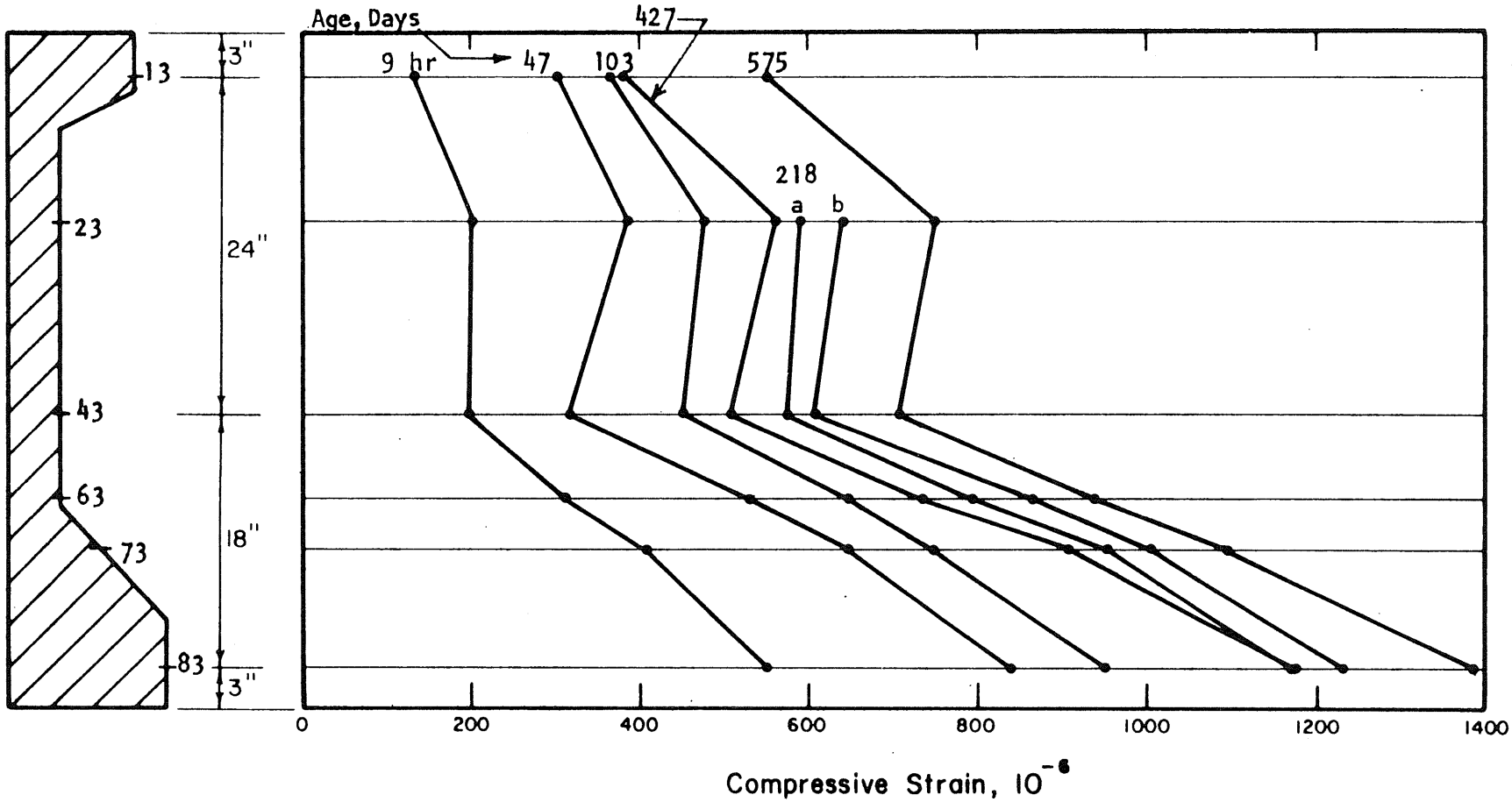

Fig. 4.19 STRAIN DISTRIUBTION AT SECTION 27.5 In. FROM SOUTH END OF BX-3

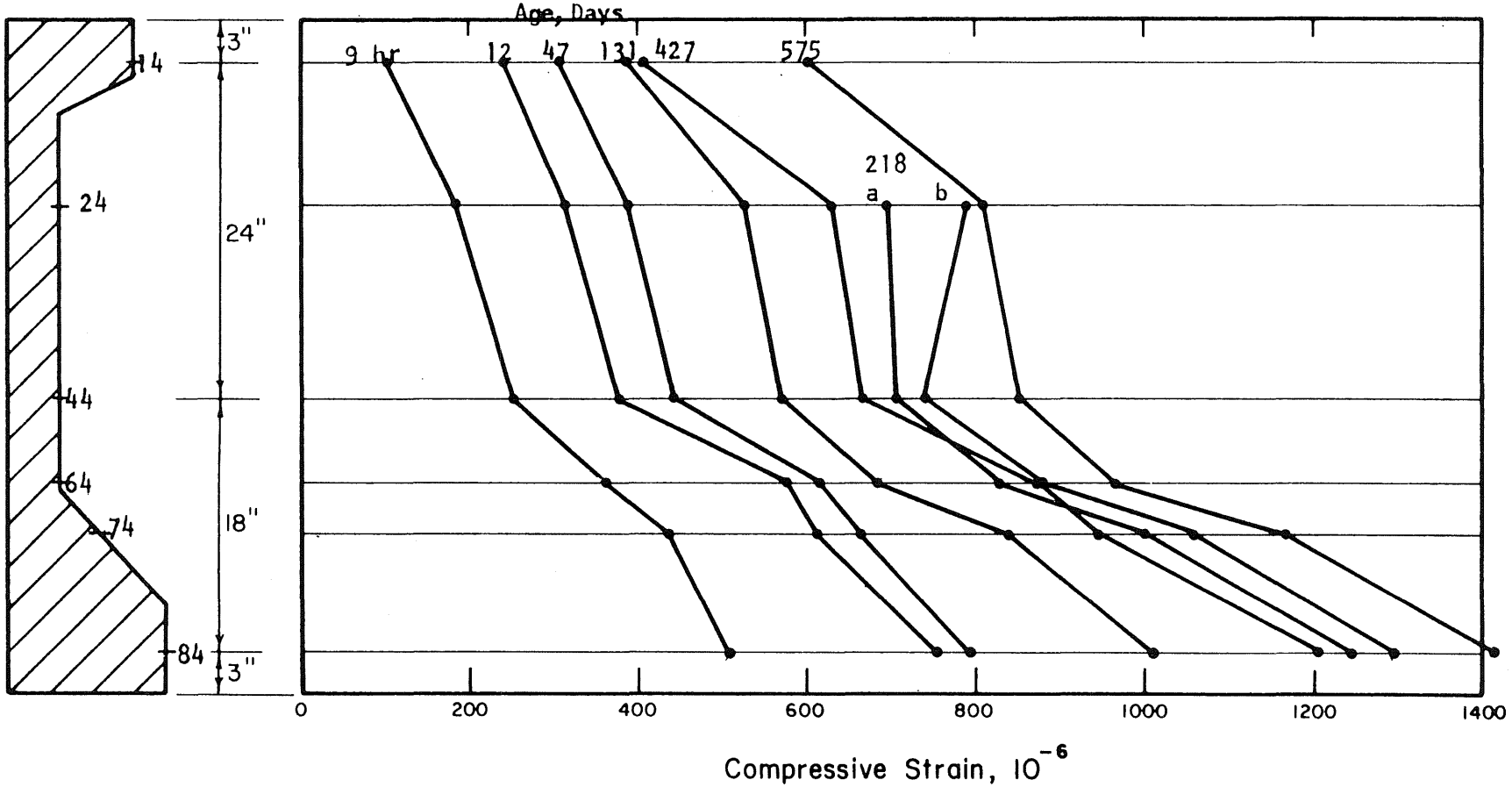

Fig. 4.20 STRAIN DISTRIBUTION AT SECTION 37.5 in. FROM SOUTH END OF BX-3

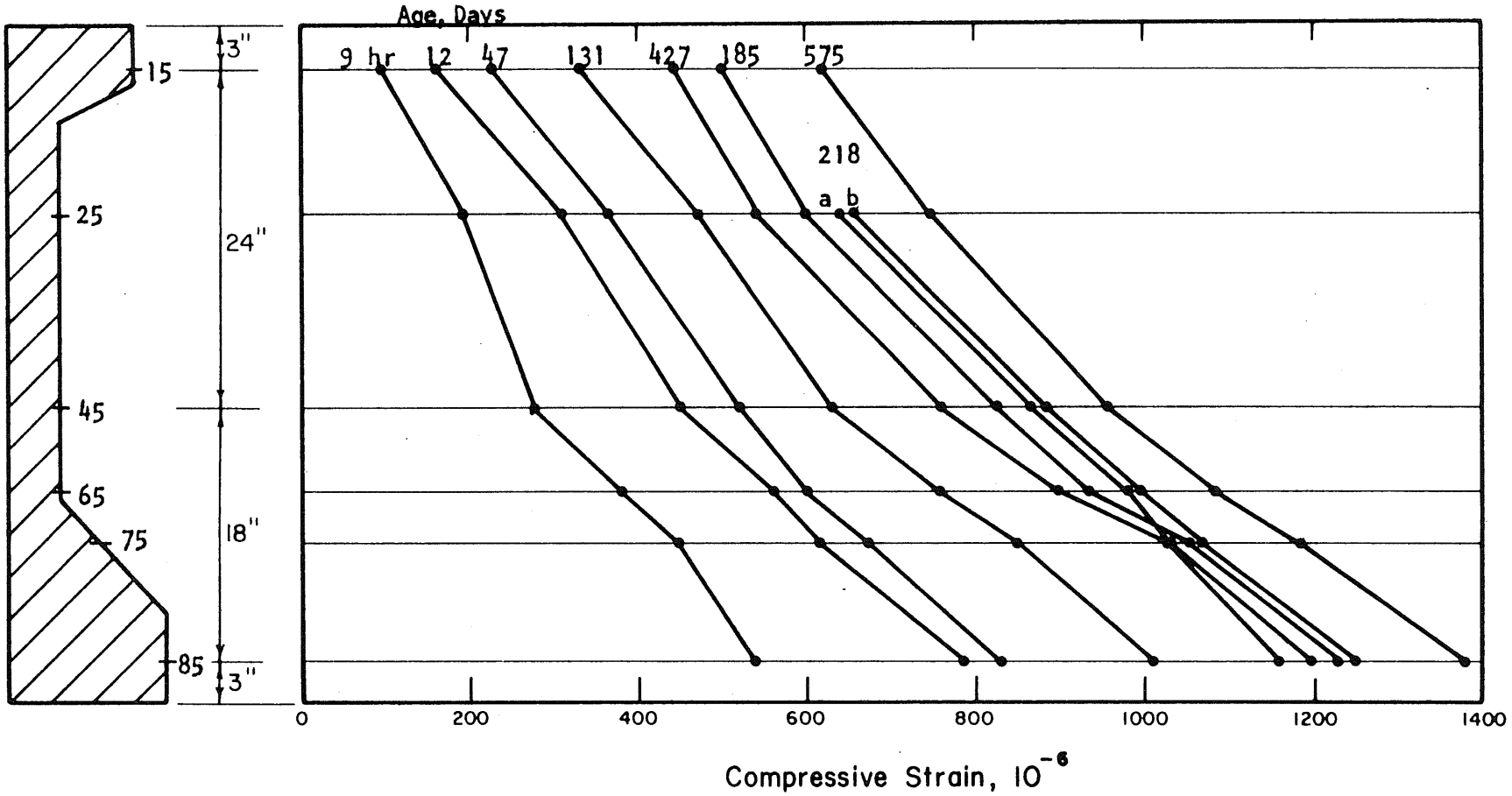

Fig. 4.21 STRAIN DISTRIBUTION AT SECTION 47.5 in. FROM SOUTH END OF BX-3

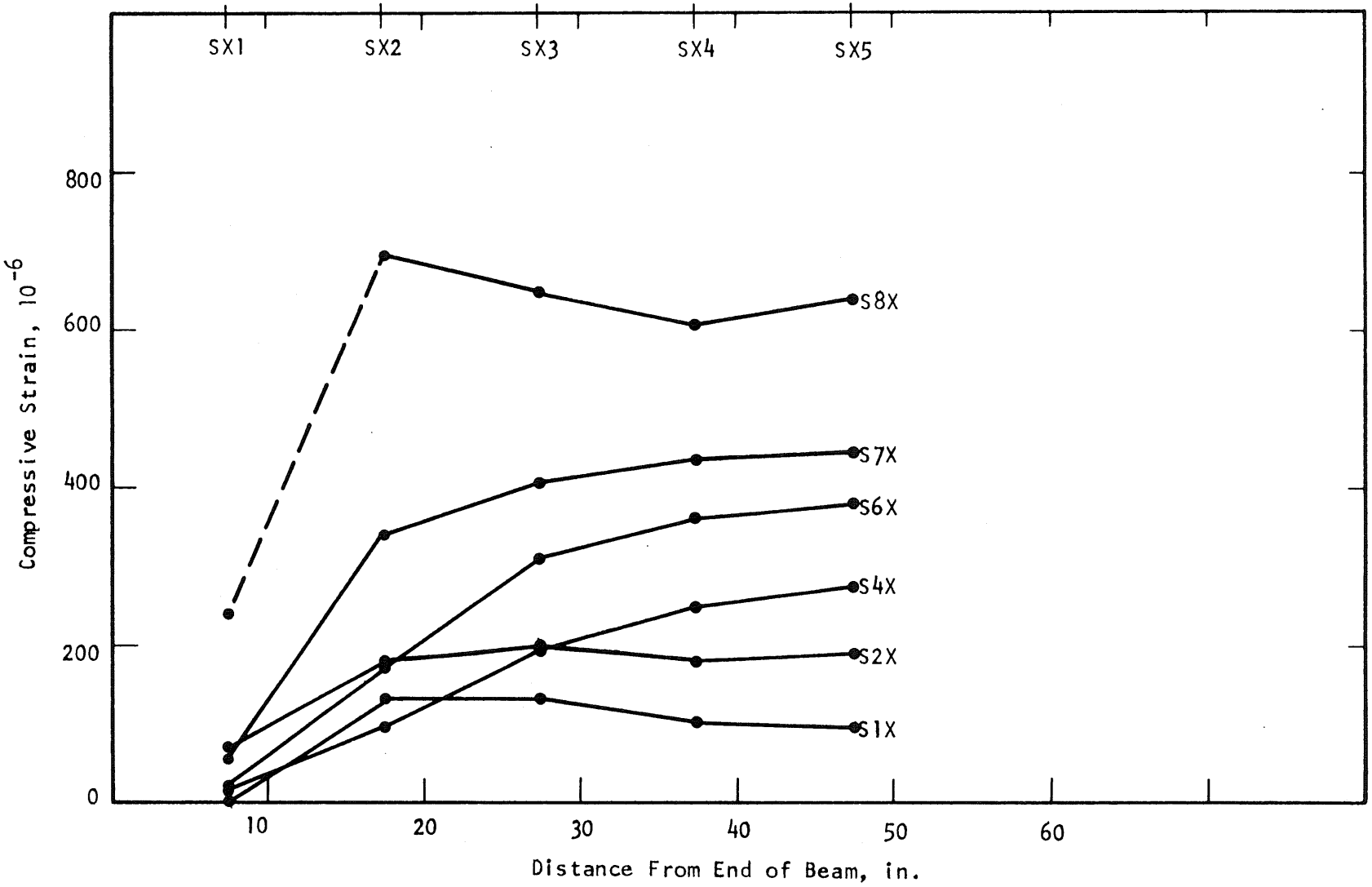

Fig. 4.22 DISTRIBUTION OF LONGITUDINAL STRAIN ALONG BX-3 NEAR SOUTH END AT RELEASE

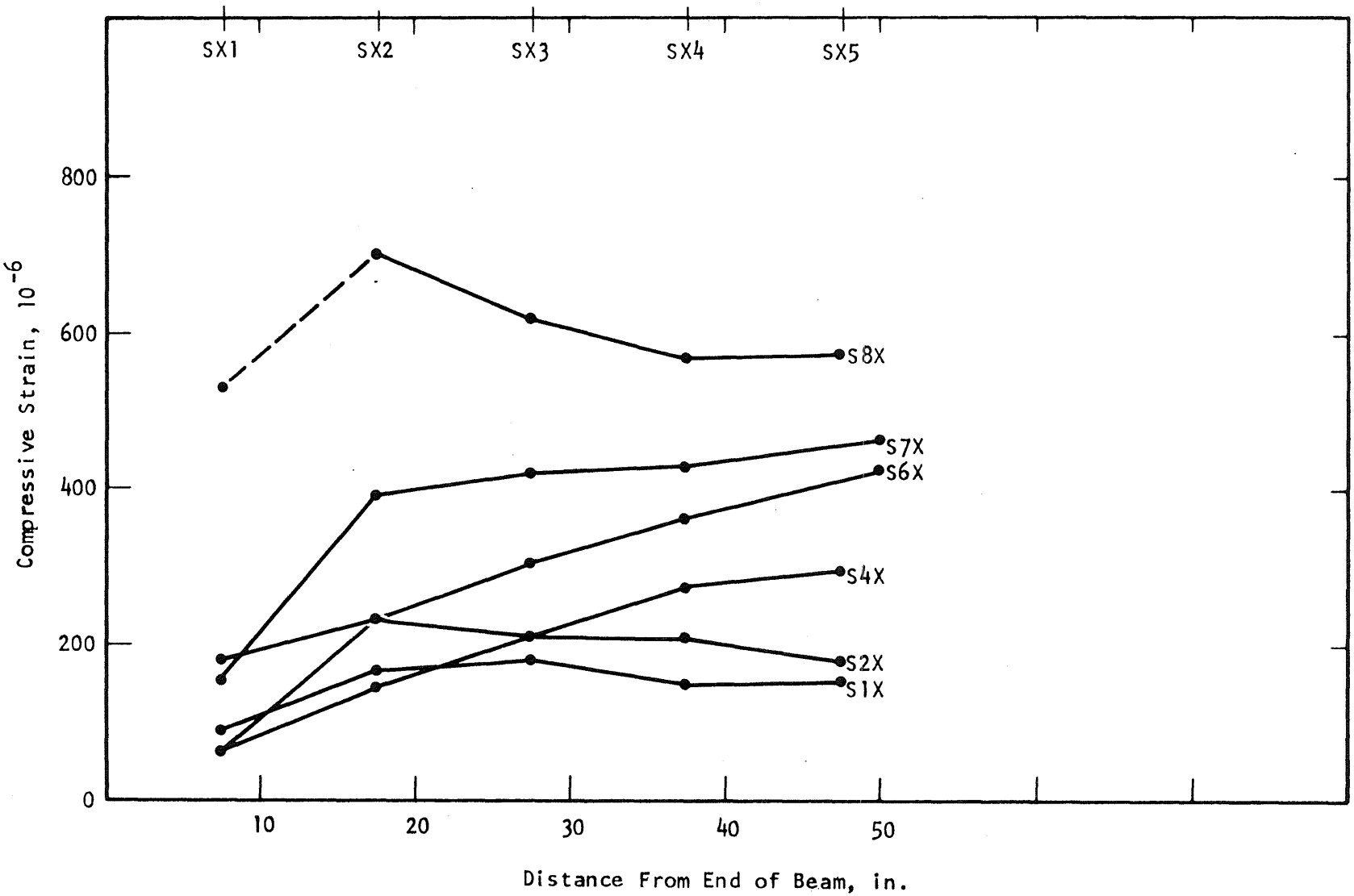

Fig. 4.23 DISTRIBUTION OF LONGITUDINAL STRAIN ALONG BX-4 NEAR SOUTH END AT RELEASE

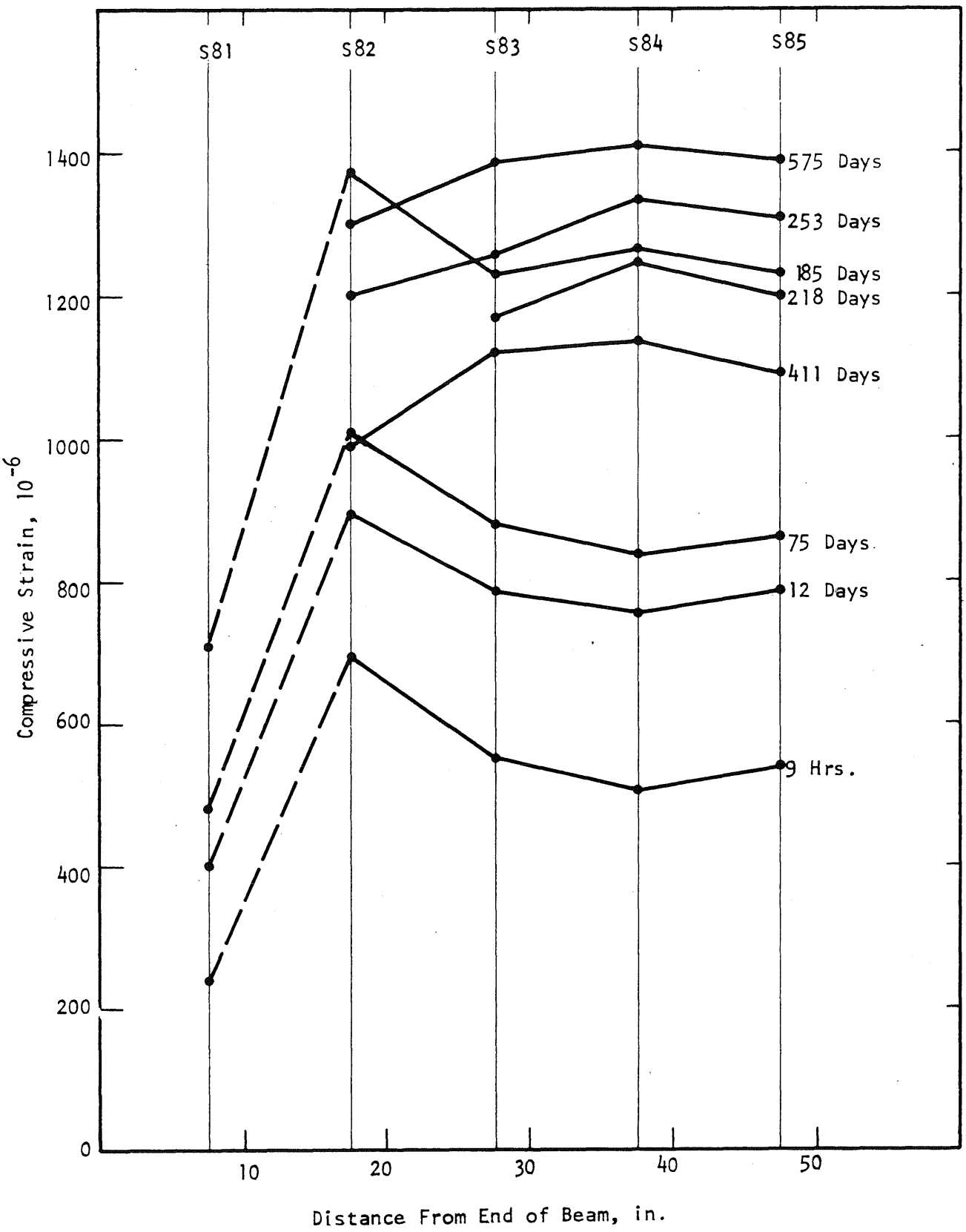

Fig. 4.24 STRAINS ALONG GAGE LINE S8X AT VARIOUS TIMES - BX-3

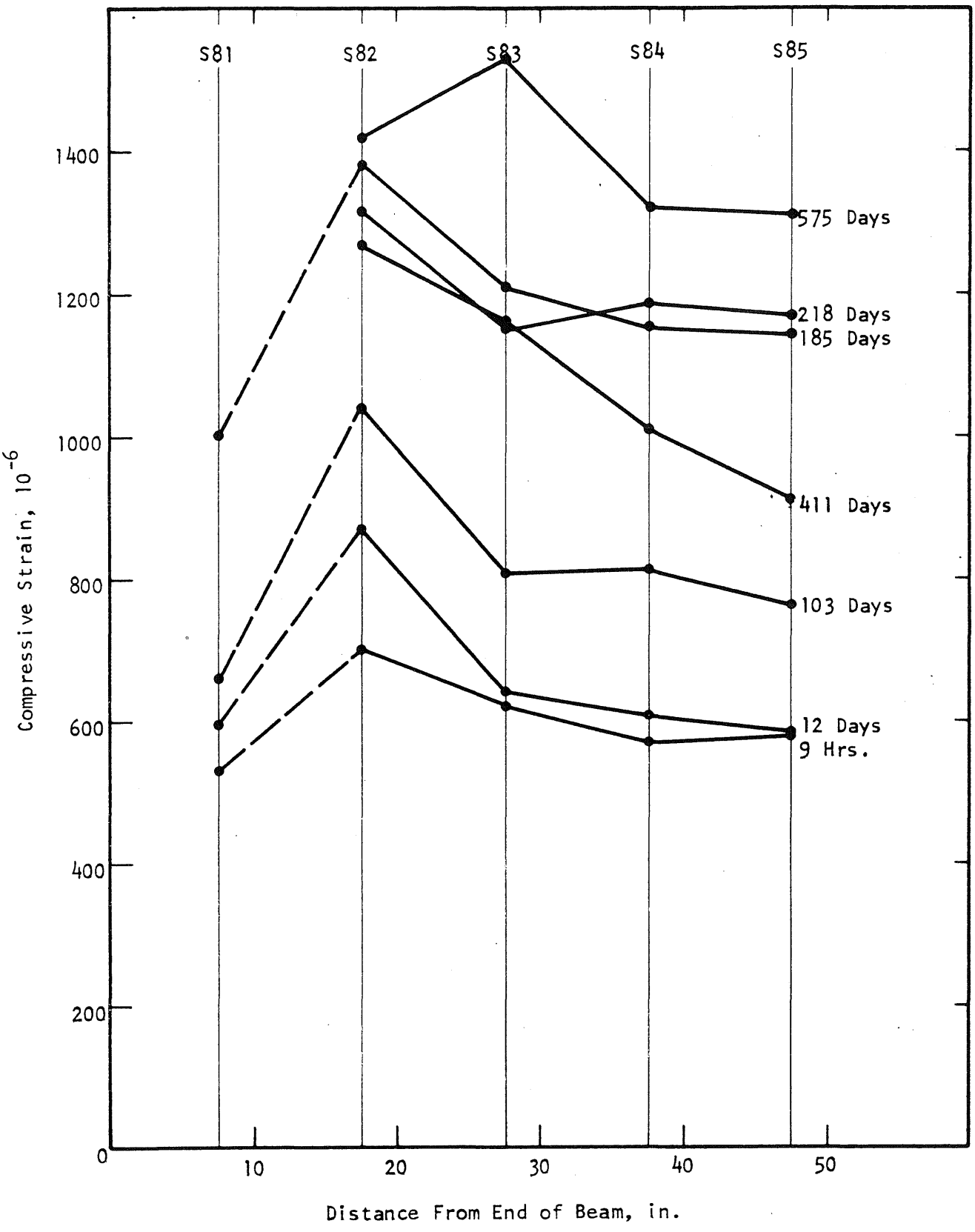

Fig. 4.25 STRAINS ALONG GAGE LINE S8X AT VARIOUS TIMES - BX-4

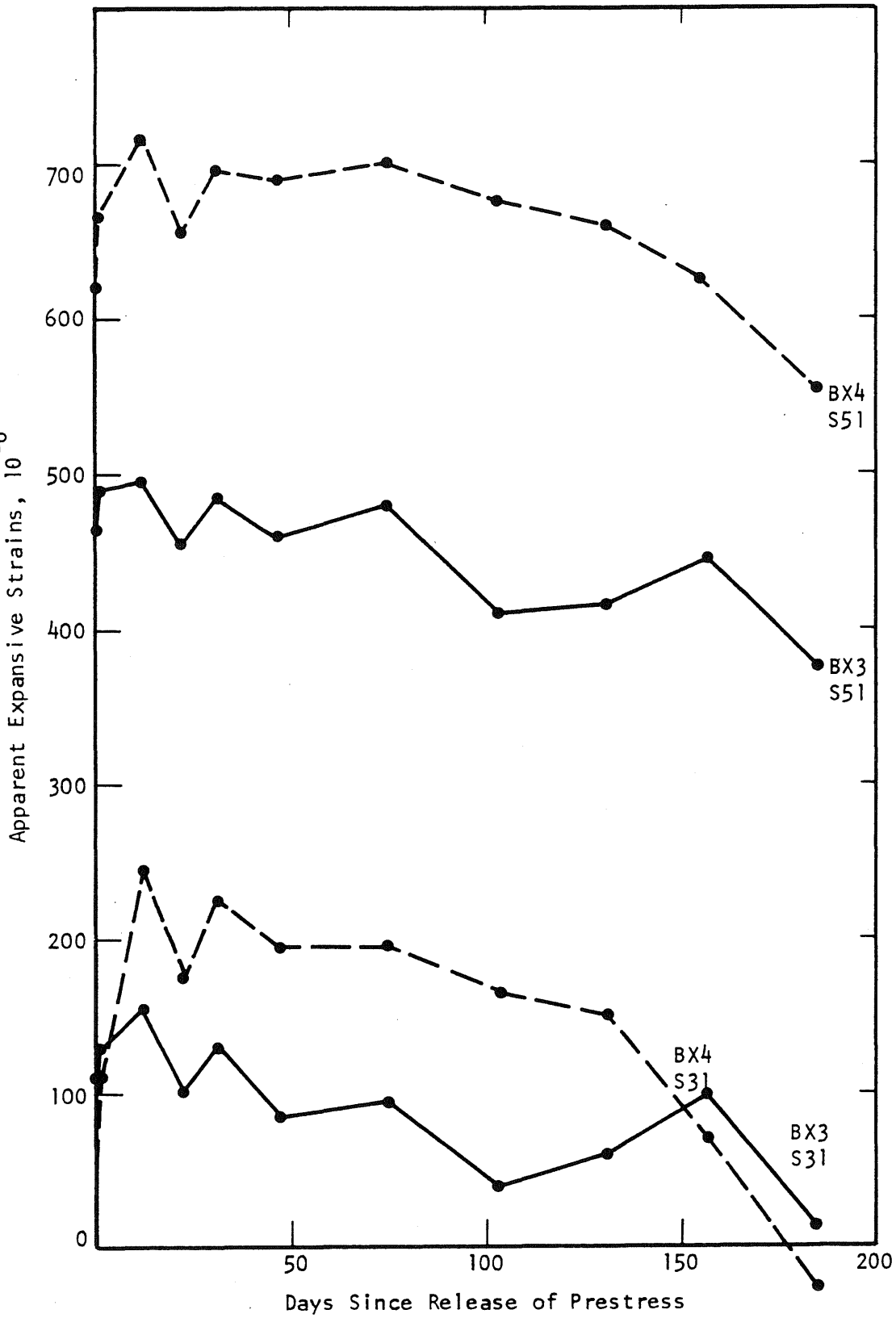

Fig. 4.26 VERTICAL STRAINS VS TIME AT SOUTH ENDS OF BEAMS

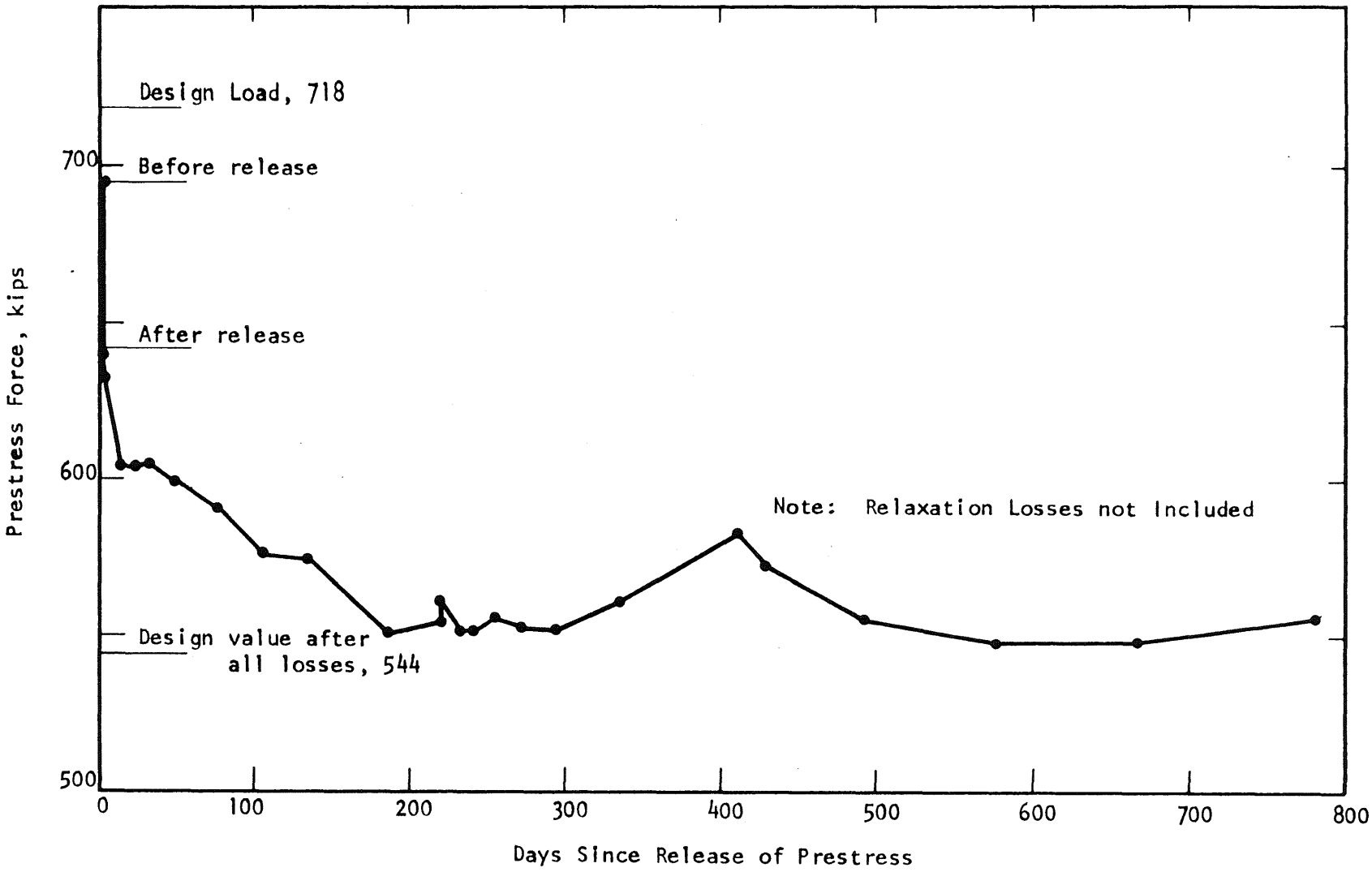

Fig. 4.27 PRESTRESSING FORCE VS TIME, BX-3

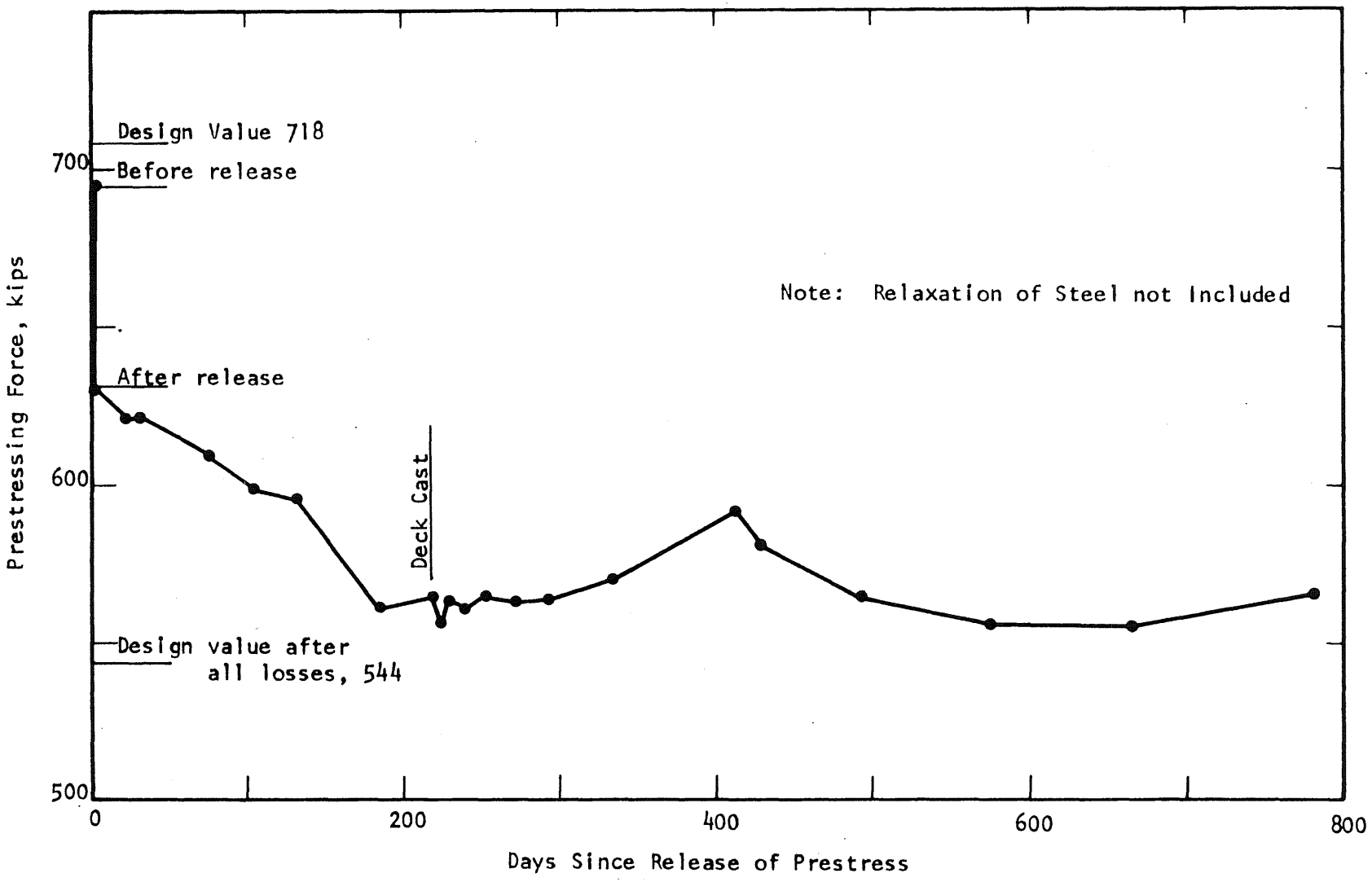

Fig. 4.28 PRESTRESSING FORCE VS TIME, BX-4

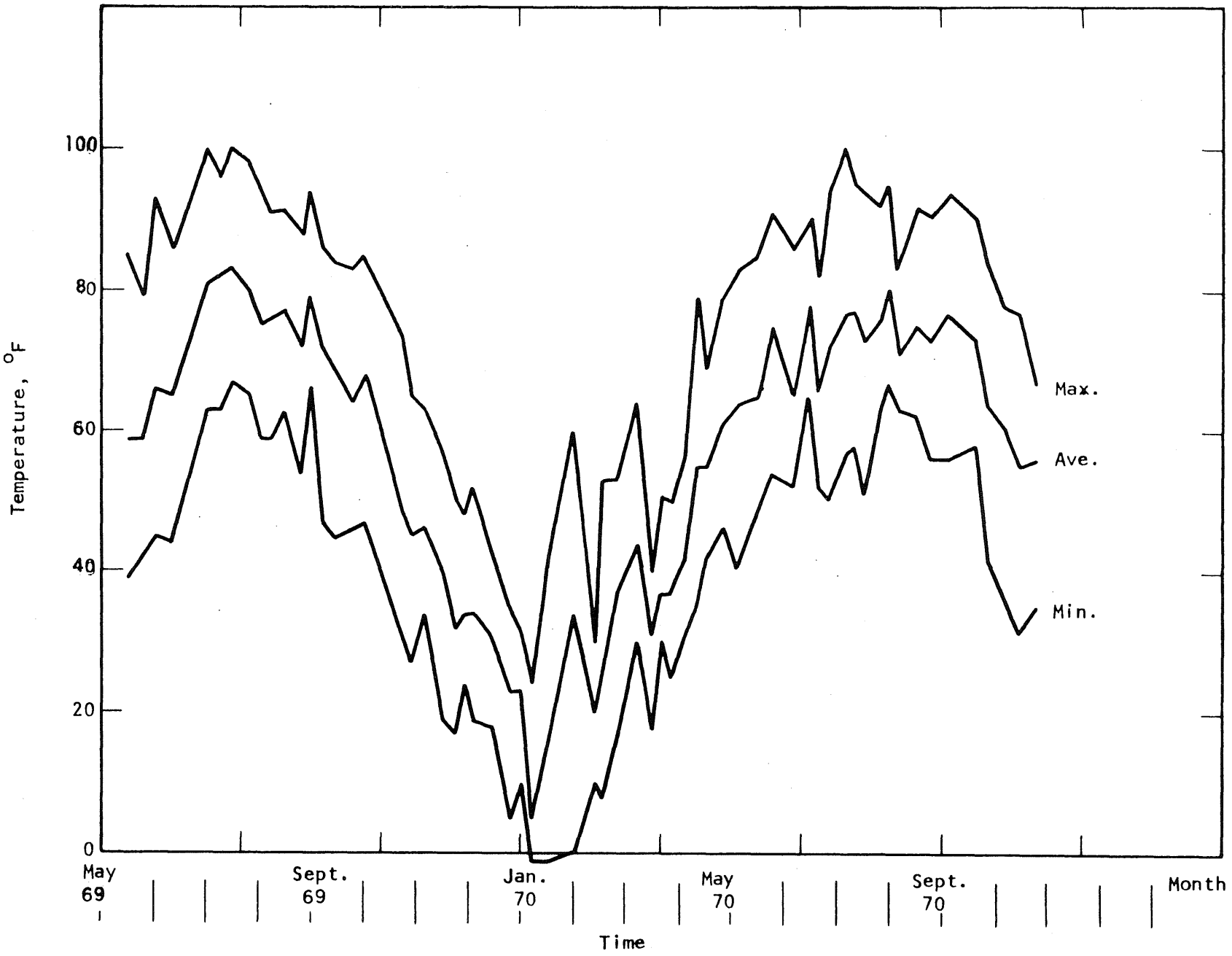

Fig. 5.1 WEEKLY TEMPERATURE RECORD, TUSCOLA

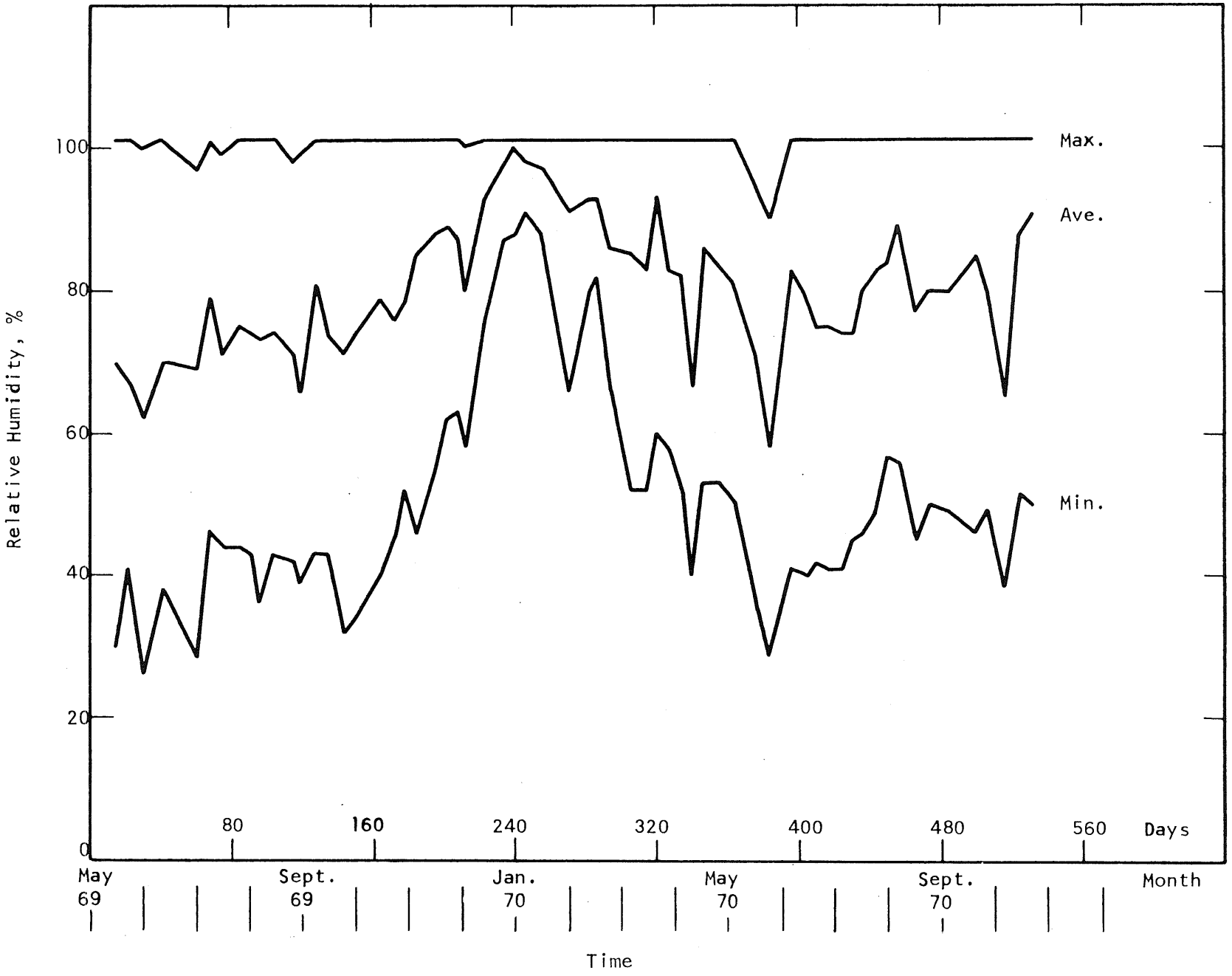

Fig. 5.2 WEEKLY RELATIVE HUMIDITY RECORD, TUSCOLA

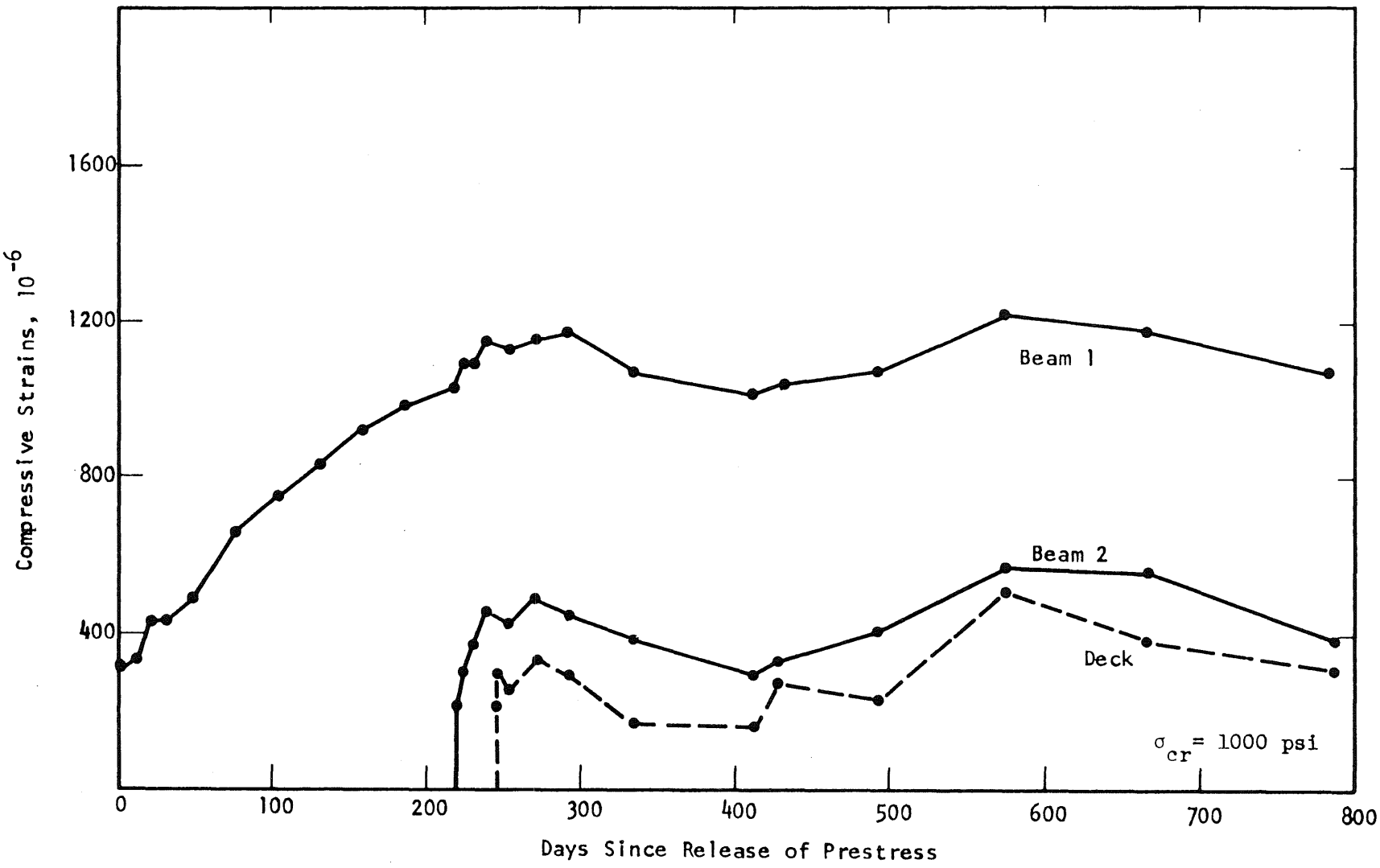

Fig. 5.3 TOTAL STRAIN-TIME CURVES FOR CREEP CYLINDERS IN THE FIELD

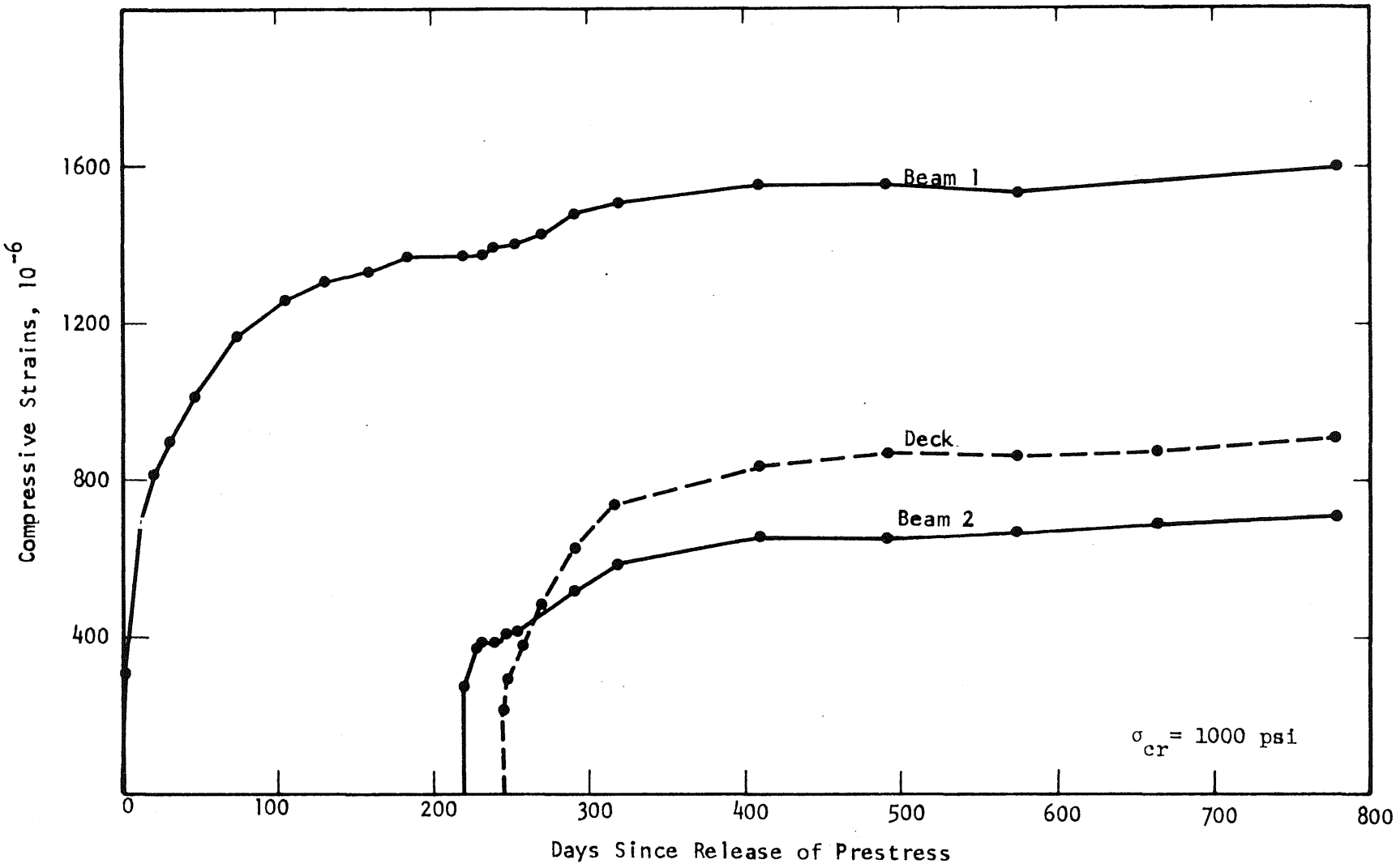

Fig. 5.4 TOTAL STRAIN-TIME CURVES FOR CREEP CYLINDERS IN THE LAB

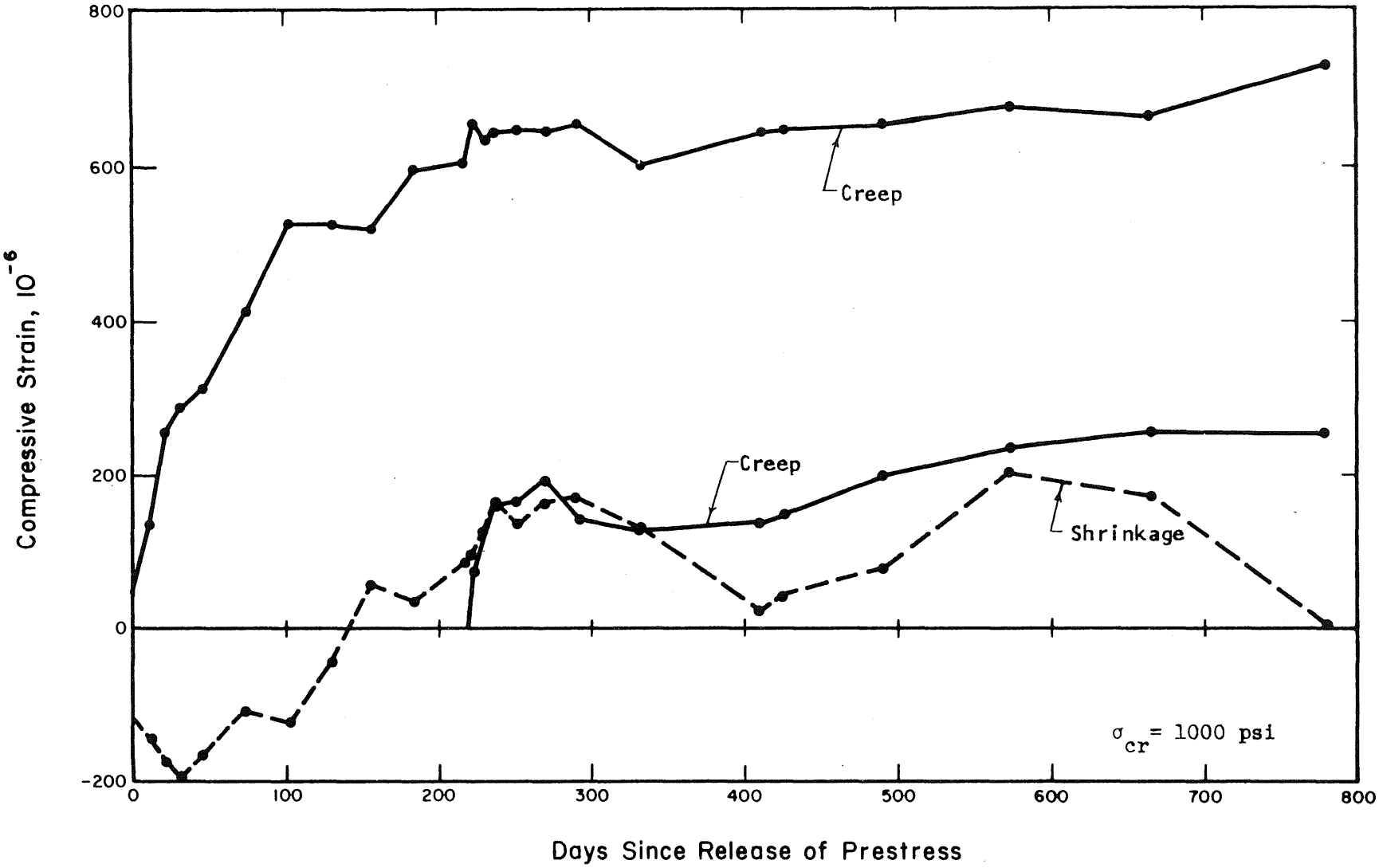

Fig. 5.5 CREEP AND SHRINKAGE OF FIELD-STORED BEAM CONCRETE CYLINDERS

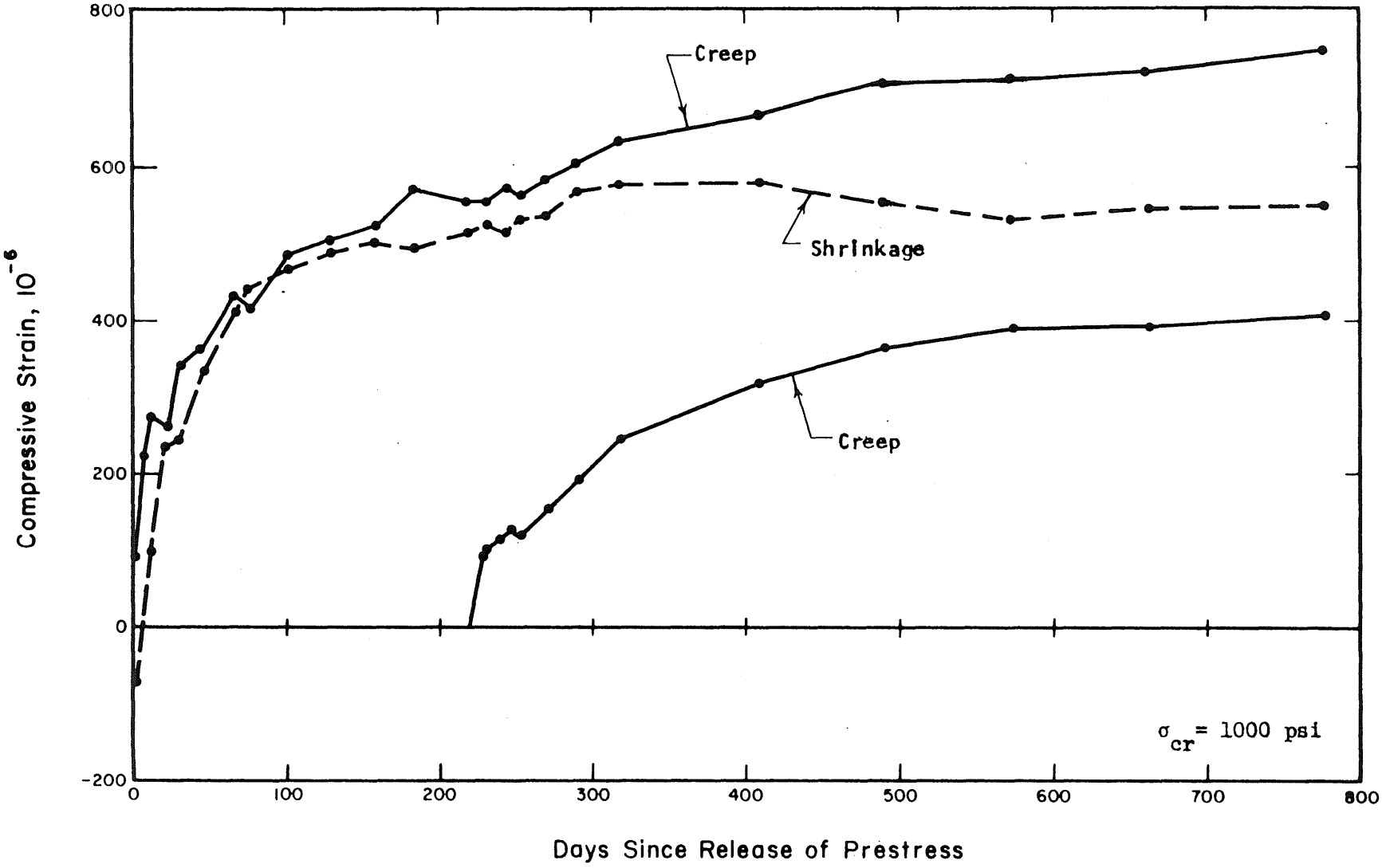

Fig. 5.6 CREEP AND SHRINKAGE OF LABORATORY STORED BEAM CONCRETE CYLINDERS

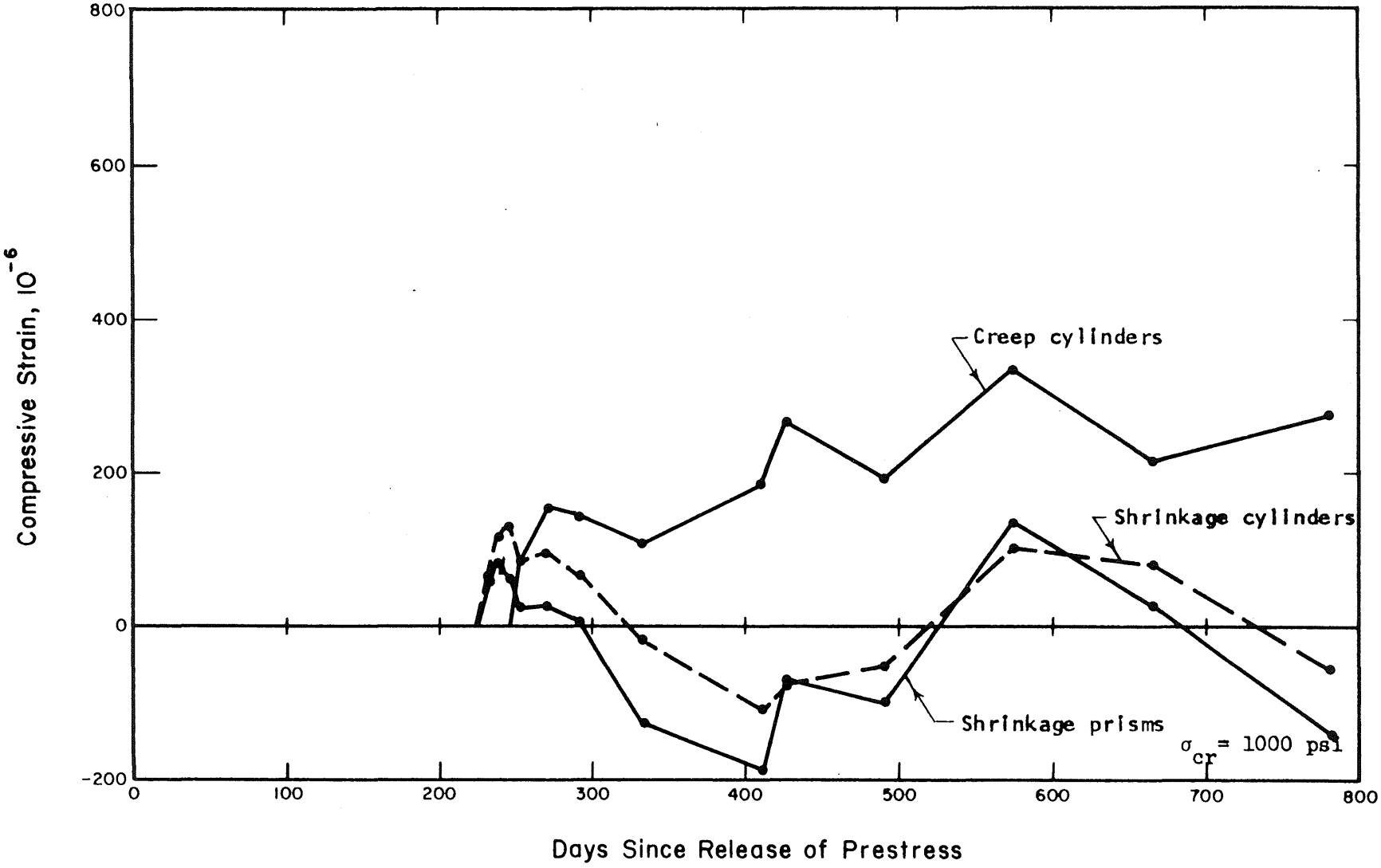

Fig. 5.7 CREEP AND SHRINKAGE OF FIELD STORED DECK CONCRETE SPECIMENS

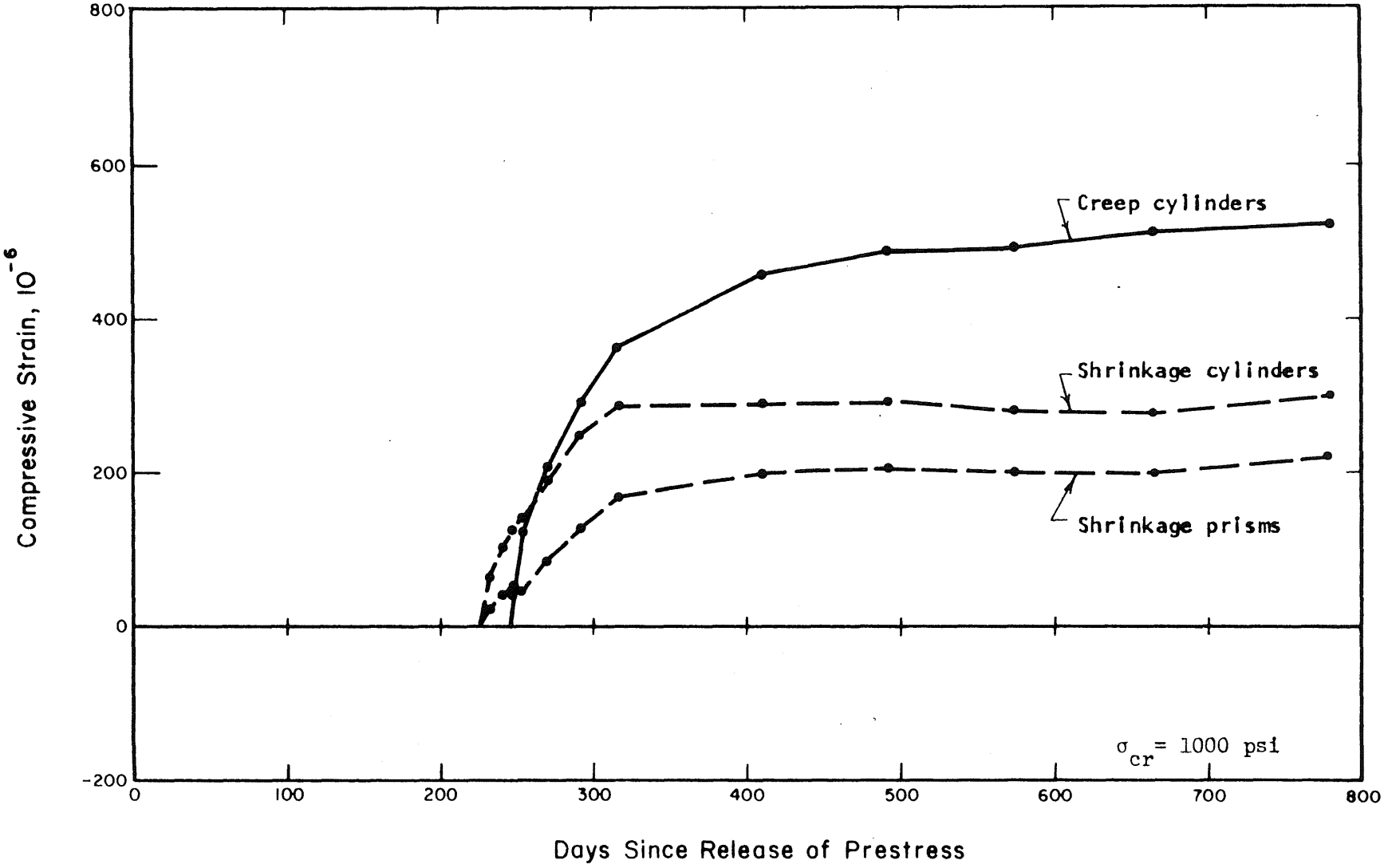

Fig. 5.8 CREEP AND SHRINKAGE OF LABORATORY STORED DECK CONCRETE SPECIMENS

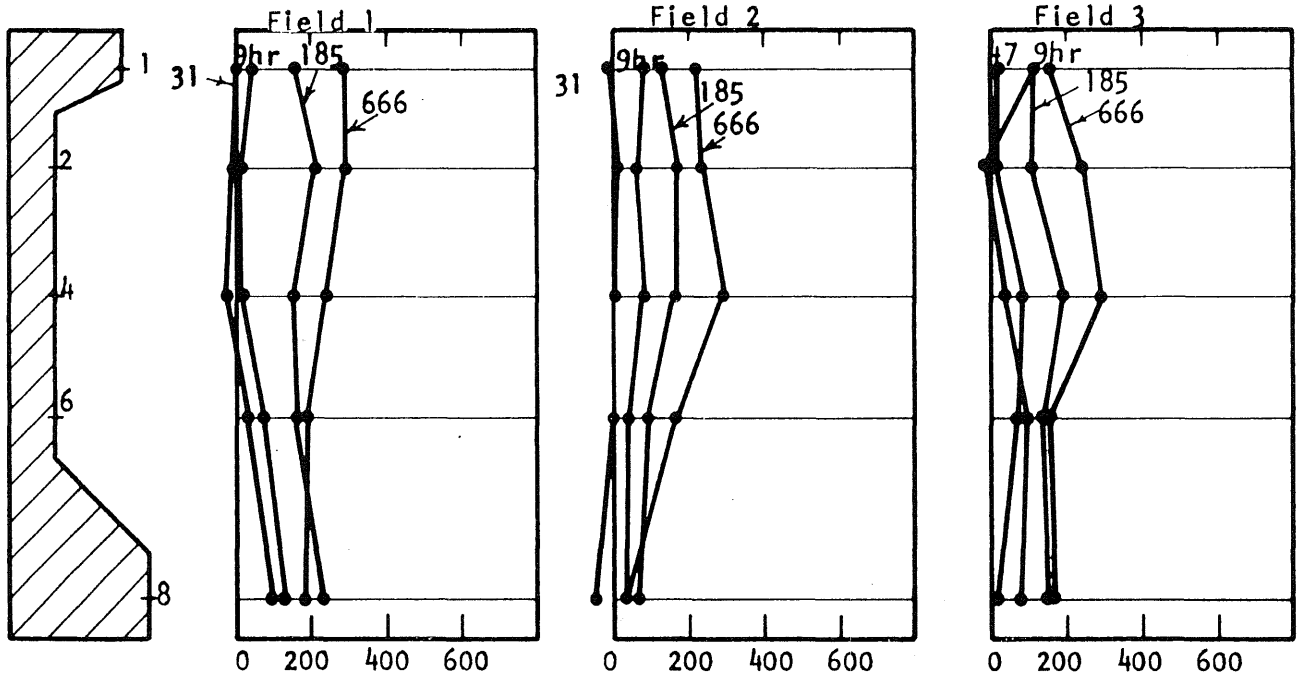

Fig. 5.9 STRAINS IN TWO-FT BEAMS, FIELD

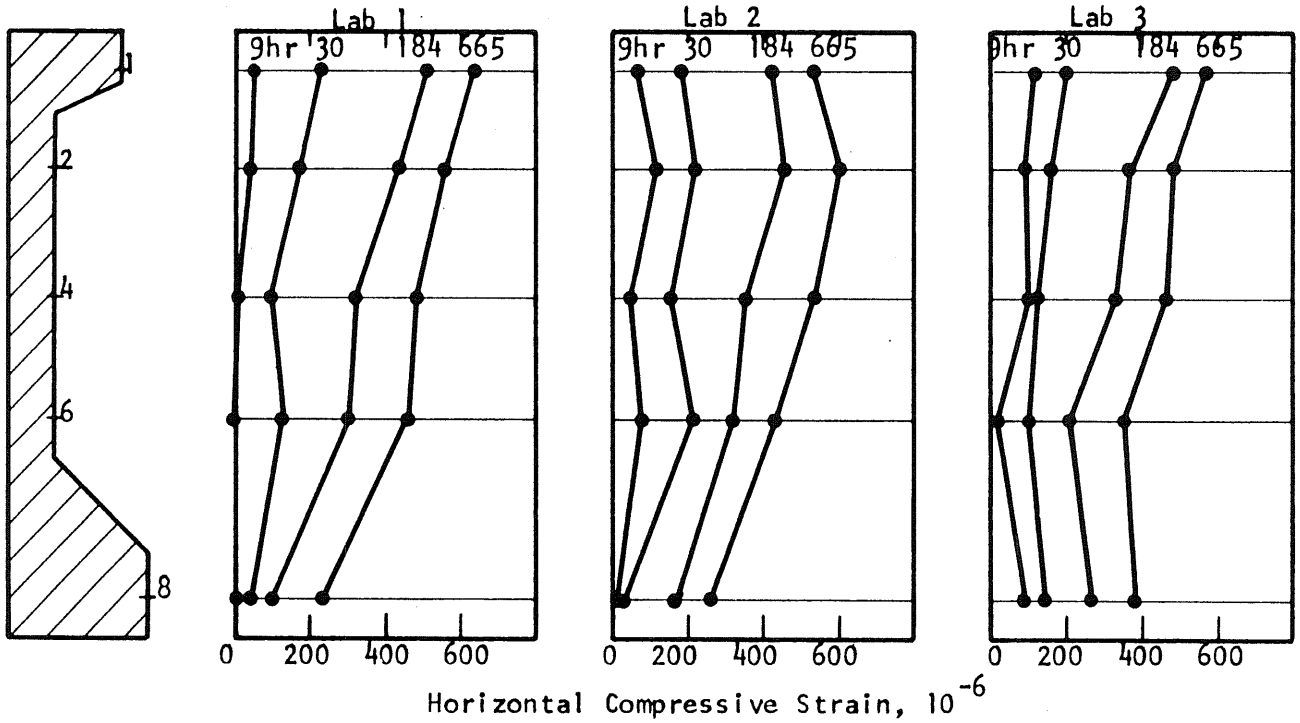

Fig. 5.10 STRAINS IN TWO-FT BEAMS, LAB

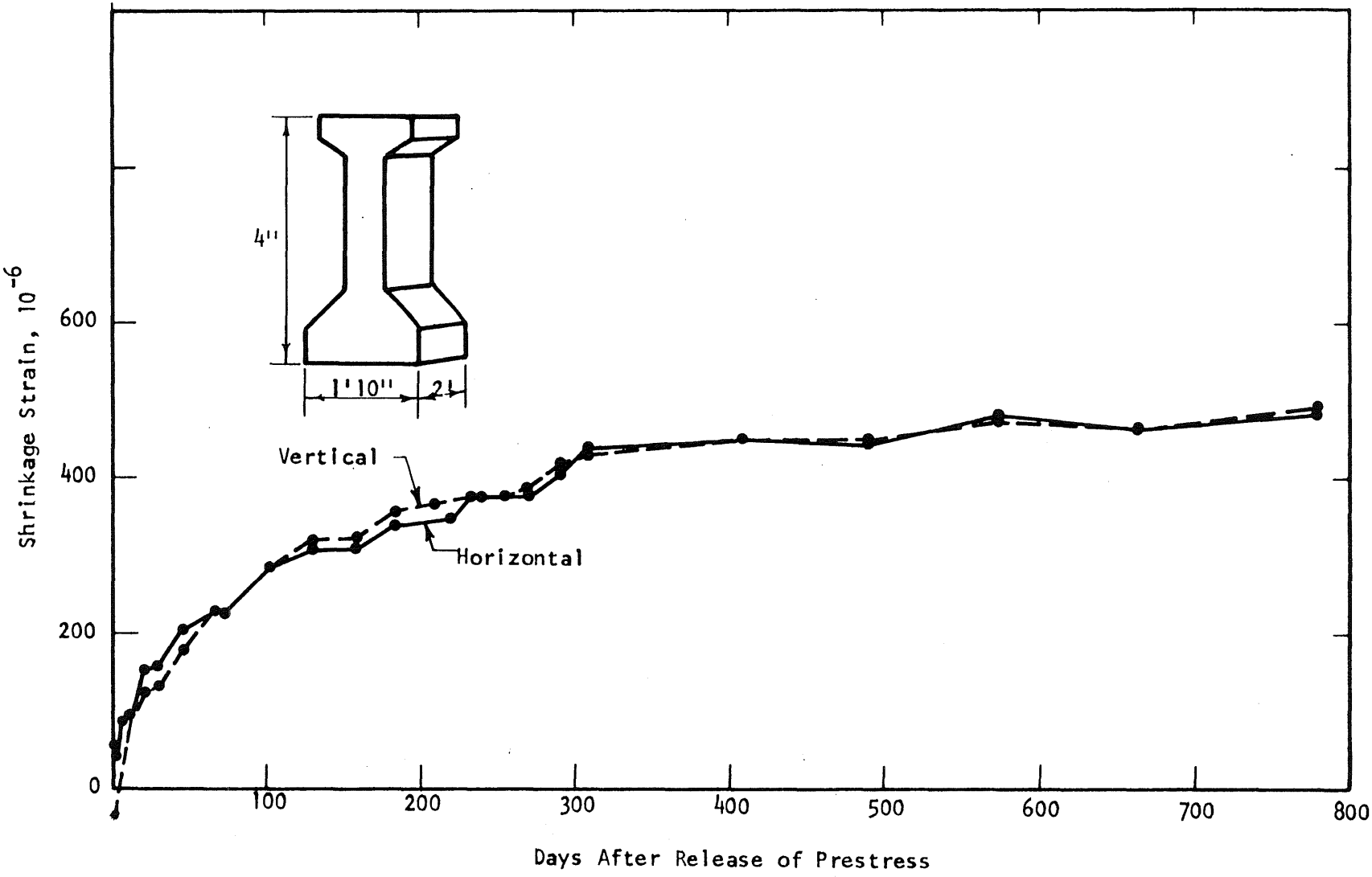

Fig. 5.11 HORIZONTAL AND VERTICAL SHRINKAGE OF TWO-FT BEAM L-2

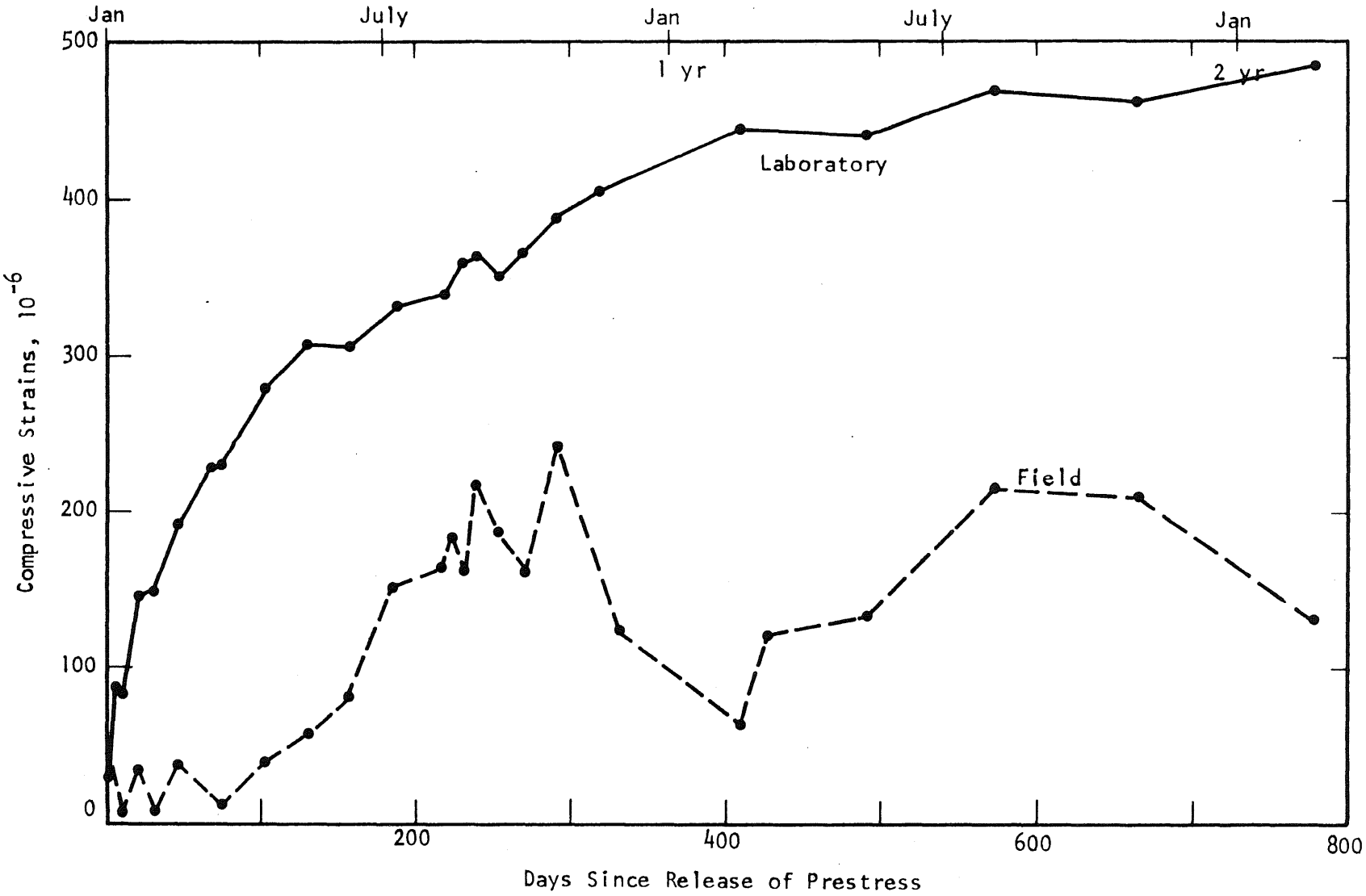

Fig. 5.12 HORIZONTAL SHRINKAGE-TIME CURVES FOR TWO-FT BEAMS

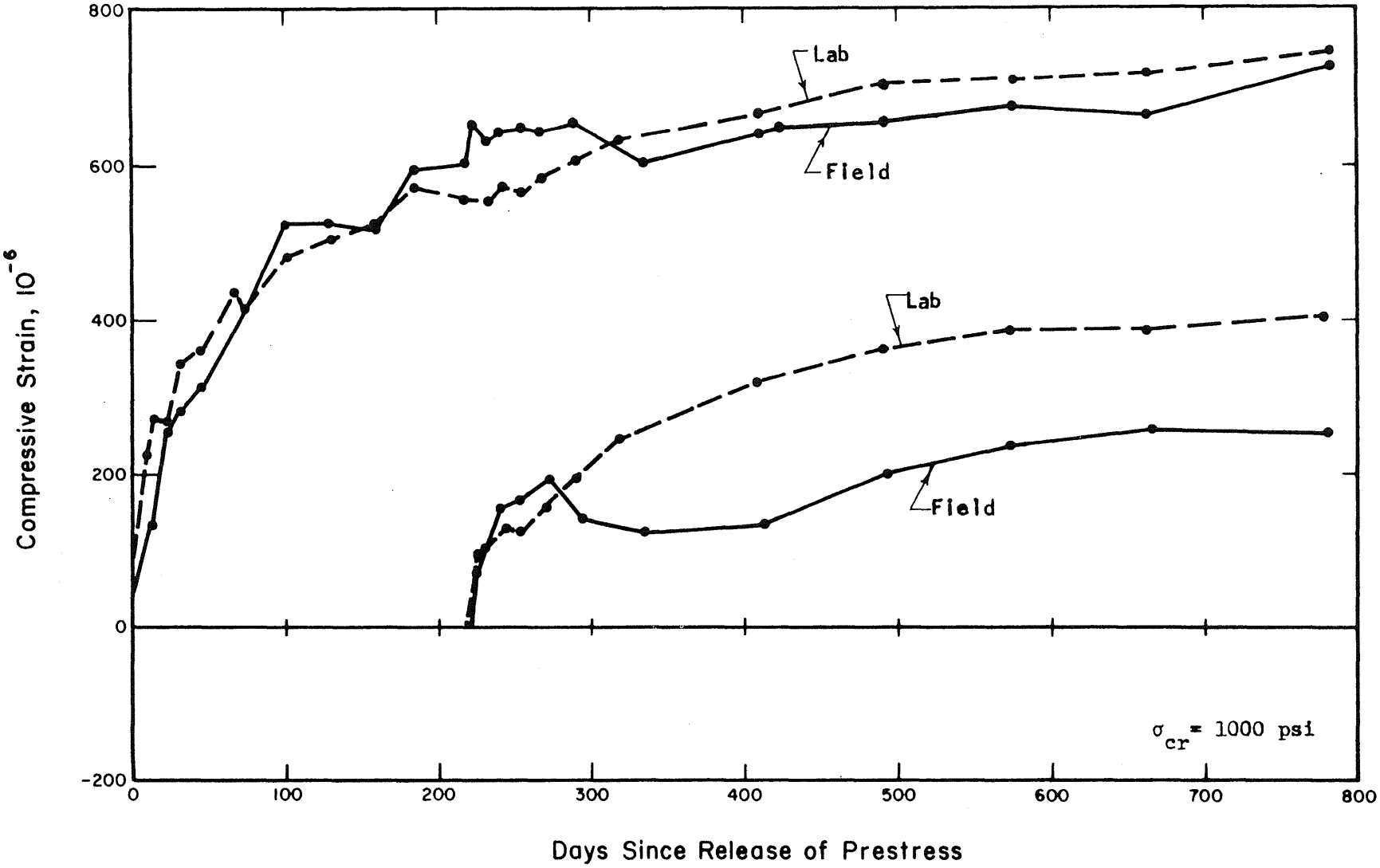

Fig. 5.13 CREEP STRAIN VS TIME CURVES FOR BEAM CONCRETE

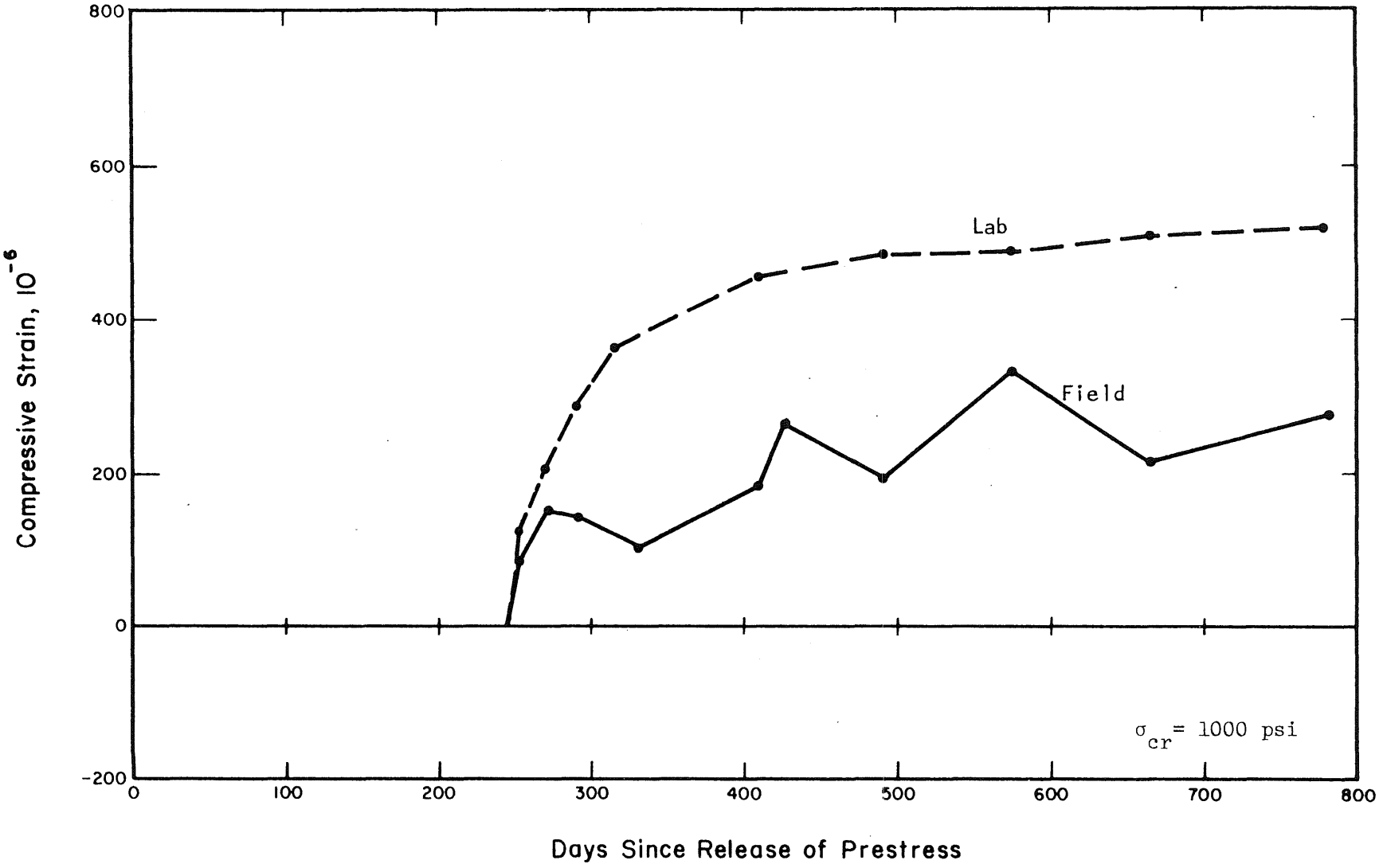

Fig. 5.14 CREEP STRAIN VS TIME CURVES FOR DECK CONCRETE